TECHNISCHE UNIVERSITÄT MÜNCHEN

Klinik für Kinderkardiologie und angeborene Herzfehler des Deutschen Herzzentrums München des Freistaates Bayern

Visualization of flow in the ascending aorta: bicuspid aortic valves compared to tricuspid aortic valves

Christine Lyko

Vollständiger Abdruck der von der Fakultät für Medizin
der Technischen Universität München zur Erlangung des akademischen Grades eines
Doktors der Medizin
genehmigten Dissertation.

Vorsitzender: Univ.-Prof. Dr. E.J. Rummeny
Prüfer der Dissertation:
1. Univ.-Prof. Dr. J. Hess, Ph.D.
2. apl. Prof. Dr. G. Schmidt

Die Dissertation wurde am 13.03.2012 bei der Technischen Universität München eingereicht und durch die Fakultät für Medizin am 11.12.2013 angenommen.

Contents

Abbreviations

4D	four-dimensional
AAo	aszendierende Aorta
ACC	American College of Cardiology
AHA	American Heart Association
AI	aortic insufficiency
AVR	aortic valve replacement
BAV	bicuspid aortic valve
Bcl-2	b-cell-lymphoma-2
BSA	body surface area
CHD	congenital heart disease
cm	centimeter
CMN	cystic media necrosis
CMR	cardiovascular magnetic resonance
CoA	coarctation of the aorta
CT	computed tomography
d	days
DICOM	Digital Imaging and Communications in Medicine
e.g.	for example/ exempli gratia
ECG	electrocardiography
ECM	extracellular matrix
FOV	field of view
f	female
Hz	Hertz
kg	kilogram
LCA	left coronary artery
LVOT	left ventricular outflow tract
m	meter
m^2	square meter
mm	millimeter

MR(I)	magnetic resonance (imaging)
ms	millisecond
MVP	mitral valve prolapse
MMP	matrix metalloproteinase
n	number
n.s.	non significant
p	pressure
p.	page
PC	phase contrast
PC-CMR	phase contrast cardiovascular magnetic resonance
PC-MR	phase contrast magnetic resonance
P_{dia}	diastolic pressure
PE	phase encode
PFO	patent foramen ovale
pp.	pages
P_{sys}	systolic pressure
PV	phase velocity
RCA	right coronary artery
retro	retrospective
rf	radiofrequency
ROI	region of interest
RVOT	right ventricular outflow tract
s	second
SD	standard deviation
SI	stiffness index
S/P	status post
TAV	tricuspid aortic valve
TE	time to echo
TR	time to repetition
Venc	velocity encoding
VSMC	vascular smooth muscle cell
yrs	years

1 Introduction

1.1 Historical Background

The first anatomical characterization and estimation of the bicuspid aortic valve (BAV) can already be found in the 16th century. Leonardo da Vinci (1452-1519) drafted aortic valves with two, three and four valvular cusps and concluded that just the tricuspid valve had optimal geometric properties with an optimal relation between anatomical structure and valvular function (O'Malley et al. 1952, p. 506). In 1844 it was first described as a pathological curiosity by Paget; in 1866 Peacock recognized its liability to calcific stenosis; and in 1886, Osler first associated BAV disease with infective endocarditis (Yener et al. 2002, p. 264; Paget J. 1884, pp. 162–188; Peacock TB. 1866, p. 204; Osler W. 1886, pp. 185–192). The association between BAV and aortic disease like aortic aneurysm, aortic dissection and rupture was first described by Abott in 1928 (Abbott ME. 1928, pp. 574–618), and McKusick reported on the association between BAV and Erdheim cystic medial necrosis in 1972 (Siu et al. 2010, p. 2789; McKusick 1972, pp. 1026–1027). The clinical significance of the aortic valve was underlined by the work of Larson and Edwards in 1984, who noted that BAV was associated with at least a nine-fold greater risk of aortic dissection (Braverman et al. 2005, p. 471; Larson et al. 1984, pp. 849–855). The autopsy studies of Wauchope demonstrated that BAV disease is the most common congenital anomaly of the heart (Braverman et al. 2005, p. 471; Mills et al. 1978, pp. 951–957; Wauchope G. 1928, pp. 383–399).

1.2 Epidemiology – Incidence and Prevalence

BAV disease is the most common congenital heart defect, with a prevalence estimated between 0.5% and 2% (Siu et al. 2010). According to the autopsy study of Roberts, a BAV can be found in one to two percent of the population and according to Osler in 1.3 % (Roberts 1970, pp. 72–83; Osler W. 1886, pp. 185–192). In the largest reported necropsy series of Larson and Edwards involving 21,417 consecutive cases, 293

patients with BAV were found. This matches an incidence rate of 1.37% (Larson et al. 1984, pp. 849–855). In some other series the incidence is indicated from 0.4 to 2.25% (Hoffman et al. 2002, pp. 1890–1900). Remarkable is the male predominance of approximately 3:1 in patients with BAV (Basso et al. 2004, pp. 661–663; Hahn et al. 1992, pp. 283–288). Besides the general population, there are certain sections of the population with higher prevalences of BAV. More than 50% of patients with coarctation of the aorta are to have a BAV (Roos-Hesselink et al. 2003, pp. 1074–1077) and females with Turner syndrome are noted to have a higher prevalence than the general population (Braverman et al. 2005, p. 478; Sybert 1998, pp. E11).

1.3 Predisposing Factors and Genetics

The etiology of the bicuspid aortic valve is still a controversial issue in previous and recent studies. Both genetic and environmental factors may play an important role in the formation of BAV (Nora et al. 1978, pp. 205–213; Cripe et al. 2004, pp. 138–143).

1.3.1 Inherited Factors

There are a number of studies reporting of BAVs in monozygotic twins and familial clustering and thus suggesting genetic factors in the etiology of BAV (Brown et al. 2003, pp. 183–184; Godden et al. 1987, pp. 316–318; Glick et al. 1994, pp. 400–404; Emanuel et al. 1978, pp. 1402–1407). Glick and Roberts suggested a Mendelian pattern of inheritance due to a prevalence of aortic valve disease of 24% in families with more than 1 person with aortic disease (Siu et al. 2010, p. 2790; Glick et al. 1994, pp. 400–404). In a study of 41 families with one family member having surgically confirmed BAV, Emanuel et al noted the prevalence to be at least 14.6% (Emanuel et al. 1978, pp. 1402–1407; Braverman et al. 2005, p. 478). Besides recent studies have demonstrated that BAV is probably attributed to mutations in different genes with dissimilar patterns of inheritance (Siu et al. 2010, p. 2790; Cripe et al. 2004, pp. 138–143). Genes associated with BAV are NOTCH1 (gene map locus 9q34.3) (Garg et al. 2005, pp. 270–274; Mohamed et al. 2006, pp. 1460–1465; McKellar et al. 2007, pp. 290–296), genes on the regions 18q, 5q and 13q (Martin et al. 2007, pp. 275–284), the ACTA2 gene on 10q (Guo et al. 2007, pp. 1488–1493) and the ubiquitin fusion degradation 1-like gene

(Siu et al. 2010, p. 2790). As clinical studies have reported a 9% prevalence of BAV in first-degree relatives of patients with BAV (Huntington et al. 1997, pp. 1809–1812), the current American College of Cardiology (ACC)/American Heart Association (AHA) adult congenital heart disease guidelines (Warnes et al. 2008, pp. e1-e121) suggest echocardiographic screening for BAV in first-degree relatives of patients with BAV based on this data (Siu et al. 2010, p. 2790).

1.3.2 Non-inherited Factors

Cardiac and valve morphogenesis occur early in fetal development. At the beginning of valve morphogenesis, early in fetal development, the extracellular matrix thickens and forms an endocardial cushion that finally shapes 4 cardiac valves (Siu et al. 2010, p. 2790). In this context Eisenberg and Fedak suggest in their studies a molecular abnormality in extracellular matrix proteins as cause of incorrect cusp formation during valvulogenesis (Fedak et al. 2002, pp. 900–904; Eisenberg et al. 1995, pp. 1–6). Besides the genetical factors, also abnormalities in fetal hemodynamics could be important in the development of BAV. In an earlier theory, Moore et al proposed that disproportional reduction of blood flow at the left side of the heart could lead to malformation of the aortic valve even after initially normal valvulogenesis (Moore et al. 1980, pp. 367–372). Frequent combination of BAV and CoA as well as aortic wall alterations of the ascending aorta is noted. This may be associated with embryonic neural crest cells. Some researchers have suggested anomalous behaviour of cells derived from the neural crest as a possible etiology. The proponents of this theory remarked that BAV was associated with congenital malformations of the aortic arch and other neural crest derived systems (Braverman et al. 2005, p. 474; Kappetein et al. 1991, pp. 830–836). So could anomalies occurring during the different stages of the migration of the neural crest cells be the cause of isolated or combined malformations of the aortic arch, the wall of the ascending aorta or the aortic valve (Le Lièvre et al. 1975, pp. 125–154; Kirby 1987, pp. 219–224). Other theories associate the development of BAV with endothelial nitric oxide, which is important in vascular and valve formation. Knockout mice can develop BAV because of their lack of endothelial nitric oxide synthase (Lee et al. 2000, pp. 2345–2348). To sum up, definite factors leading to the development of bicuspid aortic valves are still not known and require further research.

1.4 Morphology of the Bicuspid Aortic Valve

The bicuspid aortic valve usually consists of two unequally sized cusps, probably due to its development out of the fusion of two cusps. But the development of BAVs are more likely the result of a complex process, not simply the fusion of two normal cusps (Fedak et al. 2002, p. 900). Additionally there might exist a central raphe, where the two cusps fused, and smooth cusp margins (Braverman et al. 2005, p. 473). According to Pomerance et al in histological examinations no valve tissue could be found in the raphe (Pomerance 1972, p. 570).

The morphology of the BAV can be classified according to their leaflet morphology. Schaefer et al classified the BAV in type 1 (congenital fusion of the right and left coronary cusp, also called anterior-posterior BAV), type 2 (congenital fusion of the right and non-coronary cusp, also called right-left BAV) and type 3 (congenital fusion of the left and non-coronary cusp) (Schaefer et al. 2008, p. 1635). Patients with congenital BAV are predisposed for aortic disease like dilation and aortic dissection, but aortic dimensions are related to BAV phenotype (Schaefer et al. 2007, p. 686). About 70-80% of the BAV patients have a fusion of the right-coronary and left-coronary leaflet (Fernandes et al. 2004, p. 1649; Schaefer et al. 2008, p. 1636). Schaefer et al found out that subjects with BAV type 1 compared with those with BAV type 2 had a larger dimension and increased wall stiffness at the sinuses of Valsalva, but smaller diameter with no difference in stiffness at the aortic arch (Schaefer et al. 2007, p. 689). There is a male predominance among all subjects, but there were more women among BAV type 2 (Schaefer et al. 2008, p. 1636). Furthermore, fusion of the right-coronary and non-coronary leaflets was associated with more significant valve pathology, whereas fusion of the right-coronary and left-coronary leaflets was associated primarily with aortic coarctation and less aortic valve pathology (Fernandes et al. 2004, p. 1648; Fernandes et al. 2007, pp. 2211–2214). Fernandez et al noted that the different phenotypes of BAV are different etiological entities in mice and hamsters (Fernández et al. 2009, pp. 2312–2318). However, this fact is not proved for humans so far. Some authors showed associations between right and left-coronary fusion and severer dilatation of the ascending aorta (Thanassoulis et al. 2008, pp. 821–828), others suggested dilatation to be more progressive in patients with right and non-coronary leaflet fusion (Holmes et al.

2007, pp. 978–983). Besides there are also studies that could not found any differences in aortic dimensions in different BAV phenotypes (Buchner et al. 2010, pp. 1233–1240; Fazel et al. 2008, p. 903). So potential associations between aortopathy and different BAV phenotypes are still controversial.

1.5 Variants and Associated Congenital Cardiovascular Lesions

In association with BAV congenital variants in coronary arteries are described. Up to 57% of BAV patients are noted to have left coronary artery dominance and compared to tricuspid aortic valves (TAVs) a generally shorter left main coronary artery (Lerer et al. 1981, pp. 142–147; Higgins et al. 1975, pp. 292–296; Scholz et al. 1980, pp. 417–418). Additionally other isolated native coronary artery anomalies have been reported (Doty 2001, pp. 842–843; Takahashi et al. 1994, pp. 61–64). BAVs often coexist with other congenital cardiovascular lesions. The most common defect is coarctation of the aorta (CoA). Fifty to 75 % of patients with CoA have a BAV (Roos-Hesselink et al. 2003, pp. 1074–1077). According to Beaton et al patients with BAV and CoA had lower ascending aortic dimensions and slower rates of aortic dilatation. Furthermore, the ascending aorta did not dilate to the same degree as in BAV patients without CoA (Beaton et al. 2009, p. 266). In a study of Miller et al 34% of patients with Turner's syndrome had a BAV. It is likely the most common cardiovascular malformation after CoA (Miller et al. 1983, pp. 47–50). Aside from the Turner's syndrome, a few other syndromes may coexist with BAV, e.g. Shone's complex (Bolling et al. 1990, pp. 887–893) and Williams syndrome (Braverman et al. 2005, p. 482). In addition other congenital cardiac lesions like ventricular septal defects (Neumayer et al. 1998, pp. 1573–1582), patent ductus arteriosus (Glower et al. 1992, pp. 368–370) and atrial septal defects (Siu et al. 2010, p. 2790) may occur together with BAV.

1.6 Clinical Presentations and Complications

Valve diseases

The majority of patients with BAV are asymptomatic. The initial diagnosis of a BAV is often made in routine exams, when a systolic ejection sound is noted during auscultation (punctum maximum at the apex). When lesions like aortic stenosis or insufficiency are present, an additional murmur can be noted. The diagnosis can be confirmed by transthoracic echocardiograms. The clinical manifestation relates to the function of the aortic valve like aortic stenosis or insufficiency, aortopathy like dilatation and dissection and acquired complications such as endocarditis. In childhood BAV is often asymptomatic, but due to a progressive process symptoms can develop in adulthood. Complications like aortic dissection are rare in children with BAV (Mahle et al. 2010, p. 445). A frequent complication of BAV is calcification, which is the most common cause of isolated aortic stenosis at the same time. Thus, aortic valve replacement is required in many cases of BAV, approximately five years earlier than aortic stenosis of a tricuspid aortic valve (Yener et al. 2002, p. 265; Fedak et al. 2002, p. 901; Mautner et al. 1993, pp. 194–198). Aortic regurgitation can occur due to redundant or prolapsing cusps, endocarditis or after balloon valvuloplasty, especially in childhood and in adulthood also secondary to dilatation of the ascending aorta (Siu et al. 2010, p. 2793). Another complication of BAV is infective endocarditis occurring in 7-25% of the cases. Most BAV patients affected with endocarditis require surgery, often as an emergency event and with significant mortality (9%) (Yener et al. 2002, p. 266; Lamas et al. 2000, pp. 336–341). Aortic valves oriented anteroposteriorly have more severe regurgitation, whereas those with right-left orientation have more severe stenosis (Tadros et al. 2009, p. 884; Sonoda et al. 2008, pp. 242–248). Beyond it is notable that although only about 0.5% to 2% of the general population are born with bicuspid aortic valves, 43% of the patients who either die or are operated on for aortic valve disease do have a BAV (Robicsek et al. 2004, p. 177; Ward 2000, pp. 81–85; Roberts 1970, pp. 72–83).

Aortic Dilatation and Dissection

An association between congenital BAV and aortic wall alterations like aortic dilatation and dissection has been previously confirmed in numerous studies (Nistri et al. 1999, pp. 19–22; Hahn et al. 1992, pp. 283–288; Keane et al. 2000, pp. III35-39; Roberts et al. 1991, pp. 712–716; Pachulski et al. 1991, pp. 781–782; Ward 2000, pp. 81–85). A diameter more than two standard deviations (SD) above the mean is considered to be dilated (Hager et al. 2002, pp. 1060–1066). Dilatation of the aorta can occur at all levels, but involves the ascending aorta in the majority of cases (den Reijer et al. 2010, p. 1). The diameters of the aorta were found to be significantly larger in patients with BAV than those in persons with TAV at all levels of the aortic root (, but not at the annulus), even in patients with normally functioning aortic valve (Beroukhim et al. 2006, pp. 828–830; Hahn et al. 1992, pp. 283–288; Nistri et al. 1999, pp. 19–22). The prevalence of dilatation ranges from 7.5% to 59% at the annulus, 16% to 78% at the sinus of Valsalva, 15% to 79% at the sinotubular junction and 35% to 68% at the proximal ascending aorta (Tadros et al. 2009, p. 883; Nistri et al. 1999, p. 21; Hahn et al. 1992, p. 263). Already children with BAV had larger aortic diameters than healthy controls of the same age (Braverman et al. 2005, p. 501). The prevalence of aortic dilatation increases with age, and more dilated aortas have faster expansion rates (Tadros et al. 2009, p. 883). Additionally, dilatations associated with BAV were found to be typically asymmetric involving predominantly the right anterolateral wall of the ascending aorta (Cotrufo et al. 2005, p. 509).

Besides aortic dilatation, BAV patients are prone to aortic dissection associated with a high mortality rate. Patients with dilated aorta have a 9-fold higher risk of aortic dissection than the general population (Tadros et al. 2009, p. 884; Larson et al. 1984, pp. 849–855). Aortic diameter is the most important risk factor and significant predictor of aortic dissection besides aortic stiffness, male sex, family history, CoA and Turner syndrome (Siu et al. 2010, p. 2794). Even though the lifetime risk of dissection in patients with Marfan syndrome is higher than in patients with BAV, there are more aortic dissections due to BAV because of its high prevalence, and as it occurs earlier in life (prevalence: BAV: 0,5-2 % , Marfan: ~ 0,01%) (Tadros et al. 2009, p. 884). Today there is still a lack of data regarding progression of aortic dilatation in BAV disease.

According to Ferencik et al the mean rate of progression was about 0.9 mm/year at the ascending aorta. Thanassoulis et al reported a rate of 0.37 mm per year (Ferencik et al. 2003, pp. 43–46; Thanassoulis et al. 2008, p. 824).

Outcome and Survival

Despite this number of complications, studies have shown that the survival rates for BAV patients were not lower than for the general population. Tzemos et al showed in their follow up study of nine years a survival rate of 96% ±1 in the BAV group and 97% ±1 in the TAV group. The overall mortality of the BAV group was not significantly higher compared with age and sex matched population estimates. Predictors of primary cardiac events were older age, moderate or severe aortic stenosis and moderate or severe aortic regurgitation (Tzemos et al. 2008, pp. 1317–1325). Furthermore, patients with BAV often require valve surgery like valve replacement, Ross operations or valve repair. Indications for valve replacement are the same as for diseased TAV, but patients undergoing aortic valve replacement (AVR) are often younger than those with TAVs (Siu et al. 2010, p. 2796). Roberts et al showed that the majority of patients undergoing surgery for aortic valve disease have a congenitally malformed valve (Roberts et al. 2005, pp. 920–925). About 30% of patients, who underwent AVR will also require aortic root surgery (Siu et al. 2010, p. 2796). Whereas Yasuda et al showed that AVR could not prevent the progress of aortic dilatation in BAV (Yasuda et al. 2003, pp. II291-294), McKellar et al only found further dilatation after AVR in 9.9% of the patients with BAV (McKellar et al. 2010, p. 1629).

1.7 Causes of Dilation and Dissection in patients with BAV - State of Research

The histopathological pattern found in aortic walls in patients with BAV is cystic media necrosis (CMN) defined as elastic fiber degeneration and fragmentation together with noninflammatory vascular smooth muscle cell (VSMC) loss (Braverman et al. 2005, p. 503). CMN also was found in patients without significant aortic aneurysm, particularly at the convexity of the ascending aorta. The VSMCs are responsible for remodeling of

the aortic media and produce cellular matrix proteins like collagen, elastin, fibrillin, tenascin or proteolytic enzymes like matrix metalloproteinases (MMPs). Aortic valve and ascending aorta both develop from the neural crest cells, as do the VSMCs. Thus, there are theories of a common developmental defect involving the aortic valve and the aortic wall in patients with BAV.

Furthermore, the media of the pulmonary trunk shows histopathological changes similar to those of the media in the ascending aorta and it was observed that in some patients, who underwent Ross procedure due to aortic dilatation, the pulmonary autograft tended to dilate. Additionally, the main pulmonary trunk was recently shown to be significantly larger in patients with BAV than in patients with TAV. So a few authors support the hypothesis that aortic dilatation resulted from a common developmental defect, as the pulmonary trunk and the ascending aorta share the same embryologic origin, the conotruncus (Kutty et al. 2010, pp. 1756–1761; Tadros et al. 2009, pp. 880–890; de Sa et al. 1999, pp. 588–594).

Beside medial degeneration, several studies demonstrated a significant impairment of fibrillin-1 in BAV aortic tissues compared to TAV aortas. Deficiency of fibrillin-1 might trigger MMP production and VSMC detachment from elastin and collagen leading to matrix disruption and dilatation (Fedak et al. 2003, pp. 797–806). Moreover, tissues of BAV aneurysm have increased activity and expression of MMPs compared to tissues of aneurysms of TAV patients. MMPs are proteolytic enzymes and maintain the homeostasis of connective tissue. Particularly the level of MMP-2 was increased. It degrades type IV collagen, elastin and fibrillar collagens and it is synthesized by several cells including VSMCs in response to hemodynamic changes (Tadros et al. 2009, p. 882; den Reijer et al. 2010, p. 4). Pathological changes in smooth muscle cells and associated ECM protein expression especially found to be significantly highest in the convexity of the ascending aorta. This asymmetric pattern of matrix protein expression and medial degeneration is congruent with the asymmetry in wall stress distribution in BAVs (Cotrufo et al. 2005, p. 504). Supplementary, flow properties are known to modulate cellular signaling cascades resulting in increased expression of MMPs and growth factors, as flow abnormalities affect the endothelial surface by friction (den Reijer et al. 2010, p. 4; Tadros et al. 2009, p. 882; Lehoux et al. 2003, pp. 631–643). The maximal burden of wall shear stress caused by abnormal flow in ascending aortic

aneurysms in BAV patients manifested at the right anterolateral wall (convexity) of the ascending aorta (Bauer et al. 2006, pp. 218–220).

Previous studies showed helical flow patterns in patients with BAV and aneurysm, where bicuspid aortic valves with fusion of the right and left coronary leaflet brought out right-handed helical flow and valves with fusion of the right and non-coronary leaflet led to left-handed helical flow. Hope et al could observe these flow pattern in some BAV patients without dilated ascending aorta. Nevertheless, it is notable that also patients with CoA, previously repaired and not, patients with TOF and dilated aorta, aortic insufficiency and aortic stenosis were included in this study (Hope et al. 2010, pp. 53–61; Hope et al. 2007, pp. 1471–1479).

In conjunction with the influence of hemodynamic changes on dilatation, Holman first described the theory of poststenotic dilatation (Holman 1954, pp. 109–133). A few authors counter the hemodynamic theory with the point, that dilatation also occurs in absence of aortic stenosis and insufficiency (Keane et al. 2000, pp. III35-39; Hahn et al. 1992, pp. 283–288; Nistri et al. 1999, pp. 19–22). As a result of these aortic wall alterations affecting elasticity, the stiffnex index (SI) in the ascending aorta is noted to be significantly increased in patients with BAV compared to TAV, and distensibility to be decreased (Nistri et al. 2008, pp. 472–479; Nistri et al. 2002, pp. 369–373; Schaefer et al. 2007, pp. 686–690).

In conclusion, it is discussed to this day, if alterations in ECM protein expression and the morphology of the aortic media are cause or consequence of aortic dilatation and whether they are caused by an inheritable developmental defect or abnormal hemodynamic characteristics and consequential abnormal wall shear stress.

1.8 Treatment

Medical Therapy

ACC/AHA guidelines for the management of adults with congenital heart disease (2008) suggest that it is reasonable to give beta-blockers to patients with bicuspid valves and dilated aortic roots who are not eligible for surgical correction and who do not have moderate to severe aortic regurgitation. Beta-blockers might have an affect on the

progression of aortic dilatation, but this issue was so far just studied in patients with Marfan syndrome (Bonow et al. 2008, pp. e559). Some studies also did research about use of angiotensin II rezeptor blockers and cholesterol-lowering agents in BAV disease, but if these drugs will have a role in BAV aortopathy, has not been demonstrated yet (Siu et al. 2010, p. 2795). An endocarditis prophylaxis is according to ACC/AHA guidelines not necessary (Warnes et al. 2008, pp. e14-16).

Interventions

In many cases indications for interventions are similar to those in patients with TAV and degenerative aortic valve disease. In children and young adults with BAV and aortic stenosis, who are still growing, valvuloplasty is the first choice. In adulthood valve replacement is the most common intervention, if there is severe stenosis or insufficiency. According to the ACC/AHA guidelines for the management of adults with congenital heart disease (2008), the indication for surgery to repair the aortic root or replace the ascending aorta is constituted by a diameter of the aortic root or ascending aorta greater than 5.0 cm or a rate of increase in diameter of 0.5 cm per year or more. If patients undergo aortic valve replacement because of aortic stenosis or aortic insufficiency, repair of the aortic root or replacement of the ascending aorta is indicated with a diameter of the aortic root or ascending aorta greater than 4.5 cm (Bonow et al. 2008, pp. e559). It is also being discussed, that the ascending aorta should be replaced at the time of valve surgery even if it is smaller than 4.5 cm, because of the risk of further root dilatation after valve replacement (Siu et al. 2010, p. 2796).

The use of the Ross procedure is disputed, because of the similar wall abnormalities seen in the aorta and pulmonary trunk of BAV patients as well as reported dilatation of the pulmonary graft after the Ross procedure (de Sa et al. 1999, pp. 588–594). Anyhow, the number of Ross operations has been decreasing and it is just relevant as an alternative for children, adolescent and women, who wish to become pregnant (Bonow 2008, p. 112). However, the ideal point of time for surgical intervention in patients with BAV is not well established, because few studies have evaluated the natural progression and predictors of aortic dilatation.

1.9 Tools for Follow-up Examinations

Patients with known bicuspid aortic valve should undergo an initial transthoracic echocardiogram to assess the diameters of the aortic root and the ascending aorta. If the morphology of the aortic root or ascending aorta cannot be assessed accurately by echocardiography, cardiac magnetic resonance (CMR) or cardiac computed tomography (CT) is indicated. If the diameter of the aortic root or ascending aorta is greater than 4 cm, patients should undergo serial evaluations of aortic root/ascending aorta size and morphology by echocardiography, CMR, or CT on a yearly basis. When aortic root dilatation is detected by echocardiography, CMR or cardiac CT should be performed to further quantify severity of dilatation and involvement of the ascending aorta (Bonow et al. 2008, pp. e559). In the future serum markers such as MMPs, parameters for aortic elasticity or abnormal aortic blood flow patterns may play a role as potential predictive tools for clinical risk stratification (Siu et al. 2010, p. 2795).

1.10 Significance of CMR in patients with BAV

During the last 50 years especially 2D echocardiography as well as cardiac catheterization have been the most important tools for assessment of congenital heart disease (CHD). Invasive cardiac catheterization provided valuable information about hemodynamic properties and 2D echocardiography showed the anatomy of cardiac valves and chambers. Doppler echocardiography supplies a noninvasive tool for assessing hemodynamics and disease severity. Today echocardiography is the standard tool for initial assessment and longitudinal evaluation of patients with valvular heart disease, because of its portability, ease of use and excellent temporal-spatial resolution. However, echocardiography may be limited in patients with poor acoustic window and may be more operator dependent than other tools.

CMR has undergone an enormous development in the last 20 years, and it is today an established noninvasive tool in the diagnosis and monitoring of CHD without ionizing radiation. Increased availability and faster MR technology have made CMR more competitive with echocardiography in some aspects of CHD. Beside imaging of cardiac anatomy, it allows quantitative evaluation of cardiovascular function like valve stenosis

and regurgitation(Weber et al. 2006, p. 607; Cawley et al. 2009, p. 468).
In the last ten years 4D flow MR (or time-resolved 3D phase-contrast MR) has proven to be a reliable tool for visualization and assessment of blood flow and provides blood flow imaging with complete spatial and temporal coverage of the region of interest (Markl et al. 2004, p. 459). In patients with BAV, risk factors for dilatation and dissection like aortic diameters can be assessed as well as valve function like stenosis, regurgitation and peak velocities and visualization of blood flow patterns in the great vessels.

1.10.1 Pros and Cons of CMR

CMR not only provides anatomical evaluation in patients with CHD, but often also specific individual morphology and function of known anatomy (Fratz et al. 2008, p. 46). CMR may not be as operator dependent as cardiac echocardiography. In comparison to computed tomography there is no ionizing radiation. However, due to magnetic fields, gradients and radiofrequency pulses used in MR, in certain cases patients with ferromagnetic materials are not allowed to undergo CMR. Neurovascular clips, pacemakers, automatic implantable defibrillators, cochlear implants, metallic foreign bodies in the eye and neurostimulators are contraindications. Because of the loud noises occurring during the assessment, ear protection is prescribed. For patients with claustrophobia MR is also relatively contraindicated. The availability of MR compared to echocardiography is lower because of its size and costs, but it gets more and more available and it is an essential tool for evaluation of CHD (Bandettini et al. 2008, pp. 1485–1495; Cawley et al. 2009, pp. 468–478).

1.10.2 4D flow CMR

Phase-contrast CMR provides the acquisition of multidirectional blood velocity data. 2D multi-slice measurements require several breathhold sequences and are characterized by inconsistent and incomplete spatial volume coverage and breathhold misregistration. Furthermore, high spatial resolution in the slice direction is necessary due to the intrinsically lower signal-to-noise ratio of 2D vs. 3D spatial encoding. Additionally, it is difficult to describe and analyze flow patterns like vortices. Time

resolved 3D phase-contrast CMR (4D flow) affords high spatial resolution and blood flow visualization with complete spatial and temporal coverage of the region of interest. Anatomical and three-directional velocity data are measured in each voxel at several time points of the cardiac cycle according to temporal resolution.

Several visualization tools can be used to compute all velocity data and illustrate them in vector fields, 3D streamlines and particle traces. Streamlines are defined as static velocity field vectors in a single time frame, whereas particle traces represent a path that a massless particle would follow, if it was placed in a time varying vector field. Both are color-coded according to the local velocity magnitude. The measurement of flow data can provide important flow or vessel wall parameters such as pressure difference, peak velocity or wall shear stress (WSS) (Stalder et al. 2008, p. 1218).

4D flow MR is well established for evaluation of multidirectional blood flow velocity data in the great vessels and it allows characterization of abnormal blood flow patterns, which are not well visualized with other techniques. 4D flow CMR has already been used to detect helical and turbulent flow in patients with aneurysm of the ascending aorta and patients with BAV. PC-MR technique has been validated extensively and the accuracy of 4D CMR in comparison with 2D PC flow measurements has been confirmed by a number of studies (Markl et al. 2007, pp. 824–831; Markl et al. 2003, pp. 499–506; Markl et al. 2004, pp. 459–468; Hope et al. 2007, pp. 1471–1479; Hope et al. 2010, pp. 53–61; Weigang et al. 2008, pp. 11–16; Buonocore 1998, pp. 210–226; Frydrychowicz et al. 2008, pp. 400–407; Frydrychowicz et al. 2007b, pp. 463–472).

Aim of the Study

BAV disease is known to be associated with dilatation of the aortic root and the ascending aorta and thus patients with BAV are at significantly higher risk to develop aortic dissection.

Despite recent studies, the cause of aortic dilatation is still under discussion. On the one hand there are theories that support a common developmental defect with genetic backgrounds and a consequential intrinsic weakness of the aortic wall leading to dilatation similar to the Marfan syndrome. The supporters of this theory bring forward the argument that aortic dilatation is out of proportion to coexistent aortic stenosis or aortic insufficiency. On the other hand there is the hypothesis, that abnormal flow patterns due to the morphology of the bicuspid aortic valve result in abnormal wall shear stress in the ascending aorta and friction on the endothelial surface. This may cause modulation of cellular signaling cascades and thus alterations in the elasticity and stiffness of the aortic wall. Furthermore, there were significantly higher peak velocities seen towards the anterolateral wall of the ascending aorta, which correlate with the typical location of asymmetric aortic dilatation seen in patients with BAV. Some investigators showed a variation of dilated segments in the ascending aorta dependent on the type of leaflet fusion and explained that by abnormal flow patterns arising from different aortic valve morphologies (Schaefer et al. 2007, pp. 686–690; Guntheroth 2008, pp. 107–110; Bonow 2008, pp. 111–114; Nataatmadja et al. 2003, pp. II329-334; Hope et al. 2010, pp. 53–61; Hahn et al. 1992, pp. 283–288; Nistri et al. 1999, pp. 19–22).

Today it is possible to visualize 3-dimensional flow patterns without any contrast agents with so-called 4D flow CMR or time-resolved 3D phase-contrast MR. This technique is well established and validated for evaluation of multidirectional blood flow and velocity data (Weigang et al. 2008, pp. 11–16; Frydrychowicz et al. 2007b, pp. 463–472; Markl et al. 2003, pp. 499–506).

The ACC/AHA guidelines recommend an initial assessment of the diameter of the ascending aorta by echocardiography, CMR or CT and serial evaluation, if the diameter is > 4cm. However, calculable predictors of aortic dilatation as follow-up tools have not

been entirely investigated and validated so far. Additionally, flow patterns in the ascending aorta of patients with BAV without aortic stenosis, aortic insufficiency and dilatation and no CoA or any other cardiovascular diagnosis or previous cardiovascular surgery have not been investigated till now. Thus, a comparison of flow patterns by 4D flow MR in a matched-pair study population of patients with BAV and (sex and age matched) controls with TAV may point out relevant distinctions in blood flow patterns.

2 Methods

2.1 Study Population

From November 2008 to June 2009 a total of 18 patients (8 female and 10 male) with congenital BAV and 18 healthy control subjects were recruited and successfully underwent flow-sensitive 4D magnetic resonance imaging (MRI) of the ascending aorta. In this prospective matched-pair study the flow patterns in the ascending aorta, obtained from 4D flow MR of 18 patients with congenital BAV, were compared to those of 18 sex and age matched healthy control persons with a TAV.

Initially, 989 patients with the diagnosis BAV were identified in the database of the German Heart Centre Munich. Patient identification was performed using the in-house used program 'Filemaker Pro' and the search term „bikuspid“ (723 hits) and „bicuspid“ (266 hits). The data of each patient were adjusted with the data stored at the clinical workstation 'Ambulanz – Stationsarbeitsplatz' to detect patients with additional diagnoses.

Slight secondary cardiac diagnoses like mild aortic stenosis (< 2.5 m/s, Δ p < 25 mmHg), mild aortic regurgitation (≤ I°), PFO, aortic ectasia < 45mm and MVP were tolerated. Additionally, the including criteria contained a minimum age of eight years, a congenital bicuspid aortic valve and no previous surgery at the aortic valve and the further aortic segments.

Patient exclusion criteria were: all contraindications for MRI e.g. severe claustrophobia, aortic valve velocity > 2.5 m/s, aortic insufficiency > AI I°, connective tissue disease e.g. Marfan syndrome, velocity at the aortic isthmus > 2.5 m/s, right-to-left-shunt or left-to-right-shunt, moderate or severe valve insufficiency, pulmonary arterial hypertension, heart failure with need of treatment, suspicion of myocarditis or cardiomyopathy, heart rhythm disorders, established genetic disorders of ion channels, Fontan hemodynamics, S/P atrial reversial, oral anticoagulation, other clinical diseases (e.g. Trisomie 21, Turner-Syndrom), cardiovascular medication, a diameter of the ascending aorta ≥45mm, CoA, kinking of the aorta, arterial hypertension or any kind of previous cardiovascular surgery.

Out of 989 subjects 353 met inclusion criteria. Considering all their additional diagnoses, 624 patients with congenital bicuspid aortic valve were excluded from the study. It turned out that another 12 subjects obtained from the database actually had a TAV according to their files. There were no contact details available of 255 subjects, although addresses were requested from the registration office. Finally, 76 persons were contacted by phone, those with missing phone number (n=22) by letter containing a form for informed consent, information about the study and an education form about the CMR (see appendix).

During the telephone call the aim of the study was introduced, the interest of participation in the study was inquired and contraindications were requested. Seven patients were excluded because of exclusion criteria like cardiovascular medications, hypertension, Down syndrome amongst others. Four other contacted persons stated to have a TAV. Other 15 patients declined the participation in the study due to a far distance or lack of time (see Figure 1).

A total of 25 (14 male and 11 female) patients were included, four additional patients (three male and one female) underwent clinical CMR as part of routine examinations due to their bicuspid aortic valve. The cine retro images of the aortic valve of two female patients showed a valve consisting of three leaflets (tricuspid) and thus were attached to the control group. The CMR data of nine subjects (7 male and 2 female) could not be utilized for the analyzes for reasons like high peak velocity (>2,5 m/s) (n=3), technical failure in CMR imaging (n=2, one male and one female), error in 4D flow post-processing (n=1), marked arterial hypertension (n=1, male), too large diameter of the ascending aorta with 54.3mm (n=1) and funnel chest (n=1).

Thus, the flow data of the 18 patients remained were further processable.

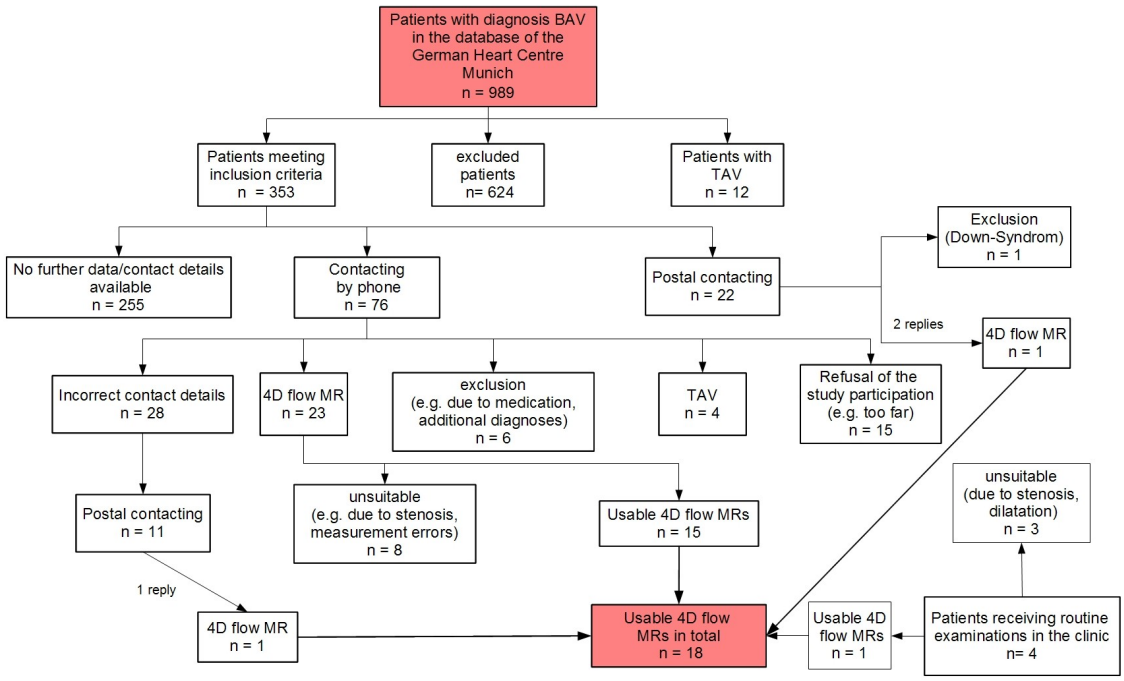

Figure 1: Flow of patients recruitment and selection

The control group was selected from the working environment and the circle of acquaintances. Criteria for selection included the presence of a congenitally normal tricuspid aortic valve and the absence of all exclusion criteria defined for the BAV group. These control persons were selected on the basis of sex and age, such that each control person was matched with a patient in the BAV group. The presence of a morphologically tricuspid or bicuspid aortic valve was confirmed by evaluation of cine retro images of the aortic valve before starting the 4D flow MR imaging.

The study protocol was approved by the institutional review board and the ethics committee of the Technical University Munich and written informed consent was obtained from all participants prior to the investigations.

The median (range) age of the BAV group was 25 years (10-44) and 25 (8-42) of the TAV group, the mean ±SD 26 years ±8.4 and 26 years ±8.0 respectively. The median of the height was 176.5 cm (138-192) in the BAV group and 174 (130-188) in the TAV group. The mean ±SD of the height was 174.7 ±12.1 for the BAV group and 173.7 ±13.8 for the TAV group. In the BAV group the median for the weight was 67.5 kg

(30.0-94.0) and the mean ±SD was 68.9 kg ±14.9 and accordingly 67.5 kg (29.0-95.0) and 68.1 kg ±16.4 in the control group. The values for the body surface area were 1.8 m^2 (1.1-2.2) for the BAV group and 1.8 m^2 (1.0- 2.2) for the TAV group.

The formula used for calculating the BSA was the Mosteller formula (Mosteller 1987, p. 1098): BSA (m^2) = $\sqrt{}$ ((weight (kg) x height (cm))/ 3600)

Detailed data are shown in Table 1 and Table 2. There were 44% (8/18) female subjects in both groups and 56% (10/18) male. There was no case with PFO or MVP in both groups.

patient #	sex	age [yrs]	type of BAV	height [cm]	weight [kg]	BSA [m^2]
1	f	26	2	180	62	1.8
2	m	24	1	192	70	1.9
3	m	44	1	183	94	2.2
4	m	32	1	182	88	2.1
5	f	27	1	162	65	1.7
6	m	20	2	170	76	1.9
7	m	29	1	178	65	1.8
8	m	44	1	183	72	1.9
9	f	10	2	138	30	1.1
10	f	32	1	165	65	1.7
11	f	20	1	169	65	1.7
12	m	22	1	187	70	1.9
13	f	20	2	173	80	2.0
14	m	27	1	175	86	2.0
15	m	28	1	185	83	2.1
16	m	18	1	180	58	1.7
17	f	24	1	173	55	1.6
18	f	24	2	170	56	1.6
mean		26.17		174.72	68.89	1.82
median		25		177	68	1.84
SD		8.37		12.13	14.9	0.25
range		10-44		138-192	30-94	1.1-2.2

Table 1: Description of the study population - BAV group

patient #	sex	age [yrs]	height [cm]	weight [kg]	BSA [m²]	age diff. [d]
1	f	25	173	59	1.7	117
2	m	25	174	65	1.8	425
3	m	42	188	95	2.2	530
4	m	34	180	92	2.1	990
5	f	28	166	64	1.7	484
6	m	20	183	77	2.0	49
7	m	30	187	76	2.0	306
8	m	40	188	80	2.0	1350
9	f	8	130	29	1.0	624
10	f	33	165	53	1.6	438
11	f	20	159	49	1.5	216
12	m	21	173	85	2.0	411
13	f	21	174	70	1.8	313
14	m	27	179	80	2.0	6
15	m	28	180	75	1.9	6
16	m	20	187	65	1.8	583
17	f	24	170	58	1.7	197
18	f	24	170	54	1.6	19
mean		26.11	173.67	68.11	1.8	392.44
median		25	174	67.5	1.84	362
SD		7.98	13.82	16.45	0.29	352.28
range		8-42	130-188	29-95	1.0-2.2	6-1350

Table 2: Description of the study population - TAV group

Studienpopulation			
group	**BAV**	**TAV**	**p-value**
number	18	18	-
age	26,2 +/- 8,4	26,1 +/- 8,0	n.s.
sex	4:5	4:5	n.s.
weight	68,9 +/- 14,9	68,1 +/- 16,4	n.s.
height	174,7 +/- 12,1	173,7 +/- 13,8	n.s.

Table 3: overview of the study population
values for age, weight and height are expressed as the mean ±SD
f: female, m: male, n.s.: not significant

2.2 Flow Data Acquisition

2.2.1 Cine and Velocity encoded Phase Contrast CMR

All participants have given informed consent and underwent flow-sensitive four-dimensional magnetic resonance, after exclusion of all contraindications for magnetic resonance and education by the physician performing the CMR. During the examination a blood pressure meter on the right upper arm, a pulse oximeter and ECG electrodes, in order to detect the heart rate during the investigation, were applied. None of the patients and healthy controls received contrast agents.

A standard cardiac 1.5 Tesla MRI-scanner (MAGNETOM Avanto®, version software VB15, Siemens Healthcare, Erlangen, Germany) and a standard cardiac 12-channel coil were used for all patients. A flow-sensitive 4D (time-resolved 3D) sequence protocol was used for flow data acquisition and measurements were taken in synchrony with the cardiac cycle and under respiratory navigation.

The localizers were planned in three orthogonal planes (sagittal, tansversal, coronal) for planning further measurements. Before starting the flow measurements, an axial cine view of the aortic valve was taken for validation of leaflet morphology (bicuspid or tricuspid), as well as a LVOT cine view and in perpendicular axis a second LVOT cine view. Thereafter measurements of three axial cine views of the aorta followed. The measurements occurred at the level of the sinuses of Valsalva, in the ascending aorta at the level of the right pulmonary artery and in the descending aorta at the level of the left pulmonary artery.

This common technique was performed as previously described (Weber et al. 2006, pp. 607–608; Cawley et al. 2009, p. 468; Rebergen et al. 1996, p. 468).

In addition blood flow measurements (PC-CMR) in the ascending aorta were performed. For this purpose a conventional phase sensitive gradient echo sequence was used in a double-oblique plane perpendicular to the dominant flow direction in the proximal ascending aorta: at the level of the sino-tubular junction after the origin of the coronary arteries and the proximal pulmonary artery about 1 cm distal the semilunar valves. Image data were collected in free-breathing.

This common technique was performed as previously described (Cawley et al. 2009, pp. 469–470; Fratz et al. 2002, p. 1511; Rebergen et al. 1993, pp. 1439–1442; Rebergen et al. 2000, p. 369; Rebergen et al. 1996, pp. 468–469; Weber et al. 2006, pp. 609–610).
The following acquisition parameters were used for PC-CMR: retrospective ECG gating, TR/TE 36.7/3.09 ms; slice thickness 6 mm; flip angle 30 degrees; rectangular field of view 320 to 500 mm; matrix 256 x 256 and number of excitations 2. At the beginning of each study, velocity encoding (VENC) was set according to the expected blood flow. Usually it was 2.0 m/s for the aorta. After the first flow maps were acquired, they were checked for aliasing. If aliasing was detected, the scan was repeated using a higher VENC (Weber et al. 2006, pp. 611–612). Data were reconstructed providing 30 magnitude (anatomic) and phase (velocity-mapped) images per cardiac cycle. Flow image data were collected in free-breathing.

2.2.2 4D Flow Measurement

After these measurements four-dimensional flow data of the thoracic aorta were acquired. The pulse sequence for 3D cine PC MRI data acquisition consists of a rf-spoiled gradient-echo sequence with velocity encoding along all 3 spatial directions. Retrospective ECG gating was used to synchronize the measurements with the cardiac cycle (Markl et al. 2007, pp. 824–831; Weber et al. 2006, pp. 607–608). Respiration control was achieved by navigator gating to minimize artifacts such as image ghosting or image blurring due to respiration (Markl et al. 2007, pp. 824–831).
Data were acquired in a sagittal-oblique volume that included the entire LVOT as well as the ascending aorta and the aortic arch with the proximal parts of the supra-aortic branches. Each volume was carefully planned and adapted to the individual anatomy. A set of localizer images was used to set the obliquity and to ensure complete coverage of the ROI.
The further imaging parameters were as follows:
volume coverage: 3D, 144x192x116 (image rows: 144, image columns: 192, number PE: 116), PE direction: ROW, FOV row: 240, FOV column: 320, spatial resolution: 2.1 x 1.7 x 2.5 mm^3, TR:39.2 ms, TE: 2.42 ms, time Frames: 16-24, flip angle: 8°-10°, band width: 455 Hz/pixel

The scans were performed with identical velocity sensitivity (venc x=venc y=venc z= 200 cm/s). A venc of 230 cm/s was used once.

All in all total scan time was in the range of 30 to 40 minutes, the 4D flow measurement on its own took about 15 to 25 minutes depending on heart rate and regularity and navigator efficiency.

The time-resolved, 3-dimensional phase-contrast magnetic resonance images were generated as previously described (Markl et al. 2007, pp. 824–831, Frydrychowicz et al. 2007a, pp. 9–15; Markl et al. 2003, pp. 499–506; Markl et al. 2004, pp. 459–468; Weigang et al. 2008, pp. 11–16; Wigström et al. 1996, pp. 800–803).

2.3 Data Processing and 3D Blood-Flow Visualization

2.3.1 Diameter and Blood Flow Measurements

The obtained cine views and the data of the PC-CMR of the ascending aorta were used to get more information of anatomy and function of the aorta. Data were processed by using the standard analysis software (Argus®, Siemens Healthcare, Erlangen, Germany).

The minimum and maximum diameters of the aortic bulbus, the ascending and the descending aorta were acquired by manually tracing a ROI (region of interest) along the margin of the vessel of interest in the magnitude image corresponding to the velocity map with subsequent projection on it. The ROI is adjusted for movements and changes in diameter of the vessel during the cardiac cycle (Rebergen et al. 1993, p. 1442). Aortic diameters were corrected for BSA by dividing diameters by (the square root of the) BSA (den Reijer et al. 2010, p. 3; Roman et al. 1989, pp. 507–512). A corrected diameter $\geq$2.2 cm/m^2 was defined as dilated (Hope et al. 2010, p. 56).

ROIs were traced in every phase of the cine series and minimal and maximal diameters in all three levels of the aorta were registered in order to gather data of anatomic conditions of patients with BAV and healthy control persons.

The blood flow parameters for the aorta were calculated from the velocity maps. Therefore, the observer traced the contour of the vessel wall (ROI) in all phases, as described above. The average and the peak phase values within each ROI were converted to average and peak velocity values that could be plotted against time. Instant volume flow was calculated from the product of average flow velocity and ROI area. In this way approximated peak velocity in the aorta and potential (exclusion criteria like) insufficiency or stenosis could be assessed. The analysis of the blood flow measurements and the vessel diameters was made once as it was previously described. (Rebergen et al. 1993, p. 1442)

2.3.2 Calculation of the Stiffness Index (SI)

The stiffness index of the ascending aorta and the descending aorta was calculated in all BAV and TAV subjects as previously described using the formula $SI = ((\ln(P_{sys}/P_{dia}))/(\Delta D/D_{dia}))$, where P_{sys} is the systolic blood pressure, P_{dia} the diastolic blood pressure and ΔD the difference between systolic and diastolic diameter (Baumgartner et al. 2005, p. 732; Schaefer et al. 2007, p. 687; Kawasaki et al. 1987, pp. 678–687; Savolainen et al. 1992, p. 691). Data were obtained from the diameter measurements in the cine views (2.3.1Diameter and Blood Flow Measurements), where the minimal diameter was used for D_{dia} and the maximal for D_{sys}. Blood pressure was measured before each performance of cine MR images (2.2 Flow Data Acquisition)

2.3.3 Evaluation of the Aortic Valve

The cine retro views of the aortic valve of all patients and control persons were evaluated by three physicians from the Department of Pediatric Cardiology and Congenital Heart Disease at the German Heart Center Munich, who are experienced in CMR in patients with congenital heart disease. After classification in the groups of TAV and BAV, all objects with BAV were subclassified in BAV type 1, type 2 or type 3. Type 1 is defined as valve with congenital fusion of the right and left coronary cusp (also called anterior-posterior BAV) and type 2, when there was congenital fusion of the right and non-coronary cusp (also called right-left BAV) (Schaefer et al. 2008, pp. 1635–1636). The congenital fusion of the non-coronary and left coronary cusp is defined as type 3 (see Figure 2) (Schaefer et al. 2008, pp. 1635–1636). Additionally, the position of the longitudinal axis of the orifice related to the RVOT was used as criteria for the classification. If the longitudinal axis of the orifice was parallel to the RVOT, the valve was classified as type 1. If it was perpendicular to it as type 2. This is illustrated in Figure 3 and Figure 4. The evaluation of the aortic valve was made once by each of the three evaluators.

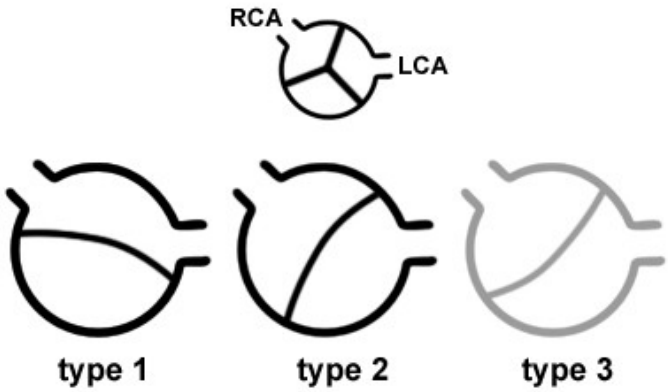

Figure 2: Type 1 is defined as congenital fusion of the right and left coronary cusp, type 2 as congenital fusion of the right and non-coronary cusp and type 3 as congenital fusion of the non-coronary and left coronary cusp. RCA= right coronary artery, LCA= left coronary artery

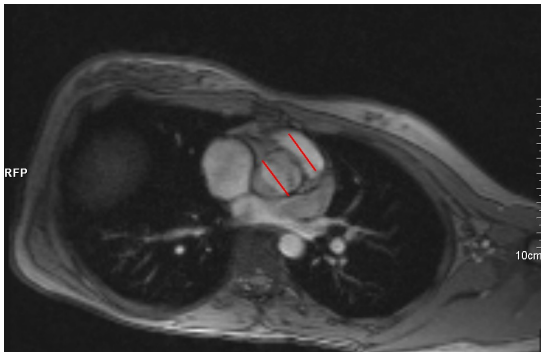

Figure 3: BAV type 1 with the longitudinal axis of the orifice parallel to the RVOT.

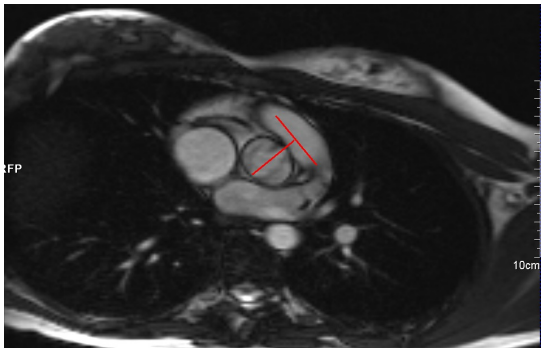

Figure 4: BAV type 2 with the longitudinal axis of the orifice perpendicular to the RVOT.

2.3.4 Preprocessing of the Velocity Data Sets

The obtained time series of velocity data sets were transferred to a standard personal computer. In the software program „copy tool“ (provided by the Institute for cardiovascular MRI Freiburg) data were converted to be compatible for further processing in the software tool Velomap (provided by the Institute for cardiovascular

MRI Freiburg, tool for import, visualization, preprocessing & converting of velocity mapping data, © Jelena Bock, University Hospital Freiburg), where they underwent semi-automated noise filtering and eddy current correction as previously reported by Walker et al., which required approximately 20 minutes (Walker et al. pp. 521–530).
A certain slice and phase in the magnitude data was chosen, where the vessel of interest, the aorta, from its valve and the ascending aorta to the arch, was well described. It differs from subject to subject, in which phase the vessel is described best. The most suitable axial slice depends on the anatomy of each individual.
The correction of standard deviation filtering, eddy current correction, anti-aliasing and delete of static tissue were already set and identical in each case. An additional time-independent PC-CMR data set was rendered as the squared sum of the individual 3D PC-CMR images, to enhance vascular regions with high flow and suppress background signals (Markl et al. 2007, p. 827). The settings for noise filtering were defined by the user. By modifying the value, the user could examine the preview of the processed velocity data and thus choose the setting with as few disturbances as possible, but good morphology of the ascending aorta at the same time. After that preparation, data underwent automatical filtering and correction procedures and data format conversion in an ensight compatible case file. All functions settings were saved in a Microsoft excel file.

2.3.5 Blood Flow Visualization

The thus obtained case file was loaded into a software package (Ensight ®; CEI, Apex, NC, USA), that offers a variety of image-processing options. The visualization included 3D streamlines and time-resolved 3D particle traces (Buonocore 1998, pp. 210–226; Wigström et al. 1999, pp. 793–799). In addition, to generate a semitransparent 3D isosurface representation of the vascular anatomy, thresholding of the PC-CMR data was used (Markl et al. 2007, p. 827). For the visualization of flow patterns the user had to modify the velocity isosurface, so that the LVOT tract was well described, by eliminating as much noise and disturbances as possible without loosing to much information of the velocity data.
The streamlines and particle traces were calculated from a limited area called „total

volume". To see the vessel of interest and to eliminate practically all noise, this area had to be minimized to the optimal size. By using a programmed instruction tool (Ensight Controller, provided by the Institute for cardiovascular MRI Freiburg), streamlines and particle traces were automatically calculated in the "total volume" that was set before. Settings used for the calculation were standardized and the same for all data sets. Calculation time was on the order of 5 to 10 minutes.

For evaluation of flow patterns, the display options of the visualized flow data were set identically in all cases. The parameters used for the visualization were: streamlines were not visible, all particle traces were animated and had the same line width (2) and the values for color encoding of the velocity were adapted (minimum: 0, maximum: 1). The visualization was saved as context file, full backup and scenario, so that the calculated data set could be restored and edited. The scenario was saved as EnLiten (.els) file and could be opened by a software program for viewing, analyzing and manipulating complex visualization scenarios (EnLiten; CEI, Apex, NC, USA). In this way the animated particle traces of the aortic outflow tract in one cardiac cycle could be viewed. Data processing was performed as previously described. (Markl et al. 2003, pp. 499–506; Markl et al. 2007, pp. 824–831; Markl et al. 2004, pp. 459–468; Frydrychowicz et al. 2007a, pp. 9–15; Frydrychowicz et al. 2008, pp. 400–407; Frydrychowicz et al. 2007b, pp. 463–472; Frydrychowicz et al. 2006, pp. 340–342; Bogren et al. 1999, pp. 861–869; Buonocore 1998, pp. 210–226; Wigström et al. 1996, pp. 800–803; Nordmeyer et al. 2010, pp. 677–683; Stalder et al. 2008, pp. 1218–1231)

2.3.6 Analysis of Blood Flow Patterns

For the blinded analysis of blood flow patterns, all scenario files were anonymized and saved with randomly generated numbers. Two independent physicians of the Department of Pediatric Cardiology and Congenital Heart Disease and the Department of Cardiovascular Surgery and one MR experienced physician of Pediatric Cardiology and Congenital Heart Disease viewed independently all 36 flow scenarios and classified each of them in a scale from 0 to 3 according to flow patterns and vortices. The classification for the flow patterns was determined before by three investigators, experienced in cardiology and MRI. 0 was defined as linear flow in the ascending aorta,

1 as less than one vortex (curvature <180°), 2 as more than one vortices (180-360°) and 3 as more than two vortices (>360°). Additionally, the graduation was referred to the diagram shown in Figure 5.

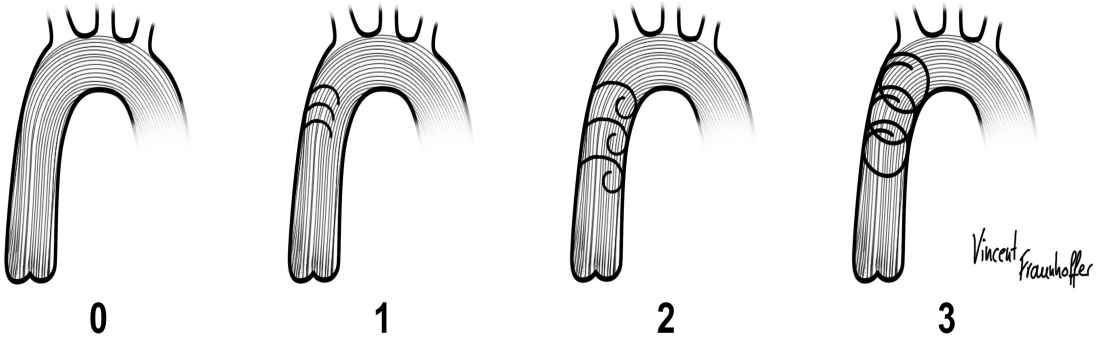

Figure 5: Classification of flow patterns from 0 to 3

2.3.7 Statistical Analysis

Data analysis was performed using the statistical software program Stat View (SAS institute, Cary, version 5.0.1) and the spreadsheet application Microsoft Office Excel version 2010. Data were presented as mean, standard deviation of the mean (±SD) and median and range (minimum to maximum).

A Wilcoxon signed rank test was used to evaluate the statistical significance of differences in flow patterns, maximal diameters of the aorta, blood pressure and stiffness index comparing patients with BAV and TAV. A Kruskal-Wallis test was used to obtain the difference in SI and aortic dimensions between BAV I and BAV II. To evaluate significant differences of flow patterns between these two groups an unpaired Mann-Whitney-U test was used.

For the calculation of the statistical significance of blood flow classification, mean values were calculated out of the graduations done by the three observers for each study subject. So 18 mean values were received in both groups and were used for the statistical analysis by a Wilcoxon signed rank test.

To determine the grade of possible dilatation in the study group, the deviation of diameters from normal aortic dimensions were calculated. A diameter that deviated more than two times of the SD was defined as dilated revealing a threshold of 3.91 cm

or 2.2cm/m^2, when the diameter is indexed for BSA (Hager et al. 2002, pp. 1060–1066; Hope et al. 2010, p. 56).

In all statistical calculations a difference was considered to be significant with a p-value ≤0.05. Diagrams were created by using the software Microsoft Office Excel and StatView.

3 Results

3.1 Data of Anatomy and Function

3.1.1 Evaluation of the Bicuspid Aortic Valve Patterns

13 of the 18 patients (72%) with bicuspid aortic valve were identified as BAV type 1 with fusion of the right and left coronary cusp, the remaining five (28%) as BAV type 2 with fusion of the right and non-coronary cusp. There was no case with fusion of the left and non-coronary cusp (type 3). Evaluation of the BAV type is described in chapter

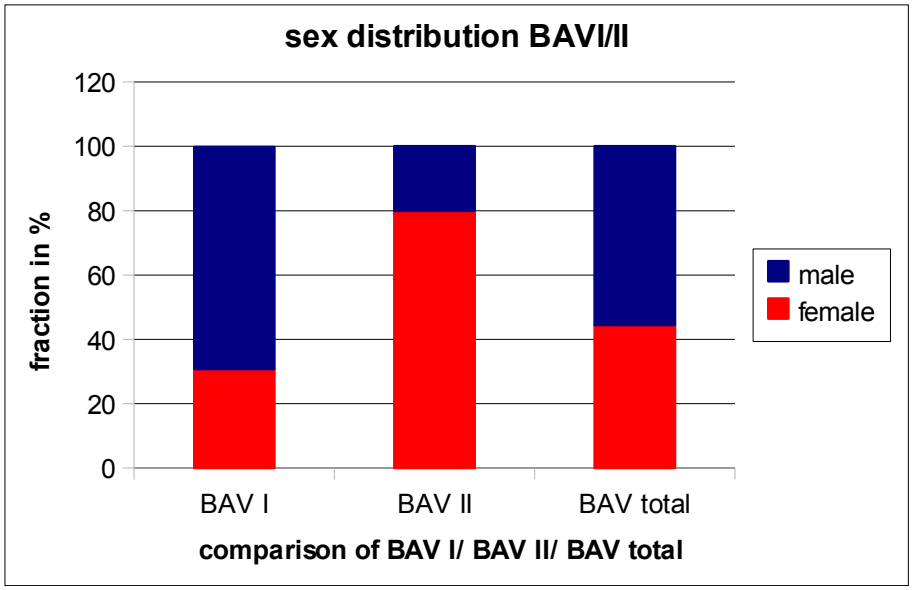

Figure 6: Ratio of women and men in different phenotypes of BAV

2.3.3 Evaluation of the Aortic Valve. There were 31 % (4/13) women of the BAV type 1 and 69% (9/13) men. The women´s fraction of the type 2 group was 80% (4/5) and the men´s 20% (1/5) (see Figure 6).The ratio BAV type 1 to BAV type 2 in the female fraction was 1:1. In the male it was 9:1(see Figure 7). Male gender predominated among BAV type 1 subjects and BAV type 2 subjects were notably more often female like it was described before by Schaefer (Schaefer et al. 2008, p. 1636).

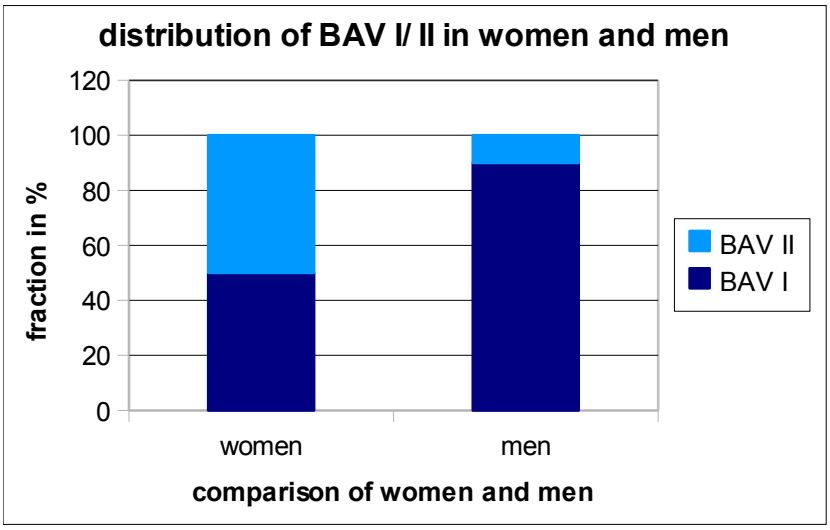

Figure 7: Distribution of BAV type 1 and 2 in women and men

3.1.2 Diameter and Function of the Aorta

Comparison of BAV and TAV Patients

The mean ±SD for P_{sys} was 110.9 ±9.6 mmHg for BAV and 107.1 ±7.7 mmHg for TAV and P_{dia} was 65.7 ±11.6 mmHg and 59.7 ±11.2 mmHg respectively. The peak velocity over the aortic valve was 150.6 ±30.65 cm/s in the BAV group and 113.9 ±23.96 cm/s in the TAV group. The performed Wilcoxon signed rank test showed no significant difference between the paired groups for P_{sys} and P_{dia}. BSA was 1.8 ±0.2 m² for BAVs and 1.8 ±0.3 m² in the control group. The mean ±SD of the diameters indexed for BSA in BAV and TAV showed 1.76 cm/m²±0.24 and 1.62 ±0.23 for the aortic bulbus, 1.89 ±0.26 and 1.57 ±0.2 for the ascending aorta and 1.05 ±0.17 and 1.08 ±0.11 for the descending aorta. The corrected diameters showed a significant difference in the ascending aorta. However, regarding the correlation with BSA, there were only two

cases of the BAV group with an ascending aortic diameter indexed for BSA greater than 2.2 cm/m^2 and thus dilated (Hope et al. 2010, pp. 53–61). A summary of all data is illustrated in Table 4. Detailed data are shown in the appendix.

	mean ±SD		
	BAV	**TAV**	**p value**
Age [yrs]	26.2 ±8.4	26.1 ±8.0	n.s.
Height [cm]	175 ±12.1	174 ±13.8	n.s.
Weight [kg]	68.9 ±14.9	68.1 ±16.4	n.s.
BSA [m²]	1.8 ±0.2	1.8 ±0.3	0.5294
P_{sys} [mmHg]	110.9 ±9.6	107.1 ±7.7	0.2209
P_{dia} [mmHg]	65.7 ±11.6	59.7 ±11.2	0.5321
bulbus aortae			
Dmax cor. [cm/m^2]	1.76 ±0.24	1.62 ±0.23	0.1771
SI	5.8 ±3.9	7.9 ±10.5	0.7299
ascending aorta			
Dmax cor. [cm/m^2]	1.89 ±0.26	1.57 ±0.2	0.0033
SI	4.8 ±3.6	3.2 ±1.0	0.0199
descending aorta			
Dmax cor. [cm/m^2]	1.05 ±0.17	1.08 ±0.11	0.4851
SI	5.2 ±4.4	3.8 ±1.3	0.4955

Table 4: Mean values ±SD are indicated. A difference was considered to be significant with a p-value ≤0.05.
n.s.: non significant

Comparison of BAV type 1 and type 2

There was no significant difference in aortic diameters, peak velocity, aortic insufficiency and blood pressure between patients with BAV type 1 and type 2.

	mean ±SD		
	BAV I	**BAV II**	**p value**
P_{sys} [mmHg]	112.6 ±10.9	109.75 ±9	n.s.
P_{dia} [mmHg]	65.7 ±11.6	59.7 ±11.2	n.s.
bulbus aortae			
Dmax cor. [cm/m²]	1.71 ±0.23	1.85 ±0.25	n.s.
SI	5.24 ±2.14	7.57 ±7.46	n.s.
ascending aorta			
Dmax cor. [cm/m²]	1.87 ±0.28	1.39 ±0.25	n.s.
SI	5.21 ±4.07	3.67 ±0.93	n.s.
descending aorta			
Dmax cor. [cm/m²]	1.03 ±0.09	1.11 ±0.29	n.s.
SI	5.49 ±4.99	4.16 ±1.76	n.s.

Table 5: Mean values ±SD are indicated. A difference was considered to be significant with a p-value ≤0.05.
n.s.: non significant

3.2 Stiffness Index

3.2.1 Comparison between BAV and TAV Patients

The analysis of the SI (dimensionless) in the BAV group revealed in a mean ±SD with 4.85 ±3.61 in the ascending aorta, 5.17 ±4.24 in the descending aorta and 5.82 ±3.95 in the aortic bulbus. The values for the TAV group were 3.23 ±1.01 in the ascending aorta, 3.79 ±1.34 in the descending aorta and 7.86 ±10.54 in the aortic bulbus (Figure 8). The Wilcoxon signed rank test showed no significant difference between the two groups for the SI in the descending aorta and the aortic bulbus. SI of the ascending aorta in the matched-pair group was significantly higher in patients with BAV (Figure 8 and Figure 9). Detailed data are shown in Table 6.

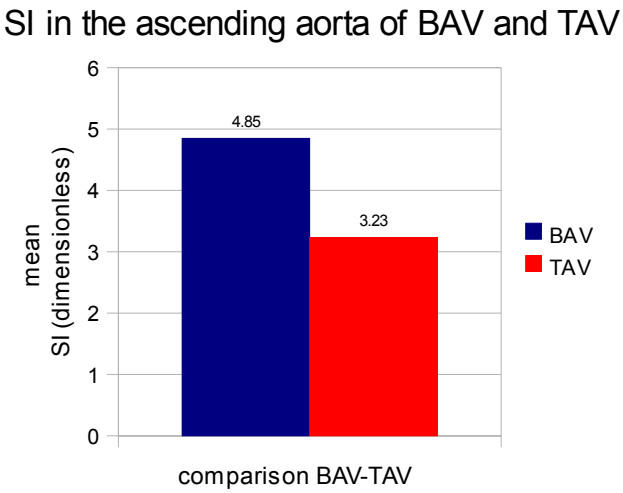

Figure 8: Comparison of the stiffness index in the ascending aorta of patients with BAV and TAV (p=0.0199)

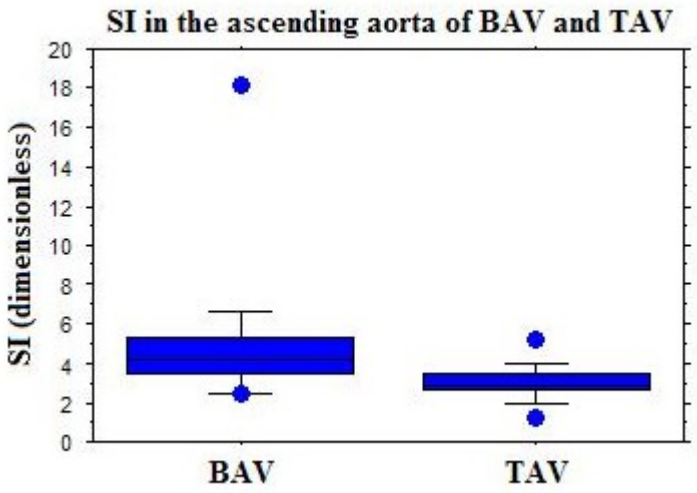

Figure 9: Box plot of the stiffness index in the ascending aorta of BAV and TAV (p=0.0199)

Comparison of Stiffness Index (SI) in the matched pairs						
	ascending aorta		descending aorta		bulbus aortae	
pair #	BAV	TAV	BAV	TAV	BAV	TAV
1	no data	5.15	no data	2.95	no data	3.11
2	3.60	no data	3.57	no data	no data	no data
3	6.64	3.16	6.88	4.27	3.84	9.69
4	2.62	no data	3.71	no data	3.33	no data
5	2.50	5.25	4.86	3.5	4.03	5.78
6	2.48	3.84	2.85	2.08	18.3	4.89
7	3.46	3.99	2.98	4.43	9.92	3.05
8	18.11	3.39	4.81	7.11	4.84	5.54
9	3.47	2.79	3.09	3.9	1.63	5.48
10	4.42	3.30	4.95	2.81	8.12	1.48
11	3.27	1.98	21.66	3.78	6.29	18.56
12	5.54	3.49	3.71	5.53	3.42	4.38
13	4.63	2.86	3.99	4.4	3.55	3.87
14	5.86	2.72	2.91	3.56	2.55	2.72
15	4.25	2.88	4.26	4.95	5.65	42.91
16	3.95	2.90	2.60	2.74	6.06	3.26
17	3.45	2.70	4.43	2.01	4.8	no data
18	4.12	1.30	6.69	2.59	6.78	3.11
mean	4.85	3.23	5.17	3.79	5.82	7.86
SD	3.61	1.01	4.42	1.34	3.95	10.54

Table 6: Comparison of the SI in the ascending and the descending aorta and the bulbus aortae in the matched pairs of BAV and TAV. Values are expressed as stiffness index (dimensionless).

3.2.2 Comparison between BAV type 1 and type 2 Patients

The SI in the BAV groups type 1 and 2 showed following data: the SI was 5.24 ±2.14 and 7.57 ±7.46 in the aortic bulbus, 5.21 ±4.07 and 3.67 ±0.93 in the ascending aorta and 5.49 ±4.99 and 4.16 ±1.76 in the descending aorta respectively. The performed Kruskal-Wallis test showed no significant difference in SI in all levels. Further data are shown in Table 7.

Comparison of Stiffness Index in BAV type 1 and type 2

	bulbus aortae		ascending aorta		descending aorta	
	type 1	Type 2	type 1	Type 2	Type 1	type2
	no data	no data	3.60	no data	3.57	no data
	3.84	18.30	6.64	2.48	6.88	2.85
	3.33	1.63	2.62	3.47	3.71	3.09
	4.03	3.55	2.50	4.63	4.86	3.99
	9.92	6.78	3.46	4.12	2.98	6.69
	4.84		18.11		4.81	
	8.12		4.42		4.95	
	6.29		3.27		21.66	
	3.42		5.54		3.71	
	2.55		5.86		2.91	
	5.65		4.25		4.26	
	6.06		3.95		2.60	
	4.80		3.45		4.43	
mean	5.24	7.57	5.21	3.67	5.49	4.16
SD	2.14	7.46	4.07	0.93	4.99	1.76

Table 7: Comparison of the SI in the bulbus aortae, the ascending and the descending aorta in the BAV groups type 1 and 2. Values are expressed as stiffness index (dimensionless).

3.3 Evaluation of Blood Flow Patterns

3.3.1 Still Frames of Flow Videos

Beneath the still frames of the obtained flow scenarios are exemplarily illustrated for three matched pairs. The mean grades of all three evaluators are indicated for each flow scenario. Exemplary still frames are shown in Figure 10 to Figure 12. Flow images of all matched pairs are demonstrated in the appendix.

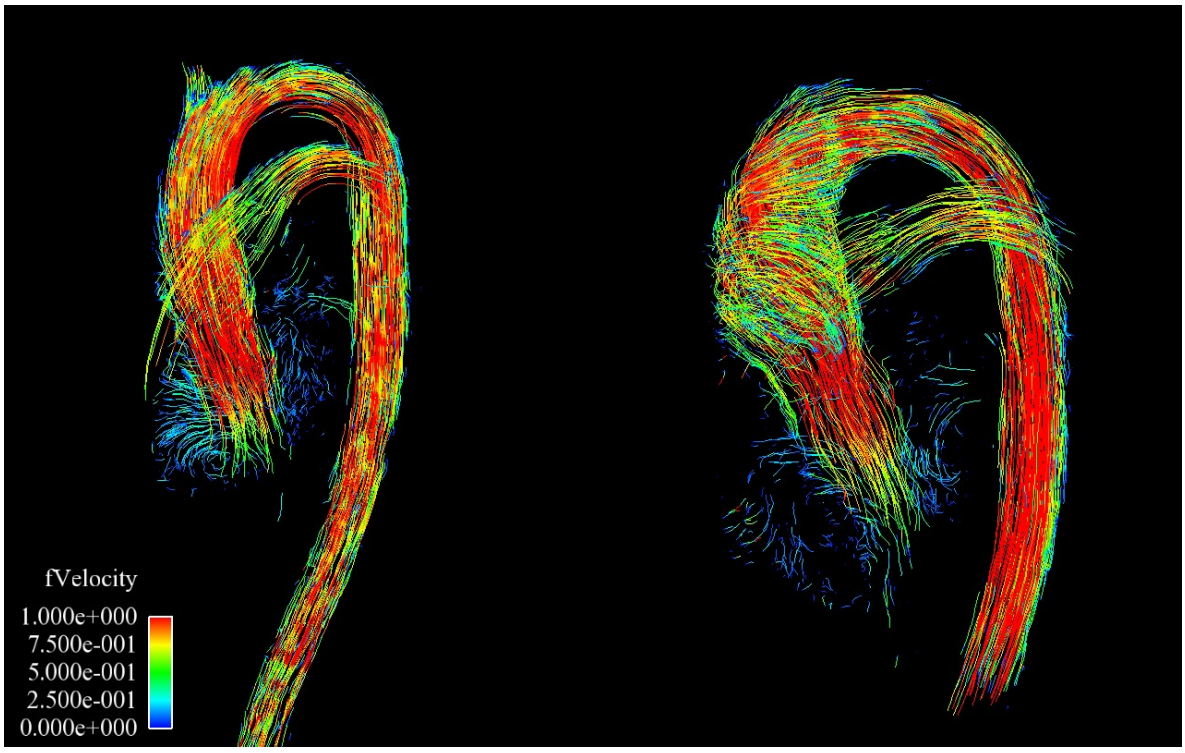

Figure 10: This image shows the particle traces of pair# 17 with the control person on the left and the patient with BAV on the right (fusion of the right and non-coronary leaflet). The mean value of flow graduation given by the three observers was 0 for the control person and 2.67 for the BAV patient.

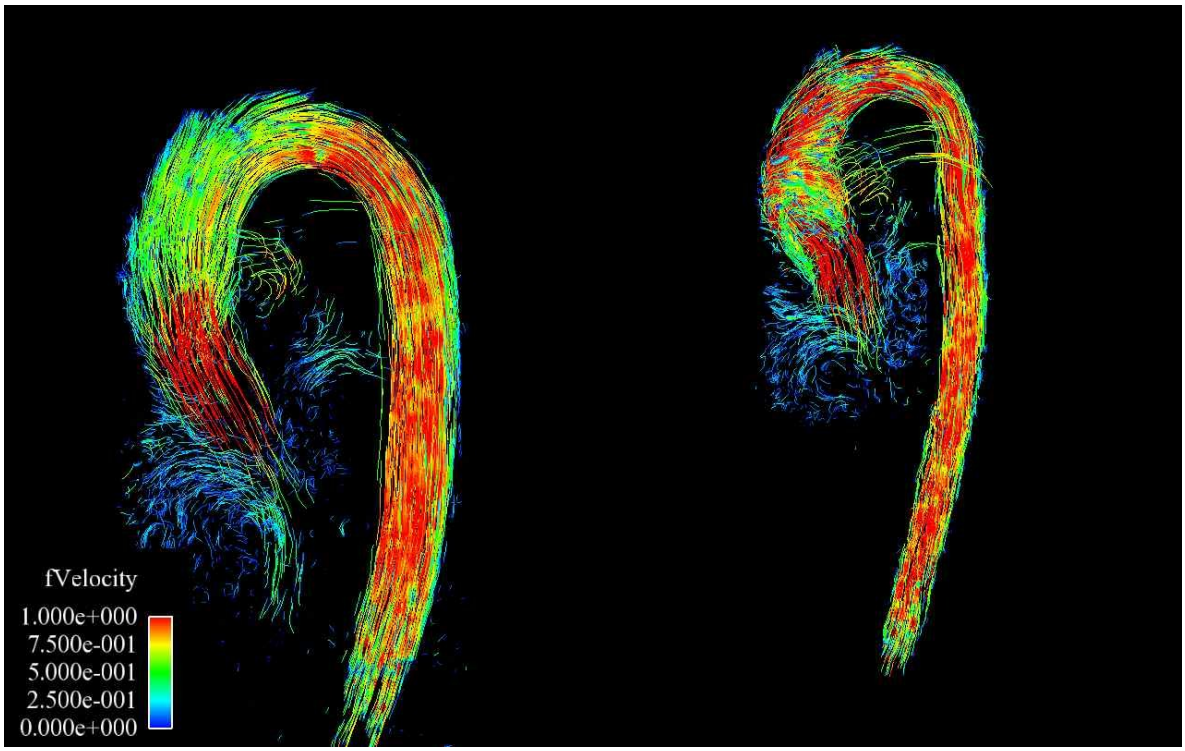

Figure 11: This image shows the particle traces of pair# 10 with the control person on the left and the patient with BAV on the right (fusion of the right and left coronary leaflet). The mean value of flow graduation given by the three observers was 0.5 for the control person and 3.0 for the BAV patient.

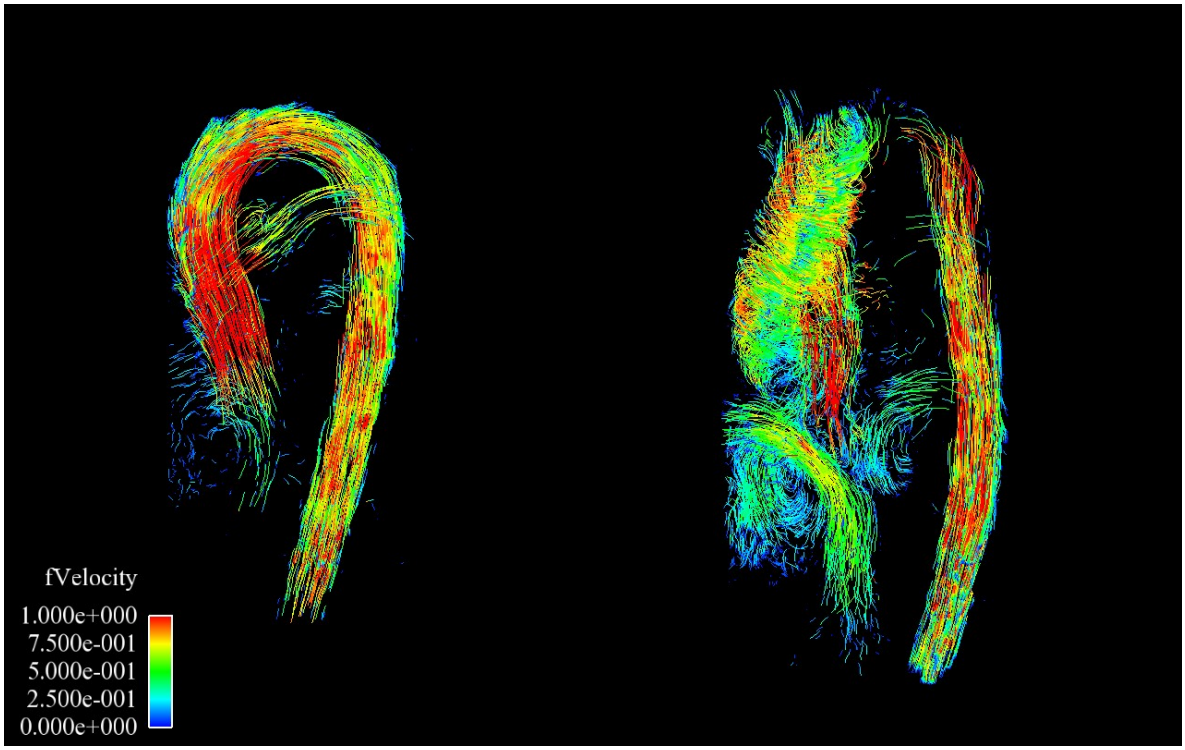

Figure 12: This image shows the particle traces of pair# 18 with the control person on the left and the patient with BAV on the right (fusion of the right and non-coronary leaflet). The mean value of flow graduation given by the three observers was 0 for the control person and 3.0 for the BAV patient.

3.3.2 Flow Classification

BAV and TAV group

The analysis of the flow patterns in patients with BAV and patients with TAV showed a significant association between vortical flow and the presence of BAV. The classification into the grades 0 to 3 according to the degree of abnormal vortical flow patterns was shown to be significantly different in the matched pairs ($p = 0.0004$) (Figure 13).

Assuming that the grades 0 and 1 are associated with tricuspid aortic valves and 2 and 3 with bicuspid valves, flow scenarios could be referred correctly to the proper leaflet morphology in 90% (SD 0.02). In the BAV group 85% (SD 0.06) of the flow scenarios were classified as grade 2 or 3. In the TAV group 94% (SD 0.06) of the flow videos

were graded as 0 or 1 and consequently only 6% as 2 or 3. These findings are illustrated in Figure 14.

In all evaluations (n = 54) of the patients with BAV (n = 18), which where performed by three observers, grade 0 was given 5 times, 1 three times, 2 eight times and 3 38 times. In the TAV group there were 28 evaluations with the grade 0, 23 with grade 1 and 3 with grade 2. None of the flow videos of the TAV group was classified as grade 3. The median (range) value given in the BAV group was 2.67 (0.33-3) and 0.58 (0-1.33) in the TAV group, the mean ±SD was 2.46 ±0.86 for the BAV group and 0.55 ±0.44 for the TAV group. The distribution of the given evaluation is shown in Figure 15.

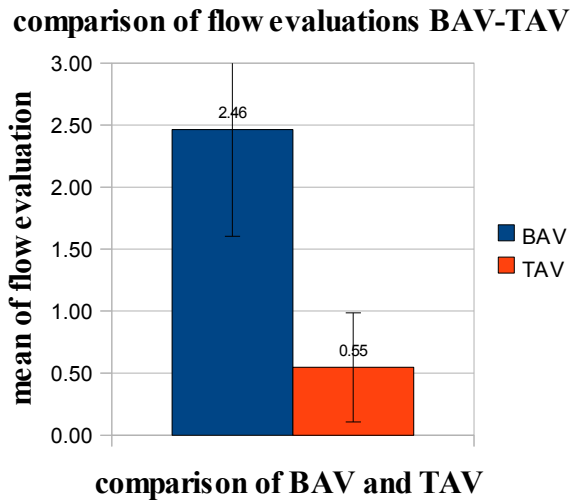

Figure 13: The mean ±SD of the flow evaluations according to the scale in Figure 5 for BAV and TAV is illustrated (p=0.0004).

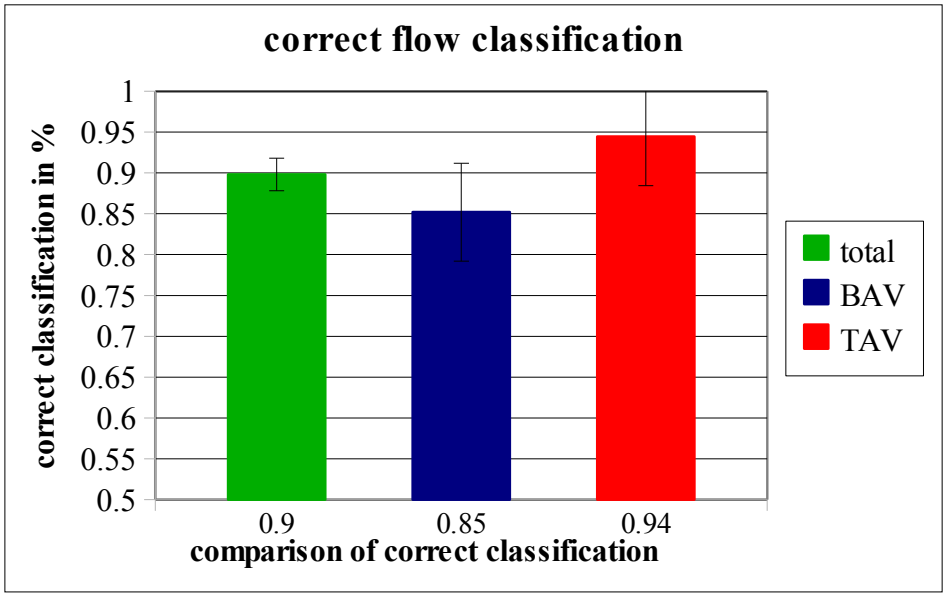

Figure 14: Assuming that the grades 0 and 1 are associated with TAV and 2 and 3 with BAV, flow scenarios could be referred correctly to the proper leaflet morphology in 90% (SD 0.02). In the BAV group 85% of the flow scenarios were classified as grade 2 or 3 (SD 0.06). In the TAV group 94% of the flow videos were graded as 0 or 1 (SD 0.06).

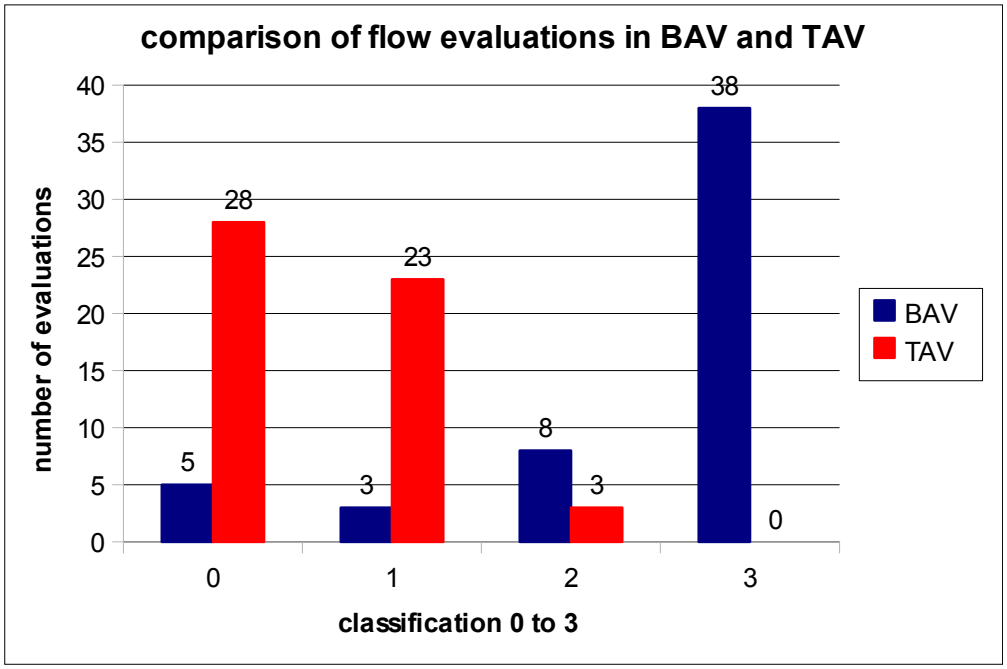

Figure 15: The number of evaluations is illustrated for each grade from 0 to 3 in the BAV and the TAV group.

BAV type 1 and 2

Comparing the patients with BAV type 1 (n = 13) and type 2 (n = 5), it was remarkable, that none of the patients with BAV type 2 was classified as grade 0 or 1 by the three observers, but grade 2 occurred two times and grade 3 13 times. In contrast grade 0 occurred five times, grade 1 three times, grade 2 six times and grade 3 25 times in the group of type 1 leaflet morphology. So all patients with BAV type 2 were classified correctly as bicuspid valve. The mean ±SD of flow graduation was 2.31 ±0.97 in the BAV group type 1 and 2.87 ±0.18 in the BAV group type 2. These results are demonstrated in Figure 16. The direction of helical flow was right-handed and towards the right anterolateral wall of the ascending aorta in almost all cases. Some authors described particularly left-handed helical flow in patients with BAV type 2 , we could not distinguish this issue (Hope et al. 2010, pp. 53–61). Just in one case with BAV type

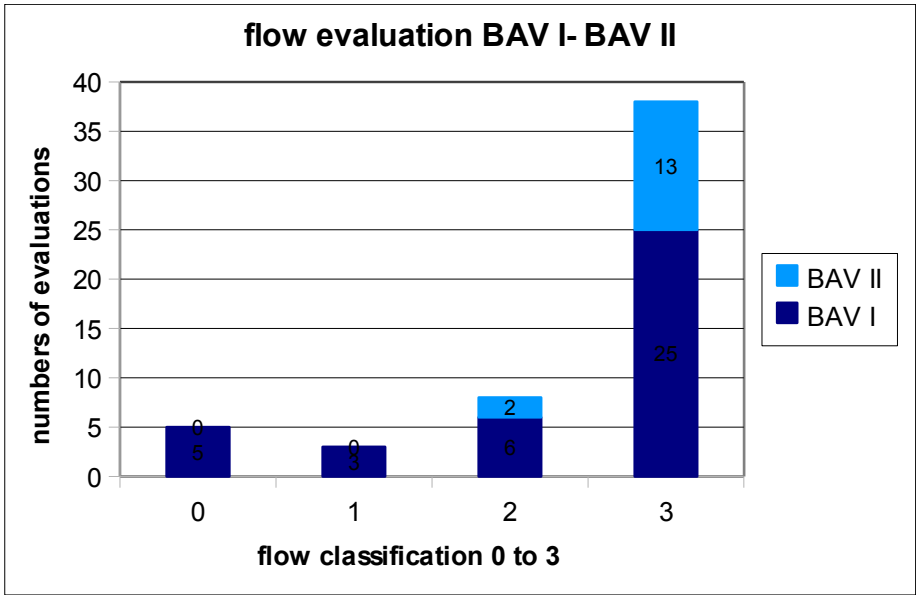

Figure 16: The distribution of flow graduation in BAV type 1 and 2 is demonstrated

2, the helical flow was viewed as left-handed. Despite remarkably severer helical flow patterns, there was no significantly difference in the flow graduation between BAV I and II (p-value = 0.0833). This may be due to the small sample size of patients with fusion of the right- and non-coronary leaflet.

Due to theories suggesting BAV type 1 and 2 to be distinct etiological diseases, we separately compared all patients with BAV type 1 with their matched partners, just as the matched pairs of the BAV type 2 group. Comparing the flow graduations with a Wilcoxon signed rank test there was significantly more helical flow in the BAV type 1 ($p = 0.0029$) and type 2 ($p = 0.0431$) group versus the matched TAV groups.

Interobserver variability

In 16 flow scenarios all three observers gave the identical classification. Four times the classification of the three observers varied between 0 and 2 and once between 1 and 3. There was no case, were the classification differed more than two grades. In all other flow evaluations the classification did not disagree more than one grade. The detailed data of the flow evaluation are listed in the appendix. The evaluation of valve fusion patterns was done by three observers. The results of all observers coincided in all cases. Measurements of the aortic diameters have been made once.

4 Discussion

The principal finding in this prospective age and sex matched pair study was a significant difference in flow patterns comparing blood flow in the ascending aorta of patients with BAV and TAV. Therefore, 4D flow CMR was used, which is well established for visualization and evaluation of multidirectional blood flow velocity, as well as for characterization of abnormal helical and vortical flow patterns (Markl et al. 2003, pp. 499–506; Frydrychowicz et al. 2007a, pp. 9–15).

Severe helical flow patterns obversely grade 2 and 3 were seen in 85% of the patients with BAV in our study. In the 18 BAV patients evaluated by three observers the blood flow was classified as grade 2 in eight cases and as grade 3 in 38 cases. In the TAV group 90% of the flow scenarios obtained by 4D flow, were classified as flow patterns without severe helical flow correspondingly grade 0 and 1. There was no case with TAV classified as grade 3. These alterations of blood flow occurred, although all diameters of the ascending aorta were within the previously defined limit of 44 mm. Additionally, in a further study with the same study population WSS in the ascending aorta was shown to be significantly higher in the BAV group than in the TAV group (Meierhofer et al. 2011).There were only two cases with an ascending aortic diameter greater than 2.2 cm/m^2 in the BAV group, pointing out, if flow abnormalities are cause or consequence of aortic dilatation. Considering the issue of the development of aortic dilatation in BAV disease, the altered flow characteristics in BAV patients are indicative of aortic wall disease due to the abnormal postvalvular hemodynamics.

The role of genetic and hemodynamic factors influencing aortic wall pathology is controversial. The similarity of the medial changes found in aortic dilatation in patients with Marfan syndrome and BAV, is used to justify a hypothesis of a genetic weakness, unless a genetic link has not been demonstrated yet in BAV with aortic dilatation in contrast to the Marfan syndrome. Moreover, Della Corte et al showed an asymmetric pattern of medial changes in BAV patients versus symmetric changes in Marfan patients, which suggests different causative mechanisms and additively argues against exclusively genetic causes of medial changes and aortic dilatation (Della Corte et al. 2006, pp. 20–27).

As the pulmonary trunk of BAV patients was found to have similar medial changes as in the aorta and to be larger than the pulmonary trunk of patients with TAV, a common developmental defect is suggested by some authors due to the fact that the pulmonary trunk, the aortic valve and the ascending aorta share a common embryonic origin, the conotruncus (de Sa et al. 1999, pp. 588–594; Kutty et al. 2010, pp. 1756–1761).

Hahn et al compared aortic root dimensions between healthy control subjects with TAV and BAV patients (n=83), separated into groups of functionally normal, mildly regurgigant, severely regurgigant and stenotic bicuspid valves. They found significantly larger aortic root dimensions in the BAV group in all hemodynamic subgroups and concluded that this fact supported their hypothesis of a genetic background in the development of aortic dilatation (Hahn et al. 1992, pp. 283–288).

Keane et al matched BAV patients with control persons for valvular lesions and showed larger aortic dimensions in BAV patients compared to TAV patients with comparable degrees of aortic valve disease. From those findings they deduced an intrinsic aortic abnormality as reason for aortic dilatation in BAV disease, as they aimed to reduce the influence of hemodynamic lesions associated with BAV. Though, an association between the severity of regurgitation and the degree of dilatation was found (Keane et al. 2000, pp. III35-39).

Nistri et al countered a hemodynamic theory with the statement, that aortic root enlargement occurred independently of hemodynamic abnormalities, as all hemodynamic perturbations had been excluded due to the study population that only included patients with normally functioning valve. Thus, they regarded flow perturbations as unlikely to influence aortic size in their study population (Nistri et al. 1999, pp. 19–22). At this point flow alterations beside aortic stenosis and regurgitation were not considered by the authors mentioned above. Bicuspid aortic valves without stenosis and regurgitation were equated with normally functioning tricuspid valves. However, we showed in our study that there are significant turbulences and helical flow patterns in the ascending aortas of patients with normally functioning BAV compared to patients with normally functioning TAV.

Several studies showed the influence of turbulent flow on changes in shear stress, which may lead to modulation of cellular signaling cascades and consequentially to alterations in the expression of genes like for MMPs and ECM proteins like fibronectin and

tenascin. MMPs are supposed to maintain the homeostasis of the connective tissue and their increased expression is expected to cause degradation of elastic proteins and apoptosis of VSMC and as a result decreased distensibility (Tadros et al. 2009, p. 882; Lehoux et al. 2003, pp. 631–643; Deplano et al. 2007, pp. 2406–2413; Cotrufo et al. 2005, pp. 504–511). Different patterns of MMP expression and activity in BAV, Marfan and idiopathic aneurysm tissue may indicate different mechanism of aortic pathophysiology, that have effect on aortic dilatation depending on the underlying etiology.

Additionally, these pathological changes in smooth muscle cells and ECM protein expression in the aortic wall were found to be asymmetrical and significantly higher in the convexity of the dilated ascending aorta or right anterolateral wall of patients with BAV, which was consistent with the asymmetrical pattern of wall stress distribution and the region that tended to dilate (Cotrufo et al. 2005, pp. 504–511; Bauer et al. 2006, pp. 218–220; Viscardi et al. 2010, pp. 1524–1594). Even non-dilated BAV aortas have higher rates of VSMC apoptosis at the convexity, suggesting an existing aortic wall pathology before dilatation occurs (Della Corte et al. 2008, pp. 8–18).

Nonetheless, it is not consistent with the theory of a common developmental defect of the entire ascending aorta. Because conversely, a hypothetical congenital wall defect that causes dilatation should induce a remodeling process uniformly involving the whole aortic circumference.

Della Corte et al found beside alterations in ECM proteins and MMP expression apoptotic VSMC death with a reduction in Bcl-2 expression and hypothesized that stress-induced early ECM changes unique to BAV convexity forward early VSMC apoptosis, at least partially through Bmf-Bcl-2 interaction, leading to progressive, typically asymmetric aortic enlargement (Della Corte et al. 2008, pp. 8–18; Tadros et al. 2009, p. 881). In an earlier study Della Corte et al reported a strict relation of an enlargement of the ascending aorta with the presence and severity of aortic stenosis and linked that fact with the hemodynamic theory (Della Corte et al. 2007, pp. 397–404).

In a study of Cotrufo et al dilated BAV aortas showed decreased levels of collagen type 1 and 2 and increased levels of fibronectin and tenascin at the convexity, which is identical with the common finding of dilatation in BAV that particularly involves the right anterolateral aspect (Cotrufo et al. 2005, pp. 504–511). Den Reijer et al showed an

association between higher MMP levels and misdirected flow patterns in dilated aortas, but could not show, if flow abnormalities were a cause or a consequence of aortic dilatation (den Reijer et al. 2010, pp. 1–13). However, MMPs are synthesized by several cells including VSMC in response to hemodynamic changes (Tadros et al. 2009, p. 882). A number of studies showed disturbed and helical flow patterns in patients with aneurysm by time-resolved 3-dimensional PC-MR (Hope et al. 2007, pp. 1471–1479; Weigang et al. 2008, pp. 11–16; Frydrychowicz et al. 2007a, pp. 9–15). Similar flow patterns have also been seen in patients with normal aortic dimensions, but additional diagnoses like aortic stenosis, insufficiency, CoA or TOF (Hope et al. 2010, pp. 53–61). Robicsek et al studied cryopreserved and then thawed human aortic roots with BAV in a left heart simulator and observed recirculation vortices that were induced by the abnormal orifice of the BAV and extended into the ascending aorta aiming toward the right (Robicsek et al. 2004, pp. 177–185).

Frydrychowicz et al showed that minor geometric changes can result in major changes in local hemodynamics (Frydrychowicz et al. 2007a, pp. 9–15). It was shown before, that in patients with BAV and aortic valve stenosis the anterolateral wall of the ascending aorta was subject to greater hemodynamic stress because of a significant higher peak systolic wall velocity. Several authors argued against the hemodynamic theory by bringing forward the argument that aortic dilatation occurs independently of coexistent valvular lesions (Bauer et al. 2006, pp. 218–220; Nistri et al. 1999, pp. 19–22; Hahn et al. 1992, pp. 283–288; Keane et al. 2000, pp. III35-39).

To rule out any cardiovascular influences, we excluded all BAV patients with dilatation, functional valve disease, cardiovascular diseases or previous surgeries and connective tissue diseases among others. Furthermore, we matched each study person for age and sex with a healthy control person. We believe this to be a strength of our study. In our study population (without stenosis and insufficiency) significant helical flow patterns were seen in 4D flow CMR. Turbulences that aimed towards the right anterolateral wall, could also be assessed in our study. This is the region, where BAV aortas tend to dilate (den Reijer et al. 2010, pp. 1–13; Cotrufo et al. 2005, pp. 504–511).

Demonstrating abnormal flow patterns in patients with normal aortic diameters, we are suggesting that the flow patterns are not secondary to dilated aortas and may be involved in the pathogenesis of aneurysm formation.

In addition, Della Corte et al showed smooth muscle cell apoptosis occurring in patients with BAV and stenotic valve without aortic dilatation, supporting this hypothesis (Della Corte et al. 2008, pp. 8–18). Barker et al found the systolic WSS in the ascending aorta of BAV patients to be significantly higher compared to TAV patients and showed a correlation between WSS and flow anomalies (Barker et al. 2010, pp. 788–800). The fact that aortic dilatation occurs only in 9.9% in BAV patients after AVR is also an argument against an intrinsic wall abnormality (McKellar et al. 2010, p. 1629).

It was remarkable that in our study the SI in the ascending aorta was significantly higher in the BAV group than in the TAV group independent of aortic diameters, as it was reported before (Nistri et al. 2008, pp. 472–479). Conspicuous is that differences in SI could only be seen in the ascending aorta, but not at other levels. These facts are indicative of hemodynamic causes of dilatation, as an intrinsic tissue disease of the aortic wall may involve all levels of the aorta and not only one single part. To our knowledge, there were only studies comparing SI at one level in BAV and TAV patients or comparing SI between different BAV phenotypes, but none comparing SI between BAV and TAV patients in different levels of the aorta (Schaefer et al. 2007, pp. 686–690; Nistri et al. 2008, pp. 472–479).There seems to be an association between abnormal flow and SI. So flow alterations may already have modified elastic properties by affecting the aortic wall and elevating WSS in the ascending aorta.

As 15% of the evaluations in the BAV group were not classified as grade 2 or 3, there arises the question whether these patients will develop an aneurysm or not and if so, when will the ascending aorta of patients with abnormal flow patterns dilate. Thus, a continuation of our study with follow-up examinations in several years including 4D flow CMR and measurement of the aortic diameters and SI may be required. We suggest that the evaluation of flow patterns in patients with BAV may help to distinguish patients at risk for aortic dilatation.

4.1.1 Study Population

In the last ten years several studies have researched on the issue of the pathogenesis of ascending aortic dilatation in BAV patients. There are also a number of studies concentrating on the hemodynamic hypothesis. Della Corte et al examined temporal and

spatial patterns of extracellular matrix and smooth muscle cell changes in the ascending aorta. They compared 12 patients with degenerative stenosis of a TAV with 14 patients with stenotic BAV. Additionally, there were some cases of aortic dilatation in both groups. In this study population smooth muscle cell apoptosis in patients with BAV occurred even in the patients without dilatation and particularly at the convexity, where the wall shear stress is to be the highest. Even though these alterations occurred before dilatation and both groups had aortic stenosis, aortic dilatation in BAV patients appears independently of abnormal valve function. Thus, a study design including only subjects with normally functioning valve would be more suggestive (Della Corte et al. 2008, pp. 8–18).

Den Reijer et al reported on an investigation in 18 pediatric BAV patients and 10 normal controls for links between abnormal blood flow patterns in the ascending aorta and aortic dilatation using velocity-encoded cardiovascular magnetic resonance. Even though they saw abnormal flow and high levels of MMP, 14 BAV patients already had a dilated aorta, so they could not distinguish, if the abnormal flow patterns were a cause or a consequence of aortic dilatation (den Reijer et al. 2010, p. 4).

Cotrufo et al compared tissue samples of the aortic wall in BAV and TAV patients. Collagen I and III were found to be decreased and fibronectin and tenascin to be increased in the concavity. Although patients with mixed valve disease were excluded, 12 patients had stenotic valves and 15 insufficient ones. In addition, all patients had already dilated aortas, so there is again the chicken or the egg problem (Cotrufo et al. 2005, pp. 504–511).

Bauer et al demonstrated that the anterolateral region of the ascending aorta in patients with BAV and aortic valve stenosis is subject to greater stress, but patients with normally functioning valve were not examined (Bauer et al. 2006, pp. 218–220).

Hope et al compared the flow patterns of 19 healthy volunteers and 13 patients with ascending aortic aneurysm of different origin (BAV, n=2) and described retrograde and helical flow patterns in the patients with aneurysm (Hope et al. 2007, pp. 1471–1479). In a further study, Hope et al reported on helical flow in 75% of patients with a BAV (n=20), among them were six patients with a dilated ascending aorta $\geq 2.2 cm/m^2$ including one patient with a diameter > 5cm, but nine with normal aortic dimensions $<2.2 cm/m^2$. However, it is notable that 16 BAV patients with CoA were included, 15 of

them were previously repaired. Additionally, there was one patient with TOF in the BAV group and seven in the control group and five BAV patients with moderate or severe aortic stenosis. As the study and the control group were not matched for age and sex, different distributions of age and sex can be seen (Hope et al. 2010, pp. 53–61).

Beaton et al showed an influence of CoA on the degree of dilatation in BAV patients. In their study children with BAV and CoA had both significantly smaller diameter of the ascending aorta and significantly slower rates of dilatation compared with age matched children with isolated BAV (Beaton et al. 2009, pp. 266–270).

Furthermore, Thanassoulis et al reported that patients with BAV, who had previously undergone coarctation repair, were those least likely to show rapid progression of aortic dilatation. So they concluded that the pathophysiology of BAV in patients who also have coarctation might differ from that of isolated BAV (Thanassoulis et al. 2008, p. 825). Thus, we suggest that a study design including both BAV patients with and without coexistent CoA, repaired or not repaired, is not suitable to examine the causes of aortic aneurysm formation in BAV disease, because of the different affects on aortic dilatation. This may be the same with other cardiac diagnoses like TOF.

To our knowledge until now only study populations divided into subgroups or mixed groups with normal, stenotic or insufficient valves, dilated aorta or additional diagnoses have been researched. This may lead to discordant and irreproducible results.

To rule out all these influences mentioned before, we attempted to find a study population that only differs in valve morphology, more precisely, either a tricuspid or bicuspid aortic valve. So patients with other cardiac diagnoses, aortic stenosis (velocity above the aortic valve >2,5 m/s) or aortic insufficiency (>AI I°), connective tissue disease or aortic diameter ≥4,5 cm were excluded. Out of 989 patients only the data of 18 BAV patients could be used for our study. Even in this study group two patients had a BSA corrected diameter of the ascending aorta >2.2 cm/m^2, which is defined as dilated.

It is almost impossible to find BAV patients with normal aortic diameters, as significantly larger aortic sizes in BAV patients were shown in several studies (Hahn et al. 1992, pp. 283–288; Keane et al. 2000, pp. III35-39). Buchner et al assessed the aortic diameters in 105 patients with BAV and reported a mean ±SD diameter of the ascending aorta of 4.1 ±0.69cm (Buchner et al. 2010, p. 1236), whereas the BAV group in our

study showed a diameter of 3.42 ±0.63 cm. Even though there were only two patients with a dilated aorta in our study group.

To gain a comparable group all patients were matched with a healthy control subject for sex and age. The median age of the BAV group was 25 years (10-44) and 25 (8-42) for TAV and there were no significant differences in weight, height, BSA or blood pressure. Thus, we assume that this age and sex matched pair study, including just healthy study objects, is suitable to compare flow patterns in order to stratify possible risks of aortic dilatation in patients with BAV.

4.1.2 BAV Phenotypes

Grading the BAV group according to the leaflet morphology, 13 of the 18 patients (72%) were allocated to BAV type 1 (fusion of the right and left coronary cusp) and five (28%) to BAV type 2 (fusion of the right and non-coronary cusp). There was no case with fusion of the left and non-coronary cusp (type 3). These findings are consistent with the distribution described by Schaefer et al.

Apart from the distribution of leaflet morphology, a male predominance in BAV type 1 was described, whereas BAV type 2 subjects were notably more often female. In our study 31% (4/13) of the BAV type 1 were women and 69% (9/13) men. The women's fraction of the type 2 group was 80% (4/5) and the men's 20% (1/5). The ratio BAV type 1 to BAV type 2 in the female fraction was 1:1. In the male it was 9:1. Even so BAV type 2 and female subjects were in minority, this distribution has been reported before, so that this study population represents all BAV patients in the general population.

Schaefer et al described different patterns of aortic elasticity and aortic root shape comparing BAV type 1 with BAV type 2. Aortic diameter was larger with type 1 than type 2 at the sinuses and smaller at the arch. At the sinuses type 1 had a higher stiffness index and lower distensibility. They suggest that differences in spatial distribution of blood flow through the different valve patterns may lead to inhomogeneous distribution of shear forces, resulting in differential gene expression and changes of the extracellular matrix (Schaefer et al. 2007, pp. 686–690).

The fact that there are regional differences in elastic properties disagrees on the one

hand with the theory of a common developmental wall defect in the ascending aorta and agrees on the other hand with the theory of different hemodynamic forces due to the orientation of the valve. So different flow patterns may lead to differential distribution of wall shear stress and this may lead to changes of aortic wall properties. Additionally, BAV type 2 is known to be associated with severer valve pathologies, especially aortic valve stenosis (Fernandes et al. 2004, pp. 1648–1651).

Due to our exclusion criteria, there was no case with aortic stenosis, but still it was remarkable that in 100% of the evaluations of BAV type 2 scenarios severe helical flow was seen. Grade 2 occurred two times in 15 evaluations and grade 3 13 times. There was no case of BAV type 2 with linear or mild helical flow.

There was no significant difference in aortic diameters, peak velocity, aortic insufficiency and blood pressure between the two phenotypes. These findings give rise to assume that the extremely abnormal flow may lead to severe changes in wall shear stress and elastic properties and thus to aortic dilatation occurring more progressively than in BAV type 1. This issue cannot be answered by our recent study, but has to be researched in further follow-up investigations (Schaefer et al. 2007, pp. 686–690; Schaefer et al. 2008, pp. 1634–1638).

We could not find a significant difference in the SI of BAV I and II at all levels of the aorta. This fact may be due to the small sample size of patients with fusion of the right and non-coronary leaflets.

As some authors regard the two phenotypes of the BAV as two distinct etiological entities, we separately compared these two groups with their matched partners (Fernández et al. 2009, pp. 2312–2318). But still there were significantly more helical flow patterns seen in both groups. So even if BAV type 1 and type 2 were two different etiological entities regarding the development of the valve, there are still abnormal flow patterns in both, that may lead to ascending aortic dilatation and wall abnormalities due to altered WSS (Meierhofer et al. 2011).

In recent studies an association of right-to-left leaflet fusion and increased rate of aortic dilatation was reported., but patients with CoA were included in the study, influencing the risk of dilatation (Thanassoulis et al. 2008, pp. 821–828). Holmes et al excluded BAV patients with concomitant CoA and found an association between right and non-coronary fusion and more rapid aortic growth, which would be compatible with severer

helical flow alterations seen in our study (Holmes et al. 2007, pp. 978–983). On the other hand Buchner et al and Fazel et al found no significant difference in aortic dimensions comparing diameters by CMR in 105 patients with BAV and varying phenotypes (Buchner et al. 2010, pp. 1233–1240; Fazel et al. 2008, p. 903).

It is still controversial, if there is a difference in the pattern of aortic dilatation dependent on aortic valve morphology and if BAV phenotypes affect the pathogenesis of aortic wall abnormalities. Therefore, further research might be necessary and it might be reasonable to pay particular attention to the potentially differing development of aortic dilatation in these two phenotypes.

4.1.3 Study Limitations

A few limitations of our study have to be considered. The principal limitation of this study is its lack of follow-up, as it was just a snapshot in time of probable developing aortic dilatation. The aim of our study was to identify and characterize abnormal flow patterns in healthy BAV patients. Data documenting progression of aortic dilatation are needed to further evaluate the proposed hypothesis that abnormal helical flow patterns affect the development of ascending aortic dilatation. Follow-up investigations after several years including assessment of flow patterns by 4D CMR flow and measurements of the aortic diameters are required.

Another point is the difference in ascending aortic diameter between the BAV and TAV group. However, all patients met the inclusion criteria with an ascending aortic diameter <45mm and there were just two cases with a BSA corrected diameter > 2.2cm/m^2, which was defined as dilated by Hope et al (Hope et al. 2010, pp. 53–61). Furthermore, significantly greater diameters in the BAV group could only be noted in the ascending aorta analogical to the localized alterations of SI, which argues against an intrinsic tissue disorder of the ascending aorta.

Although all patients with aortic stenosis and aortic valve velocity greater than 2,5 m/s were excluded, there was still a significant difference between BAV and TAV patients, probably due to the abnormal and smaller orifice of the bicuspid valve.

Another limitation of this study is the relatively simplistic quantification of abnormal blood flow by a self defined classification, where only the severity of helical flow was

evaluated, but not specific flow characteristics like different patterns of helical flow. Although, the characteristics of flow classification were closely prescribed. We did not obtain data on intraobserver variability in the evaluation of flow patterns, but interobserver variability was not notable.

Whereas remarkably severe flow alterations were seen in patients with BAV type 2, we could not distinguish different patterns of helical flow direction, as it was described by Hope et al (Hope et al. 2010, pp. 53–61). The cause of this flow difference is not known, but could be due to the different valve morphology in BAV type 1 and 2 and may lead to differences in aortic dimensions and elasticity between these phenotypes. This variation in regional dilatation is difficult to explain with a theory of intrinsic wall abnormality alone (Schaefer et al. 2007, pp. 686–690). So in future, distinctions of helical flow patterns should be considered in our flow evaluation.

Besides, only five of 18 patients with BAV had the leaflet morphology type 2, so there maybe a bias, although predominance of BAV type 1 has been reported (Schaefer et al. 2008, p. 1636). There was no significant difference in the SI of BAV type 1 and 2 in our study group, but this may be due to the small sample size of patients with BAV type 2. It was suggested that the different phenotypes of BAV are distinct diseases, which had to be considered in studies concerning on aortic dilatation in BAV (Fernández et al. 2009, pp. 2312–2318). Though BAV type 1 and 2 have been pooled in one study group, we tried to distinguish important differences in flow, SI and aortic diameters in these two phenotypes. Even so, it was difficult to find distinctions due to the small sample size.

Another issue that has to be discussed are two cases of 44 year old men with bicuspid aortic valve and severe helical flow patterns. Both were classified as grade 3 by all three observers and both had aortic diameters smaller than 44 mm. They have probably had abnormal flow patterns since their birth, but do not have a significant dilatation. This raises the question whether they will develop an aneurysm any day in life, why do some patients suffer from aneurysm earlier in life and thus, if other factors than hemodynamics play a role. So further follow-up examinations assessing flow patterns and vessel diameters are necessary.

It should be noted that velocity information may have been lost during data processing, as some modulations depend on the user. And although PC-MR data underwent eddy-current correction, remaining errors due to concomitant and non-linear gradients may

still introduce errors in the encoded velocities. Even so the flow visualization is just a calculated illustration of flow patterns out of velocity data, its accuracy of flow visualization is validated (Markl et al. 2003, pp. 499–506; Frydrychowicz et al. 2007a, pp. 9–15).

4.1.4 Conclusion

In conclusion, the bicuspid aortic valve (BAV) is the most common congenital heart defect occurring in 0.5–2% of the population. It is often associated with vascular abnormalities of the ascending aorta, such as dilatation and dissection, which are caused by accelerated degeneration of the aortic media, abnormalities of matrix disruption and apoptosis of VSMC. Furthermore, the presence of BAV is an important risk factor for progressive aortic dilatation independent of valvular function. Aortic dilatation is often asymptomatic and, if not detected, could progress to dissection or rupture, which is associated with high mortality. Therefore rapid aortic dilatation is an indication for urgent surgical intervention. However, the appropriate timing of surgical intervention in patients with BAV is not well established, because few studies have evaluated the natural progression of aortic dilatation. Especially, controversial data are available on causes of aortic dilatation in BAV and risk factors for rapid progression. Such information could improve the surveillance of patients with BAV and facilitate suitably follow-up investigations and early intervention for patients with high-risk disease, which might reduce the incidence of rare but catastrophic events such as aortic dissection and rupture.

The objective of this study was to determine possible causes of rapid progression of aortic dilatation among patients with BAV. By using 4D flow CMR imaging, that is well established for the evaluation and characterization of abnormal flow patterns in great vessels, we could demonstrate pathological flow patterns in BAV patients without concomitant lesions and with normal aortic dimensions. Regarding previous studies that showed the influence of turbulent flow on changes in shear stress, leading to modulation of cellular signaling cascades and consequentially to alterations of elastic properties in the wall of the ascending aorta, we suggest that hemodynamic properties might play an important role in the pathogenesis of aortic dilatation in BAV, in particular, as specific

alterations in the aortic media primarily occur in the right anterolateral region where the hemodynamic stress is known to be the highest.

Moreover, we propose that the characterization of blood flow may help to distinguish and follow up patients with BAV at risk for aortic dilatation in the future. However, it appears necessarily that the state of flow characteristics and aortic dimensions should be reassessed in the context of several year follow-ups, in order to establish the magnitude of influence of helical flow patterns on the progression and severity of aortic dilatation.

With this in view, it shall be referred to an additional study of the Department of Pediatric Cardiology and Congenital Heart Disease concerning on different patterns of wall shear stress in the same study population (Meierhofer et al. 2011). Whether and how flow abnormalities exactly implicate the development of aortic dilatation is not properly established. Further research is required, as the pathogenesis of aortic dilatation is a relevant issue in the adequate surveillance and surgical treatment of patients with BAV.

5 Summary

Introduction: Bicuspid aortic valves (BAV) are frequently associated with dilation, aneurysm and dissection of the ascending aorta. Two opposing hypotheses advocate either an inborn connective tissue defect or dilation secondary to altered blood flow conditions in the ascending aorta. This study was initiated to evaluate flow patterns in the ascending aorta of BAV patients compared to those in individuals with tricuspid aortic valve (TAV) using four-dimensional cardiovascular magnetic resonance (CMR).

Methods: 18 healthy individuals with normally functioning BAV, without aortic stenosis, aortic regurgitation or dilation were compared with an age and sex matched control group of volunteers with TAV. 4D blood flow data were obtained by CMR (spatial resolution = 2.1 x 1.7 x 2.5 mm^3, temporal resolution = 39.2 ms) and visualization was performed with dedicated software. Evaluation of different flow patterns was performed by three blinded observers and flow alterations were classified into four groups concerning their intensity.

Results: In 90% BAV and TAV were correctly classified in blinded evaluation of flow visualization. Abnormal helical flow patterns in the ascending aorta were seen in 85% of the evaluations in the BAV group. In the TAV group altered flow was only found in 6%. Comparison of flow patterns in the matched pairs revealed a significant difference between patients with BAV and the control group ($p = 0.0004$).

Conclusions: Patients with BAV without concomitant valve or vessel disease have a significantly different 4D flow pattern than patients with TAV. This altered flow may have an important impact on the development of aortic dilation in patients with BAV We further suggest that connective tissue defect may only be a secondary finding in these patients.

6 Zusammenfassung

Einleitung: Bikuspide Aortenklappen (BAV) sind häufig mit Dilatation, Aneurysmen und Dissektion der Aorta ascendens assoziiert. Ob ein angeborener Bindegewebsdefekt oder ein veränderter Blutfluss in der aszendierenden Aorta (AAo) zur Dilatation führt, wird kontrovers diskutiert. Das Ziel dieser Studie war die Auswertung und der Vergleich von Flussmustern in der AAo von BAV Patienten und Personen mit trikuspider Aortenklappe (TAV). Die Auswertung der Flussmuster erfolgte mit vier-dimensionaler (4D) kardiovaskulärer Magnetresonanztomographie (CMR).

Methoden: 18 gesunde Personen mit normal funktionierender BAV, ohne Aortenstenose, Aorteninsuffizienz oder Dilatation wurden mit einer nach Alter und Geschlecht gepaarten Kontrollgruppe mit TAV verglichen. Die 4D Flussdaten wurden mit CMR gewonnen (räumliche Auflösung = 2.1 x 1.7 x 2.5 mm^3, zeitliche Auflösung = 39.2 ms). Die Visualisierung erfolgte mit geeigneter Software. Drei geblindete Beobachter werteten die unterschiedlichen Flussmuster aus. Die Flussveränderungen wurden je nach ihrer Stärke in vier Gruppen eingeteilt.

Ergebnisse: In der geblindeten Auswertung der Flussvisualisierung wurden 90% der BAV und TAV korrekt klassifiziert. Bei 85% der Auswertungen der BAV Gruppe wurden abnormale helikale Flussmuster gesehen. In der TAV Gruppe zeigte sich nur in 6% veränderter Fluss. Beim Vergleich der Flussmuster der gematchten Paare ergab sich ein signifikanter Unterschied zwischen den BAV-Patienten und der Kontrollgruppe ($p = 0.0004$).

Schlussfolgerung: BAV-Patienten ohne begleitende Klappen- oder Gefäßerkrankungen haben signifikant unterschiedliche 4D Flussmuster im Vergleich zu Personen mit TAV. Es ist möglich, dass dieser veränderte Fluss eine wichtige Bedeutung für die Entwicklung einer Aortendilatation bei BAV-Patienten hat. Außerdem scheint der Bindegewebsdefekt nur ein sekundärer Befund bei Patienten mit BAV zu sein.

References

Abbott ME. Coarctation of the adult type. II. A statistical study and historical retrospect of 200 recorded cases, with autopsy, of stenosis or obliteration of the descending arch in subjects above the age of two years… Am. Heart J. 3 (1928): 574-618.

Bandettini, W. P., Arai, A. E. Advances in clinical applications of cardiovascular magnetic resonance imaging. Heart 94 (2008): 1485–1495.

Barker, A. J., Lanning, C., Shandas, R. Quantification of hemodynamic wall shear stress in patients with bicuspid aortic valve using phase-contrast MRI. Ann Biomed Eng 38 (2010): 788–800.

Basso, C., Boschello, M., Perrone, C., Mecenero, A., Cera, A., Bicego, D., Thiene, G., Dominicis, E. de. An echocardiographic survey of primary school children for bicuspid aortic valve. Am. J. Cardiol. 93 (2004): 661–663.

Bauer, M., Siniawski, H., Pasic, M., Schaumann, B., Hetzer, R. Different hemodynamic stress of the ascending aorta wall in patients with bicuspid and tricuspid aortic valve. J Card Surg 21 (2006): 218–220.

Baumgartner, D., Baumgartner, C., Mátyás, G., Steinmann, B., Löffler-Ragg, J., Schermer, E., Schweigmann, U., Baldissera, I., Frischhut, B., Hess, J., Hammerer, I. Diagnostic power of aortic elastic properties in young patients with Marfan syndrome. J. Thorac. Cardiovasc. Surg. 129 (2005): 730–739.

Beaton, A. Z., Nguyen, T., Lai, W. W., Chatterjee, S., Ramaswamy, P., Lytrivi, I. D., Parness, I. A., Srivastava, S. Relation of coarctation of the aorta to the occurrence of ascending aortic dilation in children and young adults with bicuspid aortic valves. Am. J. Cardiol. 103 (2009): 266–270.

Beroukhim, R. S., Kruzick, T. L., Taylor, A. L., Gao, D., Yetman, A. T. Progression of aortic dilation in children with a functionally normal bicuspid aortic valve. Am. J. Cardiol. 98 (2006): 828–830.

Bogren, H. G., Buonocore, M. H. 4D magnetic resonance velocity mapping of blood flow patterns in the aorta in young vs. elderly normal subjects. J Magn Reson Imaging 10 (1999): 861–869.

Bolling, S. F., Iannettoni, M. D., Dick, M., Rosenthal, A., Bove, E. L. Shone's anomaly: operative results and late outcome. Ann. Thorac. Surg. 49 (1990): 887–893.

Bonow, R. O. Bicuspid aortic valves and dilated aortas: a critical review of the ACC/AHA practice guidelines recommendations. Am. J. Cardiol. 102 (2008): 111–114.

Bonow, R. O., Carabello, B. A., Chatterjee, K., Leon, A. C. de, Faxon, D. P., Freed, M. D., Gaasch, W. H., Lytle, B. W., Nishimura, R. A., O'Gara, P. T., O'Rourke, R. A., Otto, C. M., Shah, P. M., Shanewise, J. S. 2008 Focused update incorporated into the ACC/AHA 2006 guidelines for the management of patients with valvular heart disease: a report of the American College of Cardiology/American Heart Association Task Force on Practice Guidelines (Writing Committee to Revise the 1998 Guidelines for the Management of Patients With Valvular Heart Disease): endorsed by the Society of Cardiovascular Anesthesiologists, Society for Cardiovascular Angiography and Interventions, and Society of Thoracic Surgeons. Circulation 118 (2008): e523-661.

Braverman, A. C., Güven, H., Beardslee, M. A., Makan, M., Kates, A. M., Moon, M. R. The bicuspid aortic valve. Curr Probl Cardiol 30 (2005): 470–522.

Brown, C., Sane, D. C., Kitzman, D. W. Bicuspid aortic valves in monozygotic twins. Echocardiography 20 (2003): 183–184.

Buchner, S., Hülsmann, M., Poschenrieder, F., Hamer, O. W., Fellner, C., Kobuch, R., Feuerbach, S., Riegger, G. A. J., Djavidani, B., Luchner, A., Debl, K. Variable phenotypes of bicuspid aortic valve disease: classification by cardiovascular magnetic resonance. Heart 96 (2010): 1233–1240.

Buonocore, M. H. Visualizing blood flow patterns using streamlines, arrows, and particle paths. Magn Reson Med 40 (1998): 210–226.

Cawley, P. J., Maki, J. H., Otto, C. M. Cardiovascular magnetic resonance imaging for valvular heart disease: technique and validation. Circulation 119 (2009): 468–478.

Cotrufo, M., Della Corte, A., Santo, L. S. de, Quarto, C., Feo, M. de, Romano, G., Amarelli, C., Scardone, M., Di Meglio, F., Guerra, G., Scarano, M., Vitale, S., Castaldo, C., Montagnani, S. Different patterns of extracellular matrix protein expression in the convexity and the concavity of the dilated aorta with bicuspid aortic valve: preliminary results. J. Thorac. Cardiovasc. Surg. 130 (2005): 504–511.

Cripe, L., Andelfinger, G., Martin, L. J., Shooner, K., Benson, D. W. Bicuspid aortic valve is heritable. J. Am. Coll. Cardiol. 44 (2004): 138–143.

Della Corte, A., Bancone, C., Quarto, C., Dialetto, G., Covino, F. E., Scardone, M., Caianiello, G., Cotrufo, M. Predictors of ascending aortic dilatation with bicuspid aortic valve: a wide spectrum of disease expression. Eur J Cardiothorac Surg 31 (2007): 397-404; discussion 404-5.

Della Corte, A., Quarto, C., Bancone, C., Castaldo, C., Di Meglio, F., Nurzynska, D., Santo, L. S. de, Feo, M. de, Scardone, M., Montagnani, S., Cotrufo, M. Spatiotemporal patterns of smooth muscle cell changes in ascending aortic dilatation with bicuspid and tricuspid aortic valve stenosis: focus on cell-matrix signaling. J. Thorac. Cardiovasc. Surg. 135 (2008): 8-18, 18.e1-2.

Della Corte, A., Santo, L. S. de, Montagnani, S., Quarto, C., Romano, G., Amarelli, C., Scardone, M., Feo, M. de, Cotrufo, M., Caianiello, G. Spatial patterns of matrix protein expression in dilated ascending aorta with aortic regurgitation: congenital bicuspid valve versus Marfan's syndrome. J. Heart Valve Dis. 15 (2006): 20-7; discussion 27.

den Reijer, P. M., Sallee, D., van der Velden, P., Zaaijer, E. R., Parks, W. J., Ramamurthy, S., Robbie, T. Q., Donati, G., Lamphier, C., Beekman, R. P., Brummer, M. E. Hemodynamic predictors of aortic dilatation in bicuspid aortic valve by velocity-encoded cardiovascular magnetic resonance. J Cardiovasc Magn Reson 12 (2010): 4.

Deplano, V., Knapp, Y., Bertrand, E., Gaillard, E. Flow behaviour in an asymmetric compliant experimental model for abdominal aortic aneurysm. J Biomech 40 (2007): 2406–2413.

Doty, D. B. Anomalous origin of the left circumflex coronary artery associated with bicuspid aortic valve. J. Thorac. Cardiovasc. Surg. 122 (2001): 842–843.

Eisenberg, L. M., Markwald, R. R. Molecular regulation of atrioventricular valvuloseptal morphogenesis. Circ. Res. 77 (1995): 1–6.

Emanuel, R., Withers, R., O'Brien, K., Ross, P., Feizi, O. Congenitally bicuspid aortic valves. Clinicogenetic study of 41 families. Br Heart J 40 (1978): 1402–1407.

Fazel, S. S., Mallidi, H. R., Lee, R. S., Sheehan, M. P., Liang, D., Fleischman, D., Herfkens, R., Mitchell, R. S., Miller, D. C. The aortopathy of bicuspid aortic valve disease has distinctive patterns and usually involves the transverse aortic arch. J. Thorac. Cardiovasc. Surg. 135 (2008): 901-7, 907.e1-2.

Fedak, P. W. M., Sa, M. P. L. de, Verma, S., Nili, N., Kazemian, P., Butany, J., Strauss, B. H., Weisel, R. D., David, T. E. Vascular matrix remodeling in patients with bicuspid aortic valve malformations: implications for aortic dilatation. J. Thorac. Cardiovasc. Surg. 126 (2003): 797–806.

Fedak, P. W. M., Verma, S., David, T. E., Leask, R. L., Weisel, R. D., Butany, J. Clinical and pathophysiological implications of a bicuspid aortic valve. Circulation 106 (2002): 900–904.

Ferencik, M., Pape, L. A. Changes in size of ascending aorta and aortic valve function with time in patients with congenitally bicuspid aortic valves. Am. J. Cardiol. 92 (2003): 43–46.

Fernandes, S. M., Khairy, P., Sanders, S. P., Colan, S. D. Bicuspid aortic valve morphology and interventions in the young. J. Am. Coll. Cardiol. 49 (2007): 2211–2214.

Fernandes, S. M., Sanders, S. P., Khairy, P., Jenkins, K. J., Gauvreau, K., Lang, P., Simonds, H., Colan, S. D. Morphology of bicuspid aortic valve in children and adolescents. J. Am. Coll. Cardiol. 44 (2004): 1648–1651.

Fernández, B., Durán, A. C., Fernández-Gallego, T., Fernández, M. C., Such, M., Arqué, J. M., Sans-Coma, V. Bicuspid aortic valves with different spatial orientations of the leaflets are distinct etiological entities. J. Am. Coll. Cardiol. 54 (2009): 2312–2318.

Fratz, S., Hess, J., Schuhbaeck, A., Buchner, C., Hendrich, E., Martinoff, S., Stern, H. Routine clinical cardiovascular magnetic resonance in paediatric and adult congenital heart disease: patients, protocols, questions asked and contributions made. J Cardiovasc Magn Reson 10 (2008): 46.

Fratz, S., Hess, J., Schwaiger, M., Martinoff, S., Stern, H. C. More accurate quantification of pulmonary blood flow by magnetic resonance imaging than by lung perfusion scintigraphy in patients with fontan circulation. Circulation 106 (2002): 1510–1513.

Frydrychowicz, A., Berger, A., Russe, M. F., Stalder, A. F., Harloff, A., Dittrich, S., Hennig, J., Langer, M., Markl, M. Time-resolved magnetic resonance angiography and flow-sensitive 4-dimensional magnetic resonance imaging at 3 Tesla for blood flow and wall shear stress analysis. J. Thorac. Cardiovasc. Surg. 136 (2008): 400–407.

Frydrychowicz, A., Harloff, A., Jung, B., Zaitsev, M., Weigang, E., Bley, T. A., Langer, M., Hennig, J., Markl, M. Time-resolved, 3-dimensional magnetic resonance flow analysis at 3 T: visualization of normal and pathological aortic vascular hemodynamics. J Comput Assist Tomogr 31 (2007a): 9–15.

Frydrychowicz, A., Markl, M., Harloff, A., Stalder, A. F., Bock, J., Bley, T. A., Berger, A., Russe, M. F., Schlensak, C., Hennig, J., Langer, M. [Flow-sensitive in-vivo 4D MR imaging at 3T for the analysis of aortic hemodynamics and derived vessel wall parameters]. Rofo 179 (2007b): 463–472.

Frydrychowicz, A., Weigang, E., Langer, M., Markl, M. Flow-sensitive 3D magnetic resonance imaging reveals complex blood flow alterations in aortic Dacron graft repair. Interact Cardiovasc Thorac Surg 5 (2006): 340–342.

Garg, V., Muth, A. N., Ransom, J. F., Schluterman, M. K., Barnes, R., King, I. N., Grossfeld, P. D., Srivastava, D. Mutations in NOTCH1 cause aortic valve disease. Nature 437 (2005): 270–274.

Glick, B. N., Roberts, W. C. Congenitally bicuspid aortic valve in multiple family members. Am. J. Cardiol. 73 (1994): 400–404.

Glower, D. D., Bashore, T. M., Spritzer, C. E. Congenital aortic stenosis and patent ductus arteriosus in the adult. Ann. Thorac. Surg. 54 (1992): 368–370.

Godden, D. J., Sandhu, P. S., Kerr, F. Stenosed bicuspid aortic valves in twins. Eur. Heart J. 8 (1987): 316–318.

Guntheroth, W. G. A critical review of the American College of Cardiology/American Heart Association practice guidelines on bicuspid aortic valve with dilated ascending aorta. Am. J. Cardiol. 102 (2008): 107–110.

Guo, D.-C., Pannu, H., van Tran-Fadulu, Papke, C. L., Yu, R. K., Avidan, N., Bourgeois, S., Estrera, A. L., Safi, H. J., Sparks, E., Amor, D., Ades, L., McConnell, V., Willoughby, C. E., Abuelo, D., Willing, M., Lewis, R. A., Kim, D. H., Scherer, S., Tung, P. P., Ahn, C., Buja, L. M., Raman, C. S., Shete, S. S., Milewicz, D. M. Mutations in smooth muscle alpha-actin (ACTA2) lead to thoracic aortic aneurysms and dissections. Nat. Genet. 39 (2007): 1488–1493.

Hager, A., Kaemmerer, H., Rapp-Bernhardt, U., Blücher, S., Rapp, K., Bernhardt, T. M., Galanski, M., Hess, J. Diameters of the thoracic aorta throughout life as measured with helical computed tomography. J. Thorac. Cardiovasc. Surg. 123 (2002): 1060–1066.

Hahn, R. T., Roman, M. J., Mogtader, A. H., Devereux, R. B. Association of aortic dilation with regurgitant, stenotic and functionally normal bicuspid aortic valves. J. Am. Coll. Cardiol. 19 (1992): 283–288.

Higgins, C. B., Wexler, L. Reversal of dominance of the coronary arterial system in isolated aortic stenosis and bicuspid aortic valve. Circulation 52 (1975): 292–296.

Hoffman, J. I. E., Kaplan, S. The incidence of congenital heart disease. J. Am. Coll. Cardiol. 39 (2002): 1890–1900.

Holman, E. The obscure physiology of poststenotic dilatation; its relation to the development of aneurysms. J Thorac Surg 28 (1954): 109–133.

Holmes, K. W., Lehmann, C. U., Dalal, D., Nasir, K., Dietz, H. C., Ravekes, W. J., Thompson, W. R., Spevak, P. J. Progressive dilation of the ascending aorta in children with isolated bicuspid aortic valve. Am. J. Cardiol. 99 (2007): 978–983.

Hope, M. D., Hope, T. A., Meadows, A. K., Ordovas, K. G., Urbania, T. H., Alley, M. T., Higgins, C. B. Bicuspid aortic valve: four-dimensional MR evaluation of ascending aortic systolic flow patterns. Radiology 255 (2010): 53–61.

Hope, T. A., Markl, M., Wigström, L., Alley, M. T., Miller, D. C., Herfkens, R. J. Comparison of flow patterns in ascending aortic aneurysms and volunteers using four-dimensional magnetic resonance velocity mapping. J Magn Reson Imaging 26 (2007): 1471–1479.

Huntington, K., Hunter, A. G., Chan, K. L. A prospective study to assess the frequency of familial clustering of congenital bicuspid aortic valve. J. Am. Coll. Cardiol. 30 (1997): 1809–1812.

Kappetein, A. P., Gittenberger-de Groot, A. C., Zwinderman, A. H., Rohmer, J., Poelmann, R. E., Huysmans, H. A. The neural crest as a possible pathogenetic factor in coarctation of the aorta and bicuspid aortic valve. J. Thorac. Cardiovasc. Surg. 102 (1991): 830–836.

Kawasaki, T., Sasayama, S., Yagi, S., Asakawa, T., Hirai, T. Non-invasive assessment of the age related changes in stiffness of major branches of the human arteries. Cardiovasc. Res. 21 (1987): 678–687.

Keane, M. G., Wiegers, S. E., Plappert, T., Pochettino, A., Bavaria, J. E., Sutton, M. G. Bicuspid aortic valves are associated with aortic dilatation out of proportion to coexistent valvular lesions. Circulation 102 (2000): III35-9.

Kirby, M. L. Cardiac morphogenesis--recent research advances. Pediatr. Res. 21 (1987): 219–224.

Kutty, S., Kaul, S., Danford, C. J., Danford, D. A. Main pulmonary artery dilation in association with congenital bicuspid aortic valve in the absence of pulmonary valve abnormality. Heart 96 (2010): 1756–1761.

Lamas, C. C., Eykyn, S. J. Bicuspid aortic valve--A silent danger: analysis of 50 cases of infective endocarditis. Clin. Infect. Dis. 30 (2000): 336–341.

Larson, E. W., Edwards, W. D. Risk factors for aortic dissection: a necropsy study of 161 cases. Am. J. Cardiol. 53 (1984): 849–855.

Le Lièvre, C. S., Le Douarin, N. M. Mesenchymal derivatives of the neural crest: analysis of chimaeric quail and chick embryos. J Embryol Exp Morphol 34 (1975): 125–154.

Lee, T. C., Zhao, Y. D., Courtman, D. W., Stewart, D. J. Abnormal aortic valve development in mice lacking endothelial nitric oxide synthase. Circulation 101 (2000): 2345–2348.

Lehoux, S., Tedgui, A. Cellular mechanics and gene expression in blood vessels. J Biomech 36 (2003): 631–643.

Lerer, P. K., Edwards, W. D. Coronary arterial anatomy in bicuspid aortic valve. Necropsy study of 100 hearts. Br Heart J 45 (1981): 142–147.

Mahle, W. T., Sutherland, J. L., Frias, P. A. Outcome of isolated bicuspid aortic valve in childhood. J. Pediatr. 157 (2010): 445–449.

Markl, M., Chan, F. P., Alley, M. T., Wedding, K. L., Draney, M. T., Elkins, C. J., Parker, D. W., Wicker, R., Taylor, C. A., Herfkens, R. J., Pelc, N. J. Time-resolved three-dimensional phase-contrast MRI. J Magn Reson Imaging 17 (2003): 499–506.

Markl, M., Draney, M. T., Hope, M. D., Levin, J. M., Chan, F. P., Alley, M. T., Pelc, N. J., Herfkens, R. J. Time-resolved 3-dimensional velocity mapping in the thoracic aorta: visualization of 3-directional blood flow patterns in healthy volunteers and patients. J Comput Assist Tomogr 28 (2004): 459–468.

Markl, M., Harloff, A., Bley, T. A., Zaitsev, M., Jung, B., Weigang, E., Langer, M., Hennig, J., Frydrychowicz, A. Time-resolved 3D MR velocity mapping at 3T: improved navigator-gated assessment of vascular anatomy and blood flow. J Magn Reson Imaging 25 (2007): 824–831.

Martin, L. J., Ramachandran, V., Cripe, L. H., Hinton, R. B., Andelfinger, G., Tabangin, M., Shooner, K., Keddache, M., Benson, D. W. Evidence in favor of linkage to human chromosomal regions 18q, 5q and 13q for bicuspid aortic valve and associated cardiovascular malformations. Hum. Genet. 121 (2007): 275–284.

Mautner, G. C., Mautner, S. L., Cannon, R. O., Hunsberger, S. A., Roberts, W. C. Clinical factors useful in predicting aortic valve structure in patients40 years of age with isolated valvular aortic stenosis. Am. J. Cardiol. 72 (1993): 194–198.

McKellar, S. H., Michelena, H. I., Li, Z., Schaff, H. V., Sundt, T. M. Long-term risk of aortic events following aortic valve replacement in patients with bicuspid aortic valves. Am. J. Cardiol. 106 (2010): 1626–1633.

McKellar, S. H., Tester, D. J., Yagubyan, M., Majumdar, R., Ackerman, M. J., Sundt, T. M. Novel NOTCH1 mutations in patients with bicuspid aortic valve disease and thoracic aortic aneurysms. J. Thorac. Cardiovasc. Surg. 134 (2007): 290–296.

McKusick, V. A. Association of congenital bicuspid aortic valve and erdheim's cystic medial necrosis. Lancet 1 (1972): 1026–1027.

Meierhofer, C., Schneider, E. P., Lyko, C., Martinoff, S., Markl, M., Hess, J., and Stern, H. (2011). Wall shear stress in the ascending aorta in patients with bicuspid aortic valves differs significantly from tricuspid aortic valves. March 06, 2011, accessed August 18, 2011.

Miller, M. J., Geffner, M. E., Lippe, B. M., Itami, R. M., Kaplan, S. A., DiSessa, T. G., Isabel-Jones, J. B., Friedman, W. F. Echocardiography reveals a high incidence of bicuspid aortic valve in Turner syndrome. J. Pediatr. 102 (1983): 47–50.

Mills, P., Leech, G., Davies, M., Leathan, A. The natural history of a non-stenotic bicuspid aortic valve. Br Heart J 40 (1978): 951–957.

Mohamed, S. A., Aherrahrou, Z., Liptau, H., Erasmi, A. W., Hagemann, C., Wrobel, S., Borzym, K., Schunkert, H., Sievers, H. H., Erdmann, J. Novel missense mutations (p.T596M and p.P1797H) in NOTCH1 in patients with bicuspid aortic valve. Biochem. Biophys. Res. Commun. 345 (2006): 1460–1465.

Moore, G. W., Hutchins, G. M., Brito, J. C., Kang, H. Congenital malformations of the semilunar valves. Hum. Pathol. 11 (1980): 367–372.

Mosteller, R. D. Simplified calculation of body-surface area. N. Engl. J. Med. 317 (1987): 1098.

Nataatmadja, M., West, M., West, J., Summers, K., Walker, P., Nagata, M., Watanabe, T. Abnormal extracellular matrix protein transport associated with increased apoptosis of vascular smooth muscle cells in marfan syndrome and bicuspid aortic valve thoracic aortic aneurysm. Circulation 108 Suppl 1 (2003): II329-34.

Neumayer, U., Stone, S., Somerville, J. Small ventricular septal defects in adults. Eur. Heart J. 19 (1998): 1573–1582.

Nistri, S., Grande-Allen, J., Noale, M., Basso, C., Siviero, P., Maggi, S., Crepaldi, G., Thiene, G. Aortic elasticity and size in bicuspid aortic valve syndrome. Eur. Heart J. 29 (2008): 472–479.

Nistri, S., Sorbo, M. D., Basso, C., Thiene, G. Bicuspid aortic valve: abnormal aortic elastic properties. J. Heart Valve Dis. 11 (2002): 369-73; discussion 373-4.

Nistri, S., Sorbo, M. D., Marin, M., Palisi, M., Scognamiglio, R., Thiene, G. Aortic root dilatation in young men with normally functioning bicuspid aortic valves. Heart 82 (1999): 19–22.

Nora, J. J., Nora, A. H. The evolution of specific genetic and environmental counseling in congenital heart diseases. Circulation 57 (1978): 205–213.

Nordmeyer, S., Riesenkampff, E., Crelier, G., Khasheei, A., Schnackenburg, B., Berger, F., Kuehne, T. Flow-sensitive four-dimensional cine magnetic resonance imaging for offline blood flow quantification in multiple vessels: a validation study. J Magn Reson Imaging 32 (2010): 677–683.

O'Malley, C. D., Saunders, J. B. C. M. de. Leonardo da Vinci on the human body: The anatomical, physiological, and embryological drawings of Leonardo da Vinci. With Translations, Emendations and a Biographical Introduction by Charles D. O'Malley and J. B. de C. M. Saunders, Henry Schuman, New York (1952).

Osler W. The bicsupid condition of the aortic valves. Trans Assoc Am Physicians 2 (1886): 185–192.

Pachulski, R. T., Weinberg, A. L., Chan, K. L. Aortic aneurysm in patients with functionally normal or minimally stenotic bicuspid aortic valve. Am. J. Cardiol. 67 (1991): 781–782.

Paget J. On obstruction of the branches of the pulmonary artery. Med Chir Trans 67 (1884): 162–188.

Peacock TB. On malformations of the human heart, etc.; with original cases and illustrations. 2nd. London: Churchill, 1866. London: Churchill (1866).

Pomerance, A. Pathogenesis of aortic stenosis and its relation to age. Br Heart J 34 (1972): 569–574.

Rebergen, S. A., Roos, A. de. Congenital heart disease. Evaluation of anatomy and function by MRI. Herz 25 (2000): 365–383.

Rebergen, S. A., Niezen, R. A., Helbing, W. A., van der Wall, E. E., Roos, A. de. Cine gradient-echo MR imaging and MR velocity mapping in the evaluation of congenital heart disease. Radiographics 16 (1996): 467–481.

Rebergen, S. A., van der Wall, E. E., Doornbos, J., Roos, A. de. Magnetic resonance measurement of velocity and flow: technique, validation, and cardiovascular applications. Am. Heart J. 126 (1993): 1439–1456.

Roberts, C. S., Roberts, W. C. Dissection of the aorta associated with congenital malformation of the aortic valve. J. Am. Coll. Cardiol. 17 (1991): 712–716.

Roberts, W. C. The congenitally bicuspid aortic valve. A study of 85 autopsy cases. Am. J. Cardiol. 26 (1970): 72–83.

Roberts, W. C., Ko, J. M. Frequency by decades of unicuspid, bicuspid, and tricuspid aortic valves in adults having isolated aortic valve replacement for aortic stenosis, with or without associated aortic regurgitation. Circulation 111 (2005): 920–925.

Robicsek, F., Thubrikar, M. J., Cook, J. W., Fowler, B. The congenitally bicuspid aortic valve: how does it function? Why does it fail?. Ann. Thorac. Surg. 77 (2004): 177–185.

Roman, M. J., Devereux, R. B., Kramer-Fox, R., O'Loughlin, J. Two-dimensional echocardiographic aortic root dimensions in normal children and adults. Am. J. Cardiol. 64 (1989): 507–512.

Roos-Hesselink, J. W., Schölzel, B. E., Heijdra, R. J., Spitaels, S. E. C., Meijboom, F. J., Boersma, E., Bogers, A. J. J. C., Simoons, M. L. Aortic valve and aortic arch pathology after coarctation repair. Heart 89 (2003): 1074–1077.

Sa, M. de, Moshkovitz, Y., Butany, J., David, T. E. Histologic abnormalities of the ascending aorta and pulmonary trunk in patients with bicuspid aortic valve disease: clinical relevance to the ross procedure. J. Thorac. Cardiovasc. Surg. 118 (1999): 588–594.

Savolainen, A., Keto, P., Hekali, P., Nisula, L., Kaitila, I., Viitasalo, M., Poutanen, V. P., Standertskjöld-Nordenstam, C. G., Kupari, M. Aortic distensibility in children with the Marfan syndrome. Am. J. Cardiol. 70 (1992): 691–693.

Schaefer, B. M., Lewin, M. B., Stout, K. K., Byers, P. H., Otto, C. M. Usefulness of bicuspid aortic valve phenotype to predict elastic properties of the ascending aorta. Am. J. Cardiol. 99 (2007): 686–690.

Schaefer, B. M., Lewin, M. B., Stout, K. K., Gill, E., Prueitt, A., Byers, P. H., Otto, C. M. The bicuspid aortic valve: an integrated phenotypic classification of leaflet morphology and aortic root shape. Heart 94 (2008): 1634–1638.

Scholz, D. G., Lynch, J. A., Willerscheidt, A. B., Sharma, R. K., Edwards, J. E. Coronary arterial dominance associated with congenital bicuspid aortic valve. Arch. Pathol. Lab. Med. 104 (1980): 417–418.

Siu, S. C., Silversides, C. K. Bicuspid aortic valve disease. J. Am. Coll. Cardiol. 55 (2010): 2789–2800.

Sonoda, M., Takenaka, K., Uno, K., Ebihara, A., Nagai, R. A larger aortic annulus causes aortic regurgitation and a smaller aortic annulus causes aortic stenosis in bicuspid aortic valve. Echocardiography 25 (2008): 242–248.

Stalder, A. F., Russe, M. F., Frydrychowicz, A., Bock, J., Hennig, J., Markl, M. Quantitative 2D and 3D phase contrast MRI: optimized analysis of blood flow and vessel wall parameters. Magn Reson Med 60 (2008): 1218–1231.

Sybert, V. P. Cardiovascular malformations and complications in Turner syndrome. Pediatrics 101 (1998): E11.

Tadros, T. M., Klein, M. D., Shapira, O. M. Ascending aortic dilatation associated with bicuspid aortic valve: pathophysiology, molecular biology, and clinical implications. Circulation 119 (2009): 880–890.

Takahashi, M., Ikeda, U., Shimada, K., Takeda, H. Rare association of congenital bicuspid aortic valve, annuloaortic ectasia, and anomalous origin of left circumflex coronary artery. Cardiology 84 (1994): 61–64.

Thanassoulis, G., Yip, J. W. L., Filion, K., Jamorski, M., Webb, G., Siu, S. C., Therrien, J. Retrospective study to identify predictors of the presence and rapid progression of aortic dilatation in patients with bicuspid aortic valves. Nature clinical practice. Cardiovascular medicine 5 (2008): 821–828.

Tzemos, N., Therrien, J., Yip, J., Thanassoulis, G., Tremblay, S., Jamorski, M. T., Webb, G. D., Siu, S. C. Outcomes in adults with bicuspid aortic valves. JAMA 300 (2008): 1317–1325.

Viscardi, F., Vergara, C., Antiga, L., Merelli, S., Veneziani, A., Puppini, G., Faggian, G., Mazzucco, A., Luciani, G. B. Comparative Finite Element Model Analysis of Ascending Aortic Flow in Bicuspid and Tricuspid Aortic Valve. Artificial organs (2010).

Walker, P. G., Cranney, G. B., Scheidegger, M. B., Waseleski, G., Pohost, G. M., Yoganathan, A. P. Semiautomated method for noise reduction and background phase error correction in MR phase velocity data. J Magn Reson Imaging 3: 521–530.

Ward, C. Clinical significance of the bicuspid aortic valve. Heart 83 (2000): 81–85.

Warnes, C. A., Williams, R. G., Bashore, T. M., Child, J. S., Connolly, H. M., Dearani, J. A., del Nido, P., Fasules, J. W., Graham, T. P., Hijazi, Z. M., Hunt, S. A., King, M. E., Landzberg, M. J., Miner, P. D., Radford, M. J., Walsh, E. P., Webb, G. D., Smith, S. C., Jacobs, A. K., Adams, C. D., Anderson, J. L., Antman, E. M., Buller, C. E., Creager, M. A., Ettinger, S. M., Halperin, J. L., Hunt, S. A., Krumholz, H. M., Kushner, F. G., Lytle, B. W., Nishimura, R. A., Page, R. L., Riegel, B., Tarkington, L. G., Yancy, C. W. ACC/AHA 2008 guidelines for the management of adults with congenital heart disease: a report of the American College of Cardiology/American Heart Association Task Force on Practice Guidelines (Writing Committee to Develop Guidelines on the Management of Adults With Congenital Heart Disease). Developed in Collaboration With the

American Society of Echocardiography, Heart Rhythm Society, International Society for Adult Congenital Heart Disease, Society for Cardiovascular Angiography and Interventions, and Society of Thoracic Surgeons. J. Am. Coll. Cardiol. 52 (2008): e1-121.

Wauchope G. The clinical importance of variations in the number of cusps forming the aortic and pulmonary valves. Quart J Med 21 (1928): 383–399.

Weber, O. M., Higgins, C. B. MR evaluation of cardiovascular physiology in congenital heart disease: flow and function. J Cardiovasc Magn Reson 8 (2006): 607–617.

Weigang, E., Kari, F. A., Beyersdorf, F., Luehr, M., Etz, C. D., Frydrychowicz, A., Harloff, A., Markl, M. Flow-sensitive four-dimensional magnetic resonance imaging: flow patterns in ascending aortic aneurysms. Eur J Cardiothorac Surg 34 (2008): 11–16.

Wigström, L., Ebbers, T., Fyrenius, A., Karlsson, M., Engvall, J., Wranne, B., Bolger, A. F. Particle trace visualization of intracardiac flow using time-resolved 3D phase contrast MRI. Magn Reson Med 41 (1999): 793–799.

Wigström, L., Sjöqvist, L., Wranne, B. Temporally resolved 3D phase-contrast imaging. Magn Reson Med 36 (1996): 800–803.

Yasuda, H., Nakatani, S., Stugaard, M., Tsujita-Kuroda, Y., Bando, K., Kobayashi, J., Yamagishi, M., Kitakaze, M., Kitamura, S., Miyatake, K. Failure to prevent progressive dilation of ascending aorta by aortic valve replacement in patients with bicuspid aortic valve: comparison with tricuspid aortic valve. Circulation 108 Suppl 1 (2003): II291-4.

Yener, N., Oktar, G. L., Erer, D., Yardimci, M. M., Yener, A. Bicuspid aortic valve. Ann Thorac Cardiovasc Surg 8 (2002): 264–267.

Figures

Tables

Appendix

A Still Frames of all 18 matched Pairs

Below flow images, obtained by 4D flow MR, of all matched pairs are demonstrated with the control person on the left side and the matched patient with BAV on the right. Indicated is the mean value of the three given flow graduations.

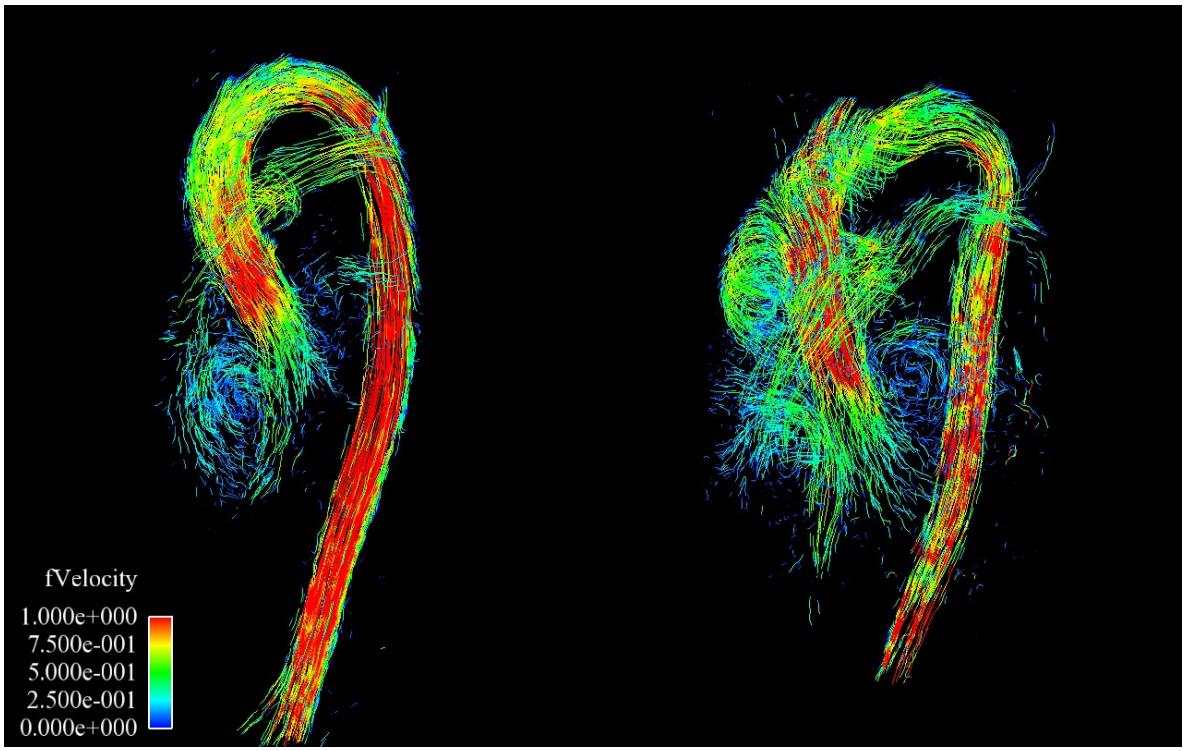

Figure A1: Pair #1 with TAV graded as 0.33 and BAV as 3.

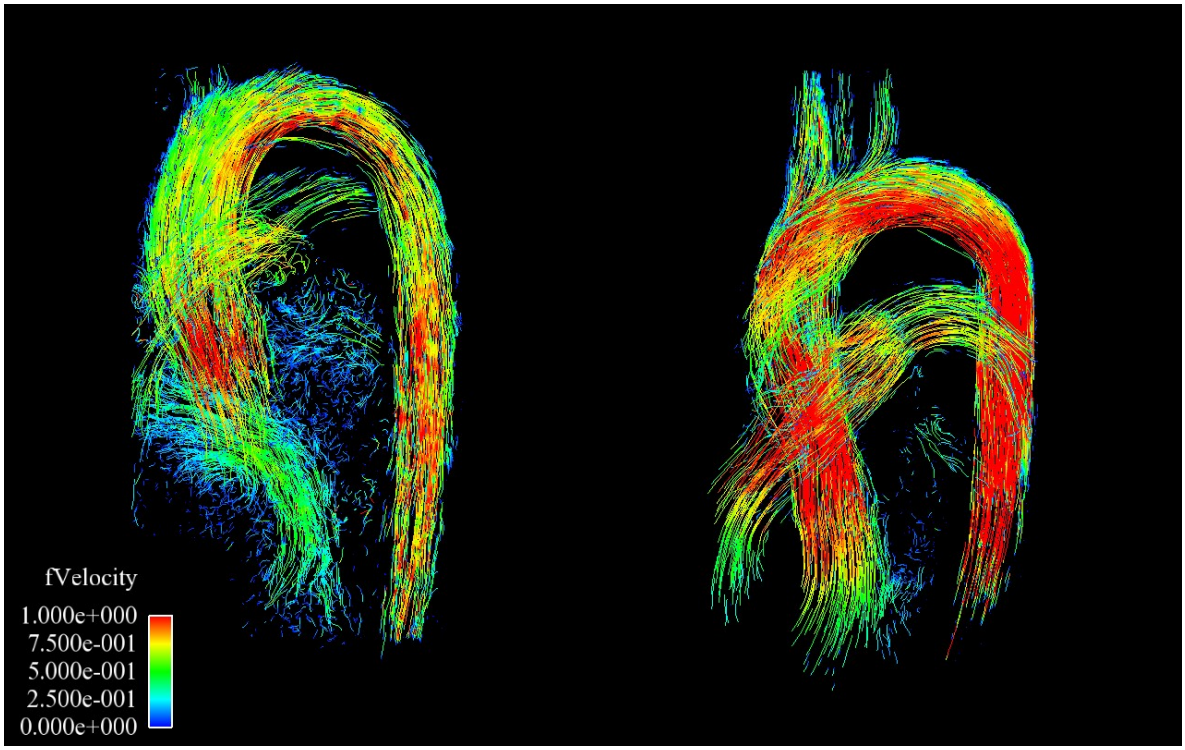

Figure A2: Pair #2 with TAV graded as 0.33 and BAV as 1.

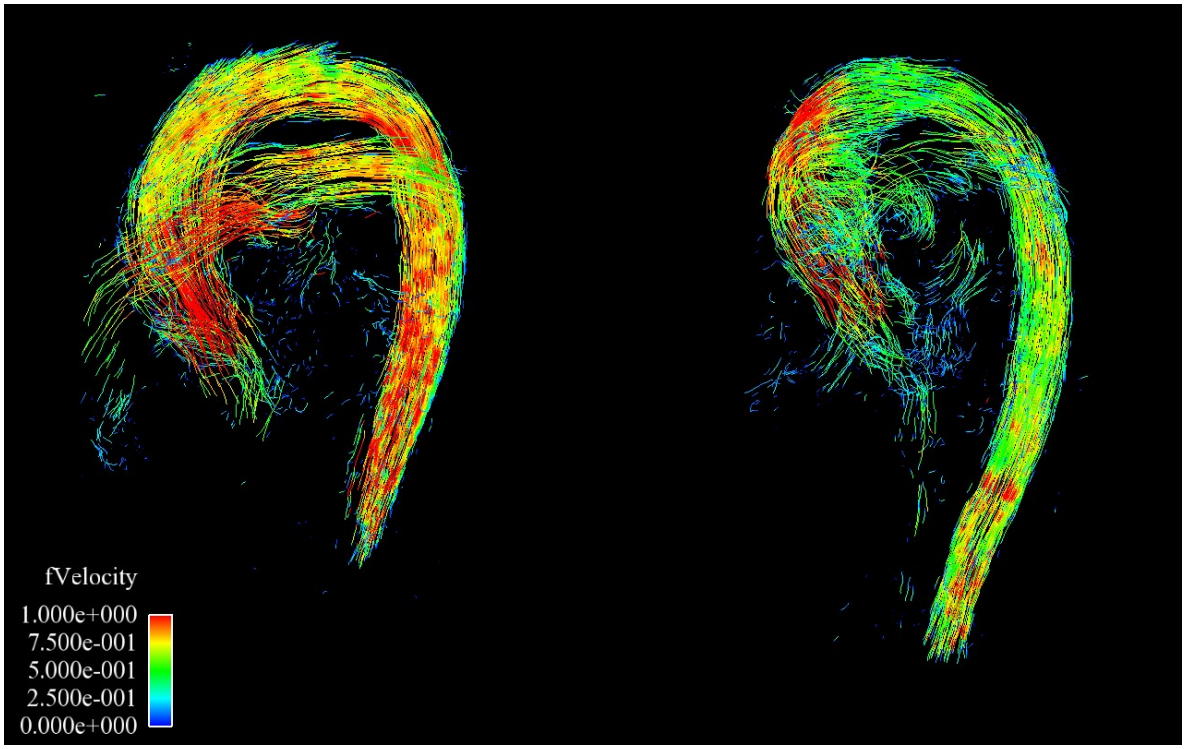

Figure A3: Pair #3 with TAV graded as 1 and BAV as 3.

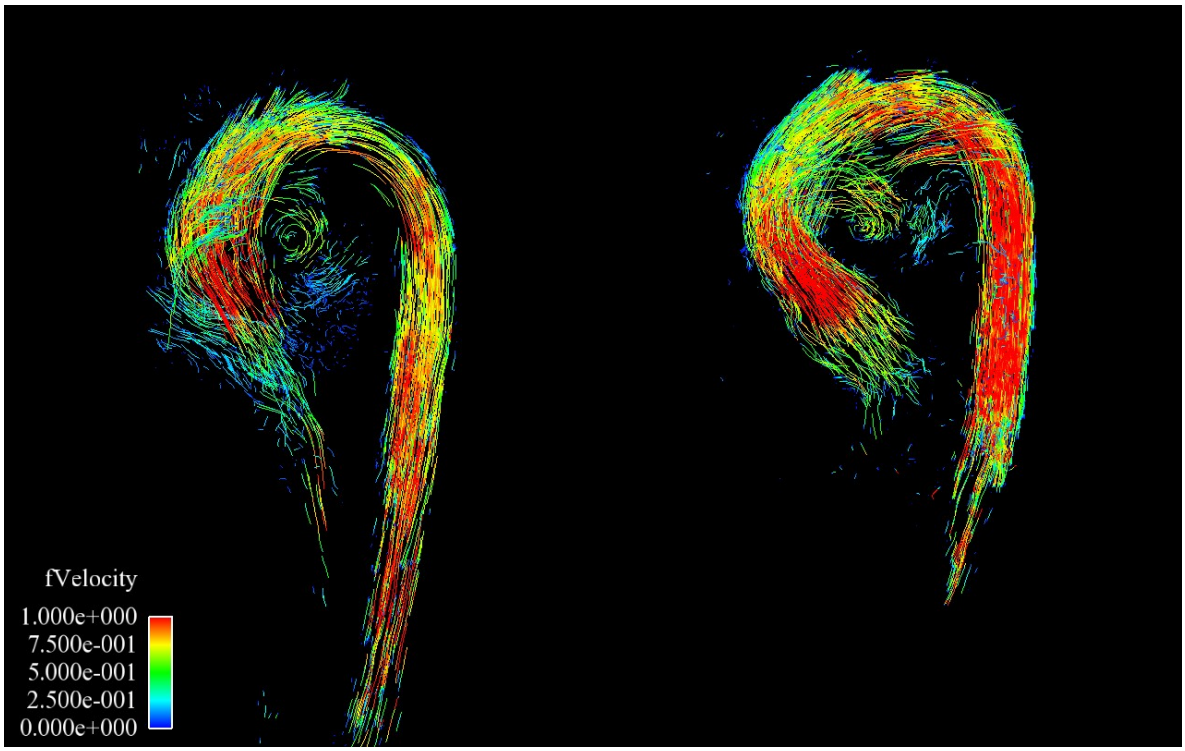

Figure A4: Pair #4 with TAV graded as 0.67 and BAV as 0.33.

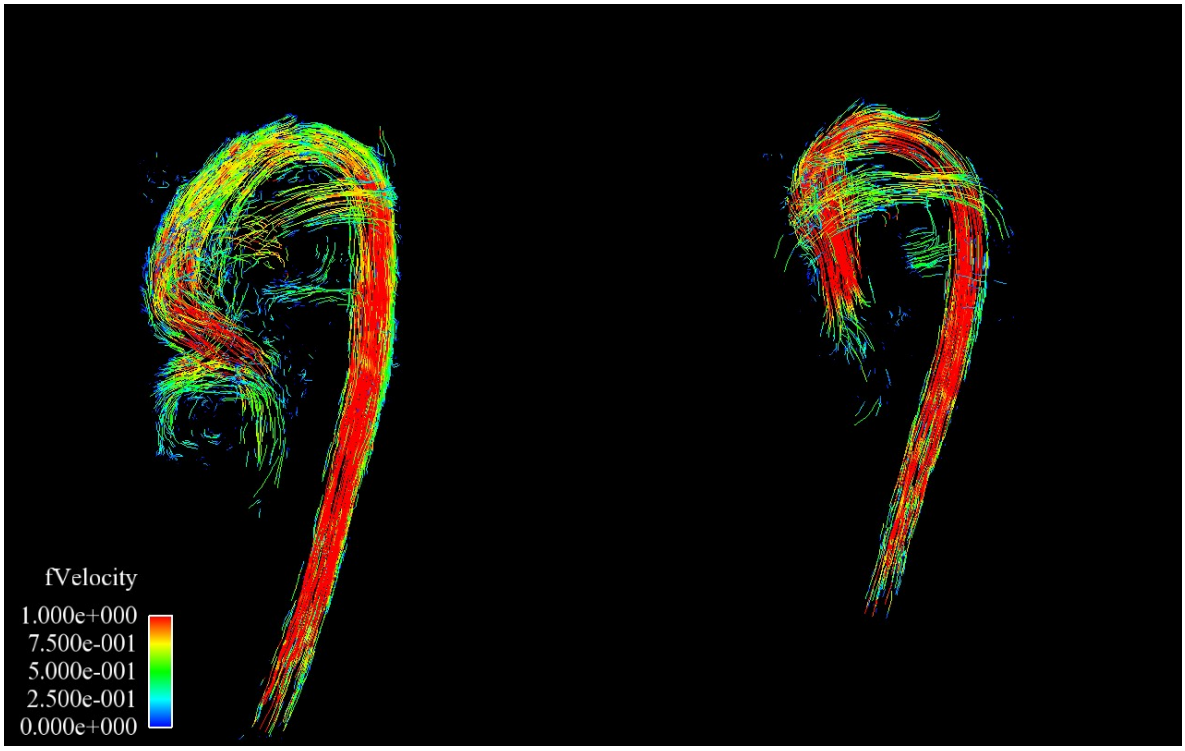

Figure A5: Pair #5 with TAV graded as 0.67 and BAV as 0.67.

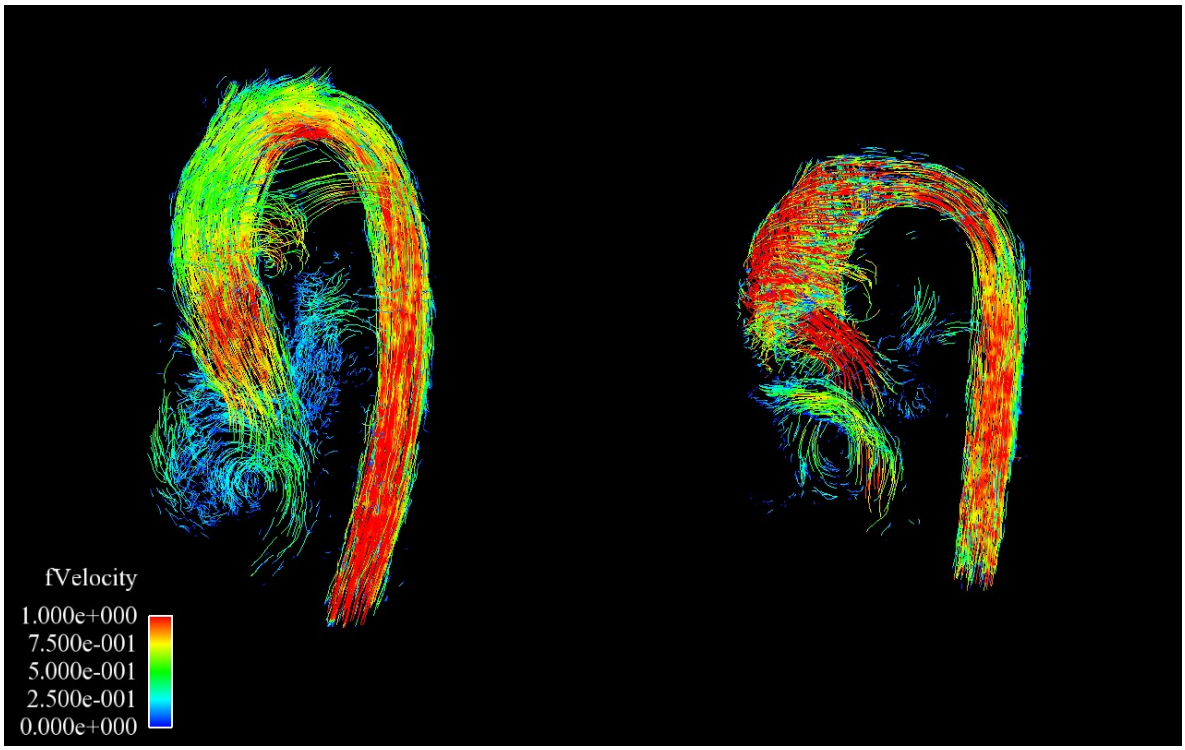

Figure A6: Pair #6 with TAV graded as 0.33 and BAV as 3.

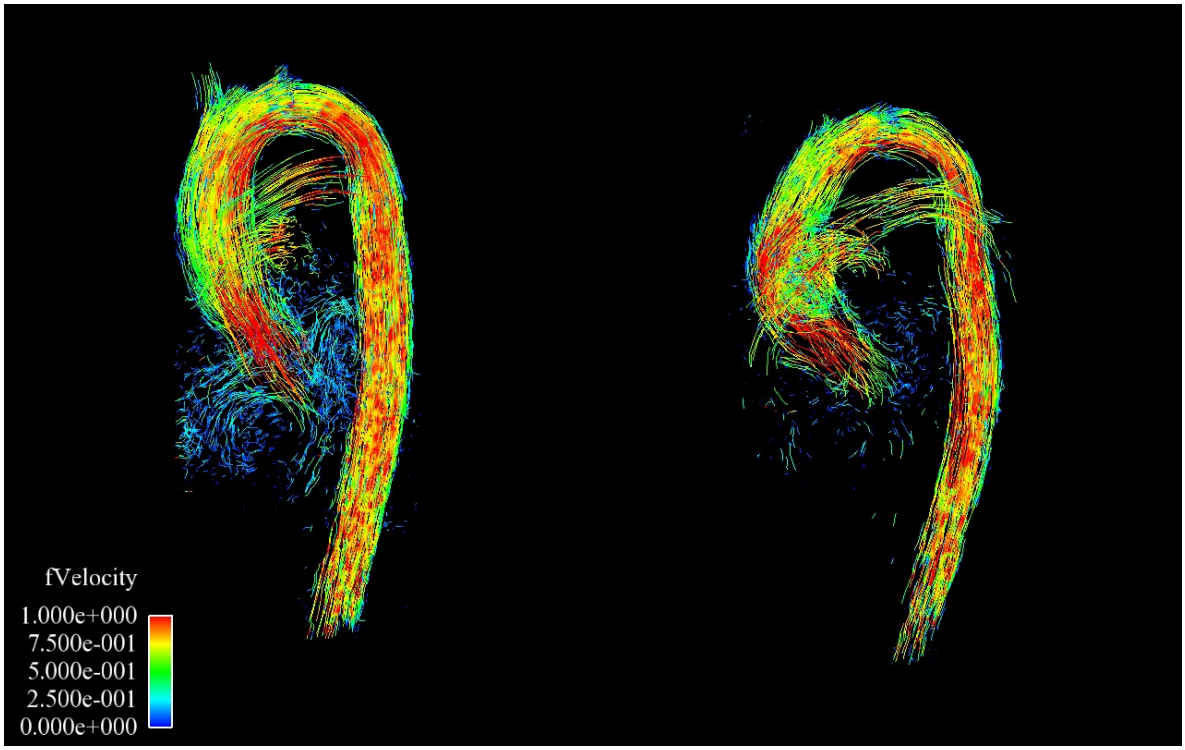

Figure A7: Pair #7 with TAV graded as 0 and BAV as 2.67.

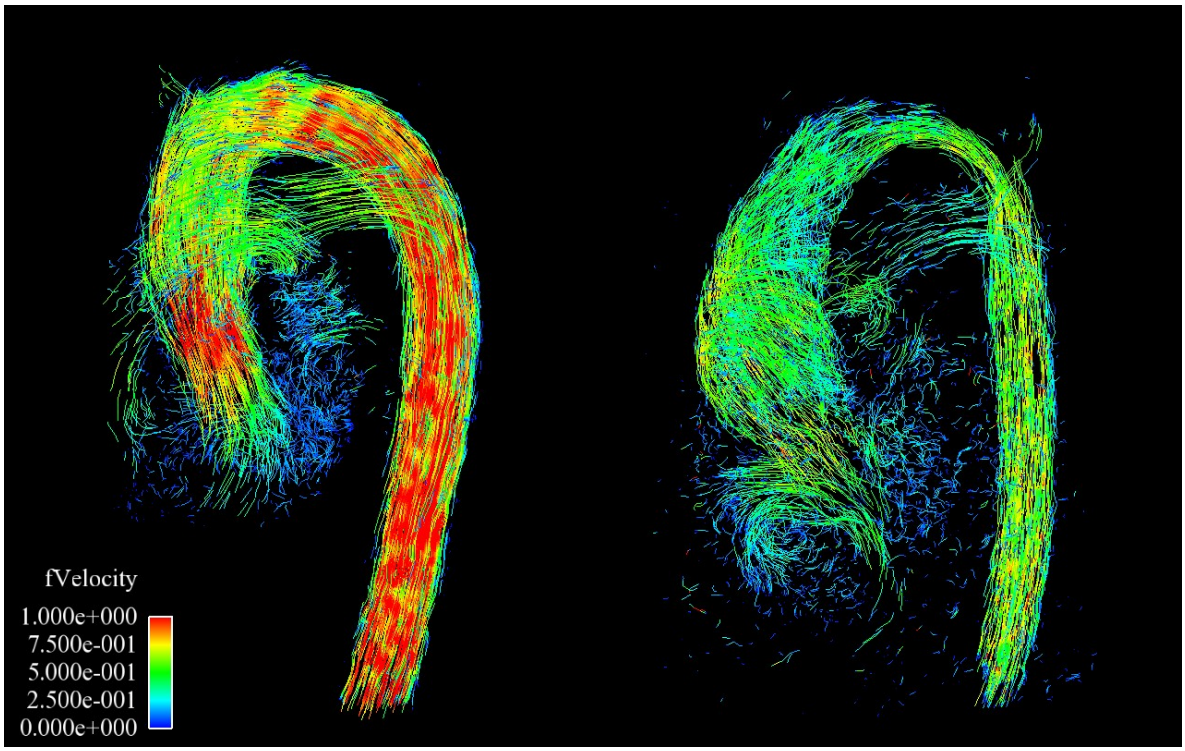

Figure A8: Pair #8 with TAV graded as 1 and BAV as 3.

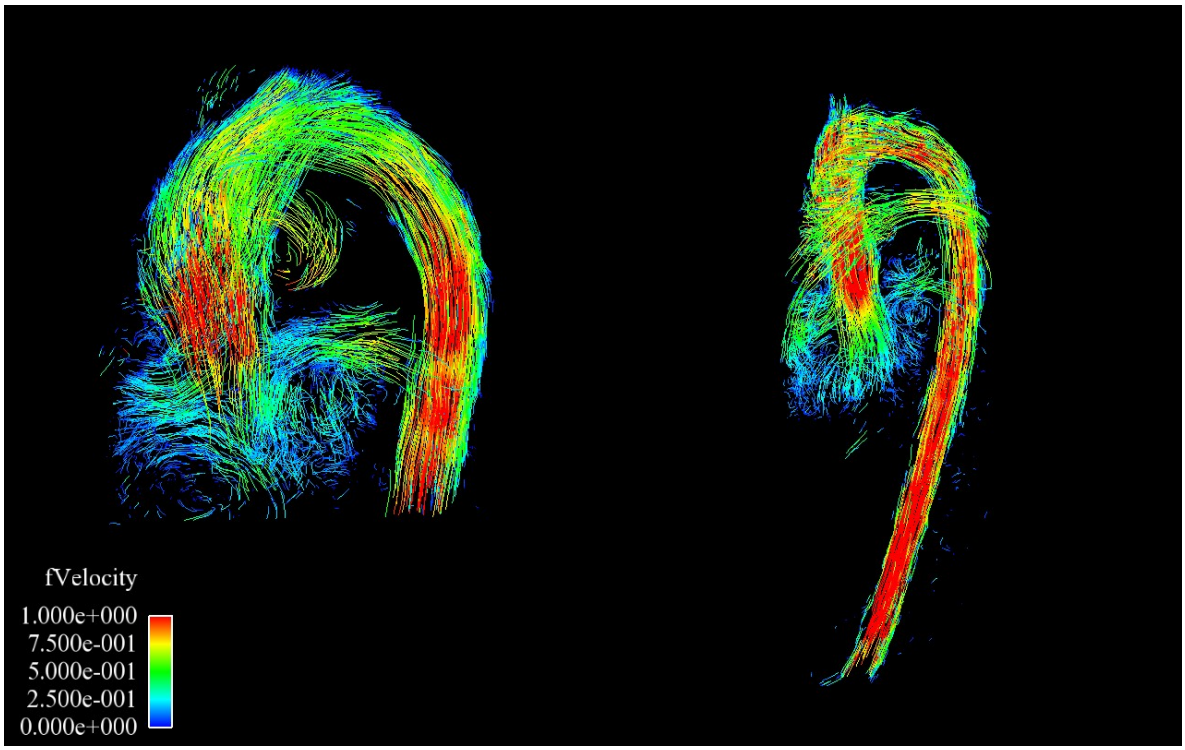

Figure A9: Pair #9 with TAV graded as 0.67 and BAV as 2.67.

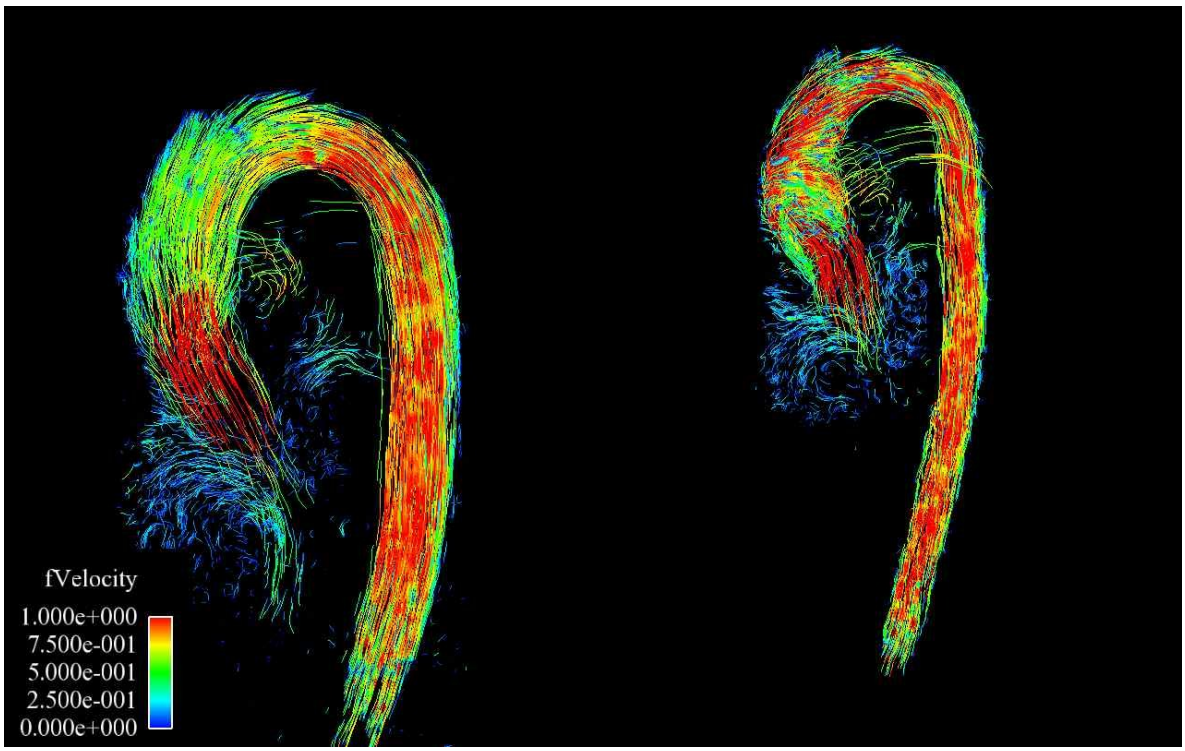

Figure A10: Pair #10 with TAV graded as 0.5 and BAV as 3.

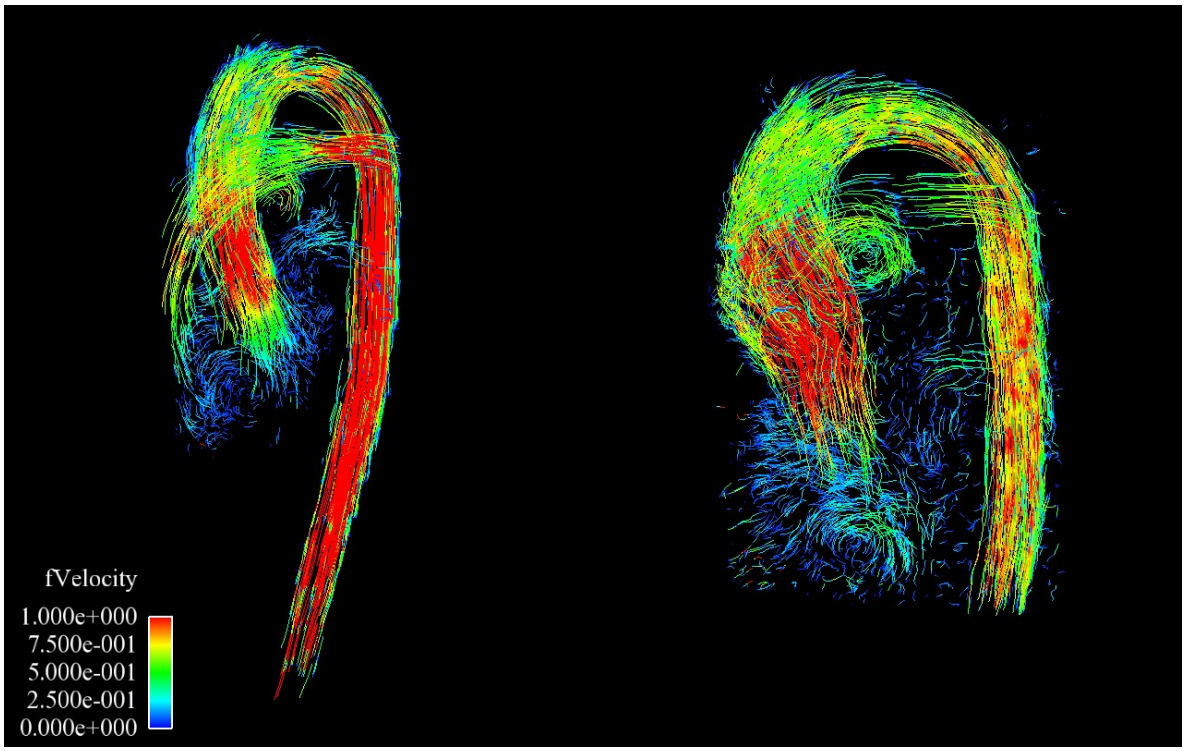

Figure A11: Pair #11 with TAV graded as 0 and BAV as 2.33.

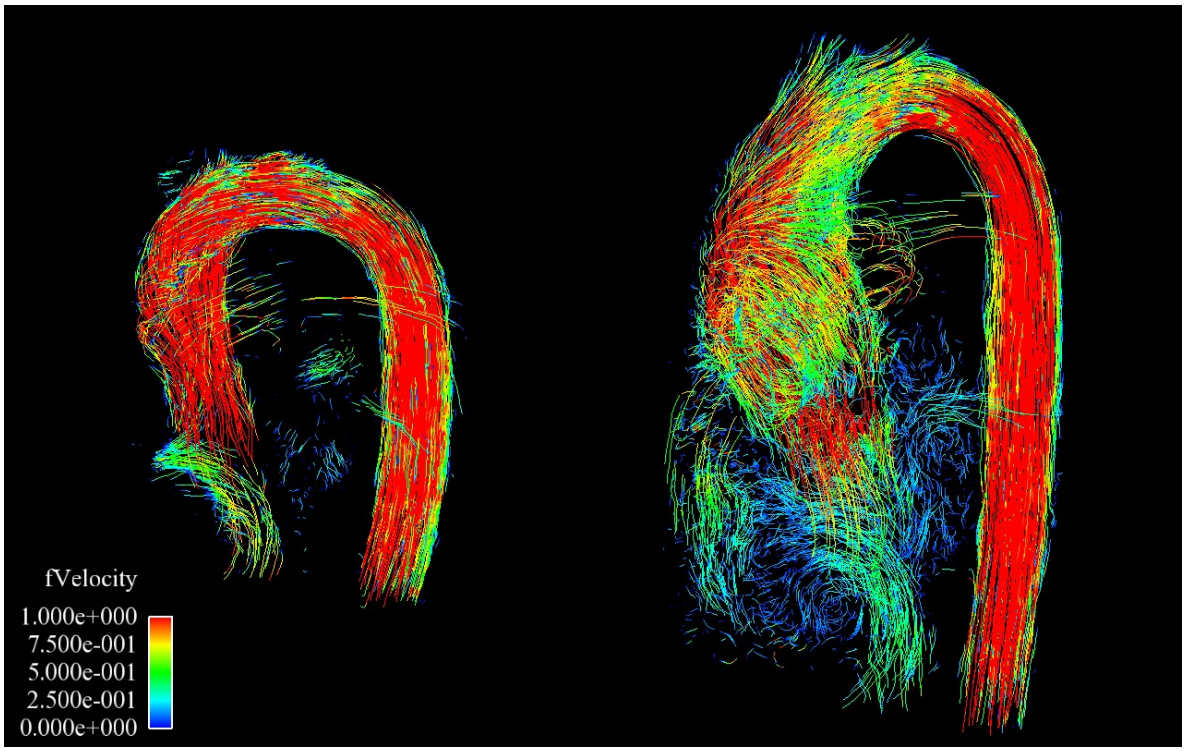

Figure A12: Pair #12 with TAV graded as 1 and BAV as 3.

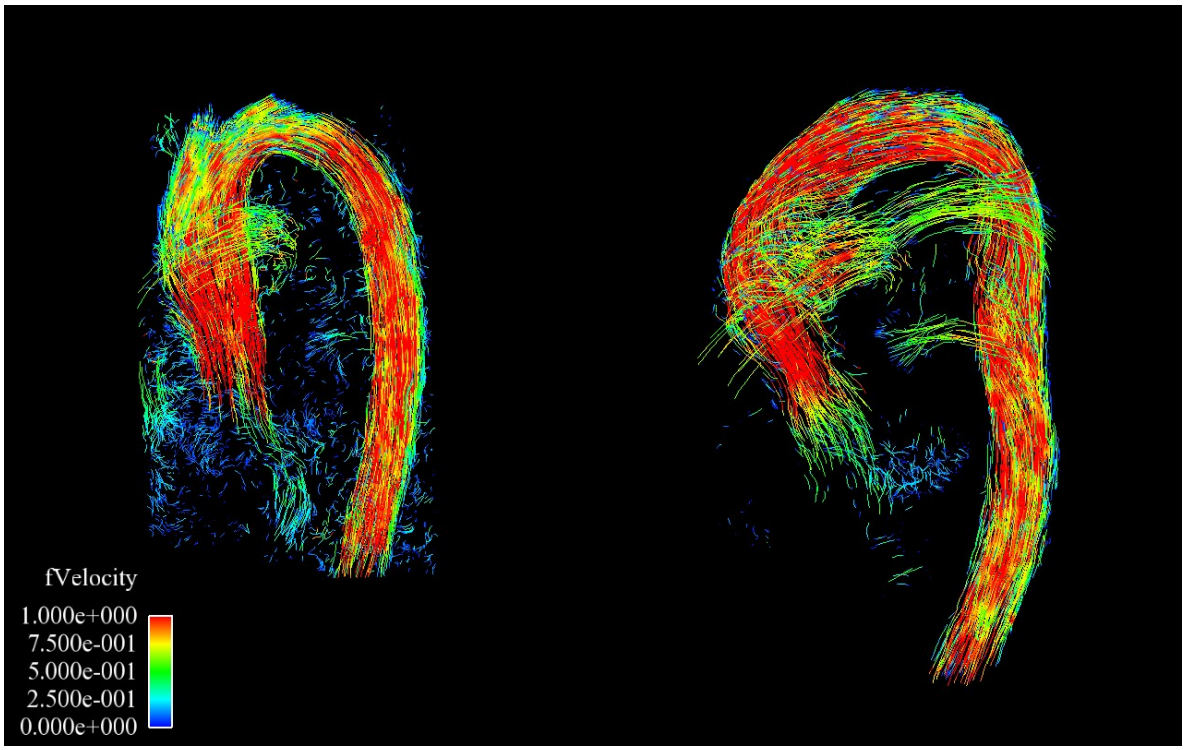

Figure A13: Pair #13 with TAV graded as 1 and BAV as 2.67.

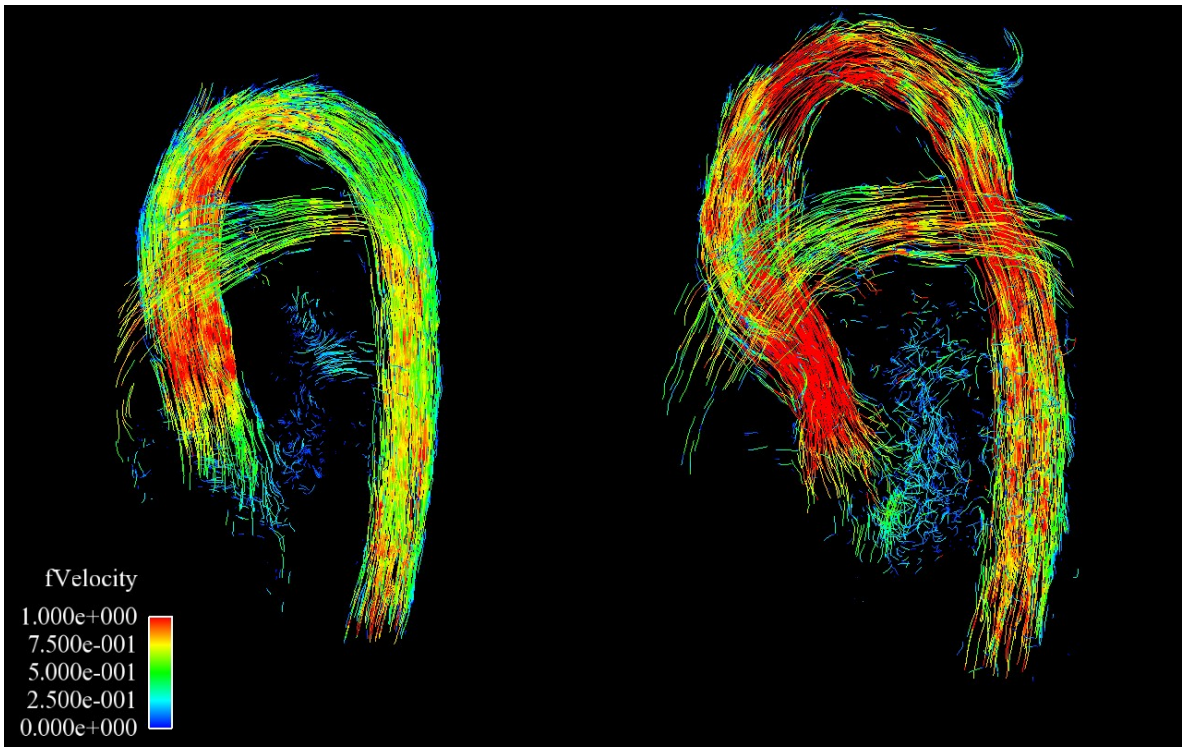

Figure A14: Pair #14 with TAV graded as 0 and BAV as 2.67.

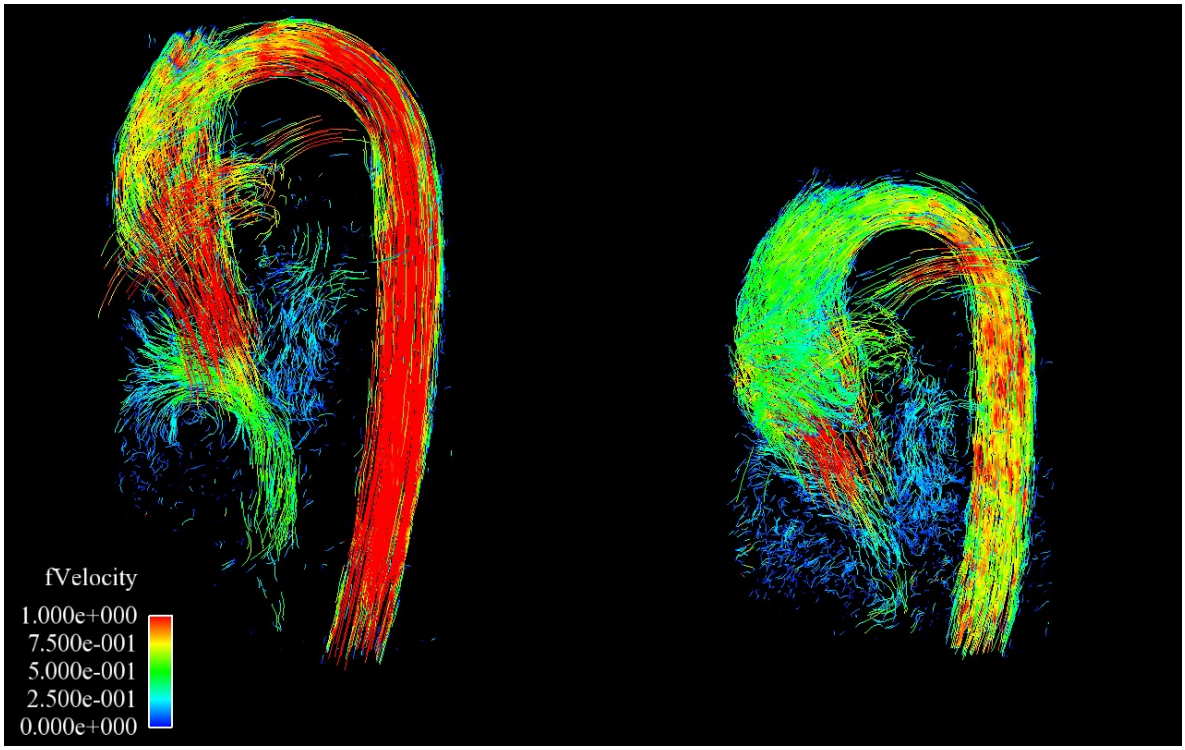

Figure A15: Pair #15 with TAV graded as 1 and BAV as 3.

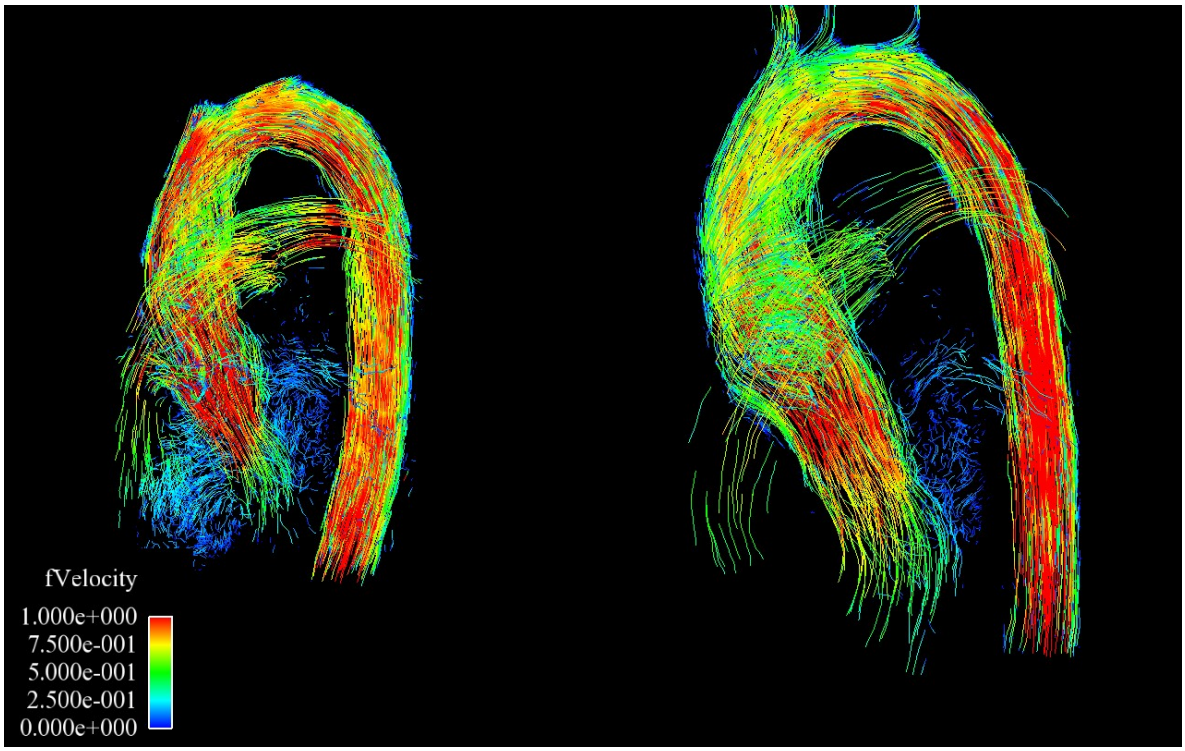

Figure A16: Pair #16 with TAV graded as 1.33 and BAV as 2.67.

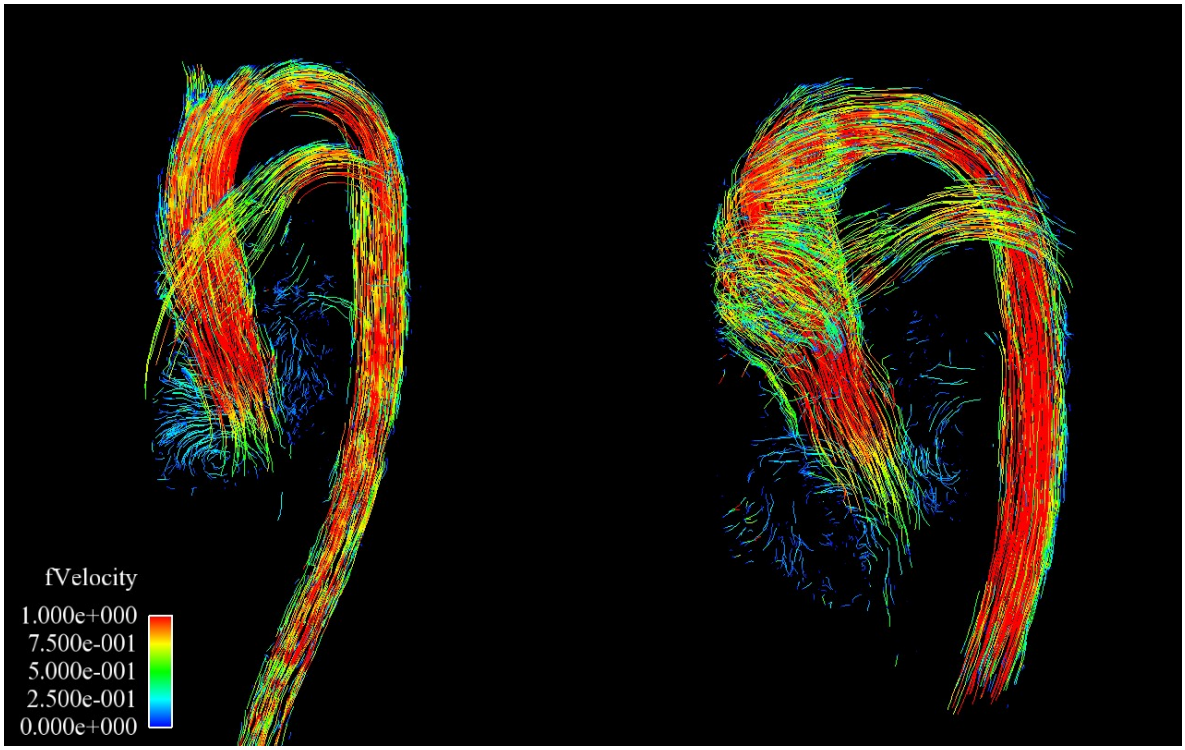

Figure A17: Pair #17 with TAV graded as 0 and BAV as 2.67.

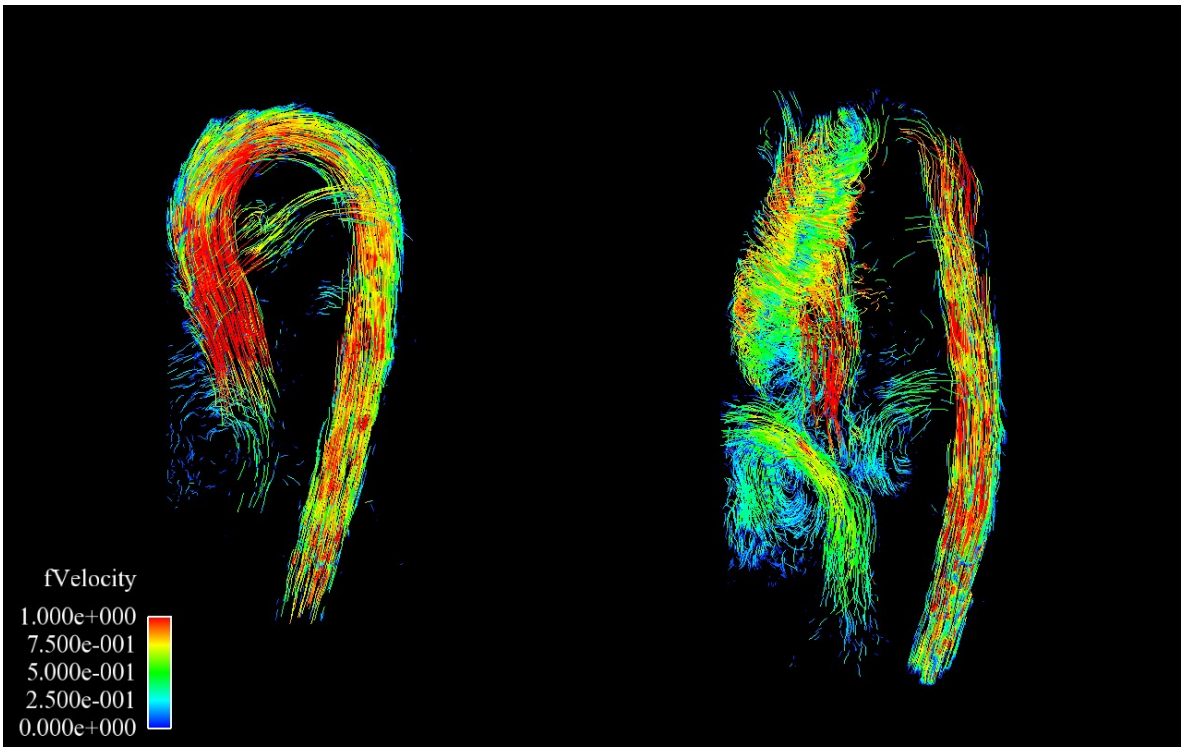

Figure A18: Pair #18 with TAV graded as 0 and BAV as 3.

B Classification of Helical Flow

Classification of helical flow (0 to 3)

initials	valve type	pair #	classification of blinded observers			
			observer 1	observer 2	observer 3	mean
S.M.	BAV II	1	3	3	3	3.00
K.M.	TAV	1	0	0	1	0.33
S.P.	TAV	2	0	1	0	0.33
S.F.	BAV	2	0	2	1	1.00
F.U.	TAV	3	1	1	1	1.00
K.H.	BAV	3	3	3	3	3.00
M.C.	TAV	4	0	1	1	0.67
R.G.	BAV	4	0	1	0	0.33
P.R.	TAV	5	1	0	1	0.67
W.S.	BAV	5	0	0	2	0.67
W.A.	BAV II	6	3	3	3	3.00
B.T.	TAV	6	0	1	0	0.33
Z.C.	BAV	7	3	2	3	2.67
B.B.	TAV	7	0	0	0	0.00
L.G.	BAV	8	3	3	3	3.00
H.H:	TAV	8	1	1	1	1.00
F.L.	TAV	9	0	1	1	0.67
W.A.	BAV II	9	2	3	3	2.67
K.A.	TAV	10	0	1	0	0.33
E.B.	BAV	10	3	3	3	3.00
O.F.	TAV	11	0	0	0	0.00
P.D.	BAV	11	1	3	3	2.33
R.L.	TAV	12	0	2	1	1.00
D.S.	BAV	12	3	3	3	3.00
D.M.	TAV	13	1	1	1	1.00
F.S.	BAV II	13	3	2	3	2.67
F.V.	TAV	14	0	0	0	0.00
M.A.	BAV	14	2	3	3	2.67
E.A.	BAV	15	3	3	3	3.00
V.F.	TAV	15	0	2	1	1.00
S.M.	BAV	16	3	2	3	2.67
Z.T:	TAV	16	1	1	2	1.33
I.L.	BAV	17	3	2	3	2.67
L.C.	TAV	17	0	0	0	0.00
R.H.	TAV	18	0	0	0	0.00
W.S.	BAV II	18	3	3	3	3.00

Table B1: The flow classifications of all three observers are demonstrated, just as the mean values. In this table BAV type 1 is indicated as BAV, and BAV type 2 as BAV II.

C Data of Study Participants

C.1 BAV group

patient #	aortic bulbus				ascending aorta				descending aorta				peak velocity aorta	aortic insufficiency
	P_{sys}	P_{dia}	D_{max}	max. diameter corrected	P_{sys}	P_{dia}	D_{max}	max. diameter corrected	P_{sys}	P_{dia}	D_{max}	max. diameter corrected		
1	no data	no data	no data	no data	no data	no data	3.71	2.11	no data	no data	1.51	0.86	129.75	1.00
2	no data	no data	no data	no data	110	58	3.58	1.85	110	60	2	1.04	165.86	1.00
3	123	78	3.96	1.81	128	83	4.08	1.87	124	81	2.23	1.02	152.75	7.00
4	123	74	3.17	1.5	125	78	3.54	1.68	123	72	2.38	1.13	123.28	6.00
5	108	63	2.46	1.44	111	59	2.92	1.71	112	59	1.46	0.85	162.50	0.00
6	105	50	3.08	1.63	109	54	3.58	1.89	111	58	2.21	1.17	231.15	6.00
7	101	58	3.21	1.79	102	60	3.46	1.93	104	59	2.13	1.19	128.55	1.00
8	103	72	4.21	2.2	102	70	4.42	2.31	103	69	2.21	1.16	115.21	1.00
9	105	55	2.15	2	97	45	2.04	1.9	92	50	1.7	1.59	131.74	0.00
10	98	46	2.7	1.56	97	44	3.1	1.8	94	44	1.73	1	193.87	1.00
11	101	61	3.1	1.77	99	61	3.33	1.91	99	60	1.77	1.01	134.77	0.00
12	128	76	4.08	2.14	123	71	4.21	2.21	126	77	1.79	0.94	156.17	4.00
13	114	75	2.75	1.4	117	73	3.03	1.55	115	72	2	1.02	158.81	4.00
14	120	67	3.17	1.55	115	75	2.5	1.22	122	63	2	0.98	171.78	3.00
15	121	83	4	1.94	124	79	4.38	2.12	122	78	2.21	1.07	131.39	3.00
16	110	56	3.29	1.93	110	66	2.88	1.69	109	69	1.67	0.98	111.05	0.00
17	113	81	2.93	1.8	124	74	3.23	1.99	128	73	1.69	1.04	131.89	2.00
18	101	56	2.75	1.69	110	51	3.56	2.19	111	49	1.47	0.9	180.08	0.00
mean	110.88	65.69	3.19	1.76	111.94	64.76	3.42	1.89	112.06	64.29	1.9	1.05	150.59	2.22
SD	9.61	11.59	0.6	0.24	10.33	11.93	0.63	0.26	11.12	10.76	0.29	0.17	30.65	2.32
median	109	65	3.14	1.78	110	66	3.5	1.9	111	63	1.9	1.02	143.76	1
range	98-128	46-83	2.15-4.21	1.88-3.04	97-128	44-83	2.04-4.42	1.75-3.2	92-128	44-81	1.46-2.38	1.12-1.64	111-144	0-7

Data of TAV group; Psys = systolic blood pressure in mmHG, Pdia = diastolic blood pressure in mmHg, Dmax = maximum Diameter in cm, Dmax corrected = Dmax indexed for BSA in cm/m²

C.2 TAV group

patient #	aortic bulbus				ascending aorta				descending aorta				peak velocity aorta	aortic insufficiency
	P_{sys}	P_{dia}	D_{max}	D_{max} corrected	P_{sys}	P_{dia}	D_{max}	D_{max} corrected	P_{sys}	P_{dia}	D_{max}	D_{max} corrected		
1	112	75	2.54	1.51	110	64	2.31	1.37	115	64	1.69	1	108.09	0.00
2	no data	no data	no data	no data	no data	no data	2.97	1.68	no data	no data	1.84	1.04	90.90	0.00
3	116	67	3.17	1.42	117	73	3.54	1.59	118	66	2.42	1.09	120.16	4.00
4	no data	no data	no data	no data	no data	no data	no data	no data	no data	no data	no data	no data	85.39	0.00
5	110	67	3.04	1.77	111	69	2.89	1.68	110	70	1.75	1.02	110.88	0.00
6	102	51	4.03	2.04	99	53	3.29	1.66	102	52	2.21	1.12	88.07	0.00
7	122	82	3.47	1.75	124	80	3.03	1.52	123	79	2.2	1.11	97.77	1.00
8	98	50	3.14	1.54	101	56	2.97	1.45	98	55	2.13	1.04	100.86	1.00
9	94	50	2.13	2.08	98	48	2.16	2.11	99	48	1.34	1.31	123.09	0.00
10	107	73	2.88	1.85	110	67	2.83	1.82	124	77	2	1.28	97.52	0.00
11	107	54	1.97	1.34	110	65	2	1.36	114	68	1.33	0.9	95.10	0.00
12	114	48	3.09	1.53	98	51	2.92	1.44	110	49	1.96	0.97	169.90	2.00
13	111	47	2.75	1.5	103	57	2.92	1.59	103	56	1.81	0.98	125.16	0.00
14	100	58	3	1.5	99	59	2.63	1.32	106	58	2	1	107.25	0.00
15	111	60	2.83	1.46	112	61	3.33	1.72	109	61	2	1.03	153.81	2.00
16	98	49	3.08	1.68	99	54	2.72	1.48	103	51	2.25	1.22	143.93	1.00
17	no data	no data	no data	no data	129	81	2.52	1.52	112	72	1.83	1.11	102.44	0.00
18	104	65	2.21	1.38	97	58	2.33	1.46	104	63	1.79	1.12	138.52	0.00
mean	107.07	59.73	2.89	1.62	107.31	62.25	2.79	1.57	109.38	61.81	1.91	1.08	114.38	0.61
SD	7.72	11.2	0.53	0.23	9.82	9.8	0.42	0.2	7.95	9.74	0.3	0.11	23.96	1.09
median	107	58	3	1.53	106.5	60	2.89	1.52	109.5	62	1.96	1.04	107.67	0
range	94-122	47-82	1.97-4.03	1.62-2.87	97-129	48-81	2-3.54	1.65-2.39	98-124	48-79	1.33-2.42	1.1-1.66	85.4-170	0-4

Data of TAV group; Psys = systolic blood pressure in mmHG, Pdia = diastolic blood pressure in mmHg, Dmax = maximum Diameter in cm, Dmax corrected = Dmax indexed for BSA in cm/m²

Acknowledgements

Herzlich bedanken möchte ich mich bei Herrn Prof. Dr. med. John Hess für die Möglichkeit an seiner Klinik zu promovieren.
Außerdem gilt mein Dank besonders Herrn PD Dr. med. Sohrab Fratz, sowie Herrn Dr. med. Christian Meierhofer, die mich die ganzen Jahre betreut haben und Antwort auf all meine Fragen hatten.
Auch bei Herrn PD Dr. med. Heiko Stern möchte ich mich herzlich für seine Unterstützung und seine Tipps bei der Durchführung der Studie bedanken, sowie für seine Beteiligung an der Flussauswertung. Hier gilt auch Frau Dr. med. Andrea Hutter mein Dank.
Vor allem möchte ich auch Philipp Schneider danken, der mir durch die Zusammenarbeit an der Studie eine große Hilfe bei der Patientenrekrutierung, Flussauswertung, Interpretation der Ergebnisse und vielen Fragen war.
Ein besonderer Dank gilt auch den Mitarbeiterinnen der Kinderambulanz, vor allem Frau Frisch, die uns durch die Vorbereitung der Blutdruckmessgeräte sehr geholfen haben.
Auch meinem Freund Vincent Fraunhoffer bin ich für seine Hilfe in der Bildbearbeitung und Erstellung von Grafiken, für die Teilnahme an der Studie als Proband, sowie für seine Unterstützung während der letzten Jahre sehr dankbar.
Nicht zu vergessen sind all die Patienten und Bekannte, die Ihre Zeit zur Verfügung gestellt und freiwillig an der Studie und an den Untersuchungen teilgenommen haben und meine Familie und Freunde, die mich während dieser Zeit unterstützt und motiviert haben.